Author:
Harvey, Lucy

Title:
Exploring the in vitro behaviour of endothelial cells in different cell culture models

Exploring the *in vitro* behaviour of endothelial cells in different cell culture models

Lucy Harvey

School of Biochemistry

November 2018

A dissertation submitted to the University of Bristol in accordance with the requirements for award of the degree of MRes in the Faculty of Life Sciences

Word count: Thirty-seven thousand, five-hundred and eighty-two

Abstract

Maintenance of vascular homeostasis requires a coordinated and regulated response by endothelial cells. ECs form the inner lining of blood and lymphatic vessels and form an interface between the luminal vessel fluid and surrounding tissue. They are hence involved in a large number of physiological processes and implicated in many pathologies. The fundamental biology of ECs must therefore be studied in order to understand the role of ECs in normal physiology and disease. My lab focusses on research into ECs and in the generation of *in vitro* EC culture models to explore its roles in angiogenesis. I aimed to analyse EC growth and proliferation under different conditions. An additional aim was to optimise a tumour angiogenesis co-culture assay, which analyses the growth of blood vessels towards tumour spheroids. Finally, I set out to study the surface polarity of a number of important cell surface proteins in human umbilical vein endothelial cells by means of surface protein labelling and analysis. A variety of *in vitro* assays were used across this work, including that for cell proliferation, tube formation and protein identification.

Optimal HUVEC culture conditions were analysed and determined. HUVEC grow and proliferate greatest in Lonza EGM-2 media, however ECs from transgenic fluorescent zebrafish larvae require alternate cell culture conditions. HUVEC also have varying growth abilities on different surfaces, with a nanostructured surface generating low confluency of cells which also developed markers of genetic instability. Optimisation of HUVEC culture conditions led to investigation of their capacity to form vascular tubules in a co-culture with normal human dermal fibroblasts. An optimal vascular density to effectively determine vascular directionality towards tumour spheroids was achieved, with future prospects to assess the angiogenic effects of growth factors and drugs in culture. Failure to develop a novel method to label HUVEC surface proteins for proteomic analysis revealed that further work on this needs to be carried out, however immunofluorescence has shown to be a valid, low-throughput method to label and identify surface proteins.

Dedication and Acknowledgements

Firstly, I would like to thank Professor Harry Mellor, Dr Ananthalakshmy Sundararaman and Jimmy Wei for their support and guidance throughout this project. Their ability to teach and demonstrate technical details has allowed me to learn a number of new laboratory techniques as well as enhance my scientific knowledge. I would especially like to express my gratitude to my supervisor, Harry, who has given up a lot of his own time to help develop me into a more independent scientist. I am enormously appreciative of his patience during the entirety of this project.

I also want to thank my dear friend Eddie, who has sat with me through countless coffee breaks. His enthusiasm and humour has made my year in the lab really entertaining, and his supportive nature has made me determined to achieve my masters.

Part of my dedication goes to my family; they are my inspiration to succeed in anything that I do, and without whom none of this would be possible. Their support has meant so much to me. I would like to express my enormous appreciation for their time and dedication that has been put towards my education and my own life journey.

Author’s Declaration

I declare that the work in this dissertation was carried out in accordance with the requirements of the University's *Regulations and Code of Practice for Research Degree Programmes* and that it has not been submitted for any other academic award. Except where indicated by specific reference in the text, the work is the candidate's own work. Work done in collaboration with, or with the assistance of, others, is indicated as such. Any views expressed in the dissertation are those of the author.

SIGNED: ..... DATE:.....

Table of Contents

CHAPTER 2 materials and Methods

CHAPTER 3 Endothelial cell proliferation assays

CHAPTER 4 Adaption of an *in vitro* angiogenesis assay to study tumour angiogenesis

Tables and Figures

Abbreviations

aEC	Arterial endothelial cell
BBB	Blood Brain Barrier
BL	Basolateral
BSA	Bovine serum albumin
CHC	Clathrin heavy chain
CNS	Central nervous system
CV	Cardinal vein
DAPI	4’6-diamidino-2-phenylindole
Dll4	Delta-like-4
DMEM	Dulbecco’s modified eagle media
EBM-2	Endothelial basal medium-2
ECM	Extracellular matrix
EDTA	Ethylenediaminetetraacetic acid
EGM-2	Endothelial cell growth medium-2
ESL-1	E-selectin ligand-1
FBS	Fetal bovine serum
FGF	Fibroblast growth factor
FN	Fibronectin
GA	Gentamicin, Amphotericin B
GLUT-1	Glucose transporter-1
HRP	Horseradish peroxidase
HPSGs	Heparin sulphate proteoglycans
HSC	Haematopoietic stem cells
HUVEC	Human umbilical vein endothelial cells
ICAM-1	Intercellular Adhesion Molecule-1
lEC	lymphatic endothelial cell
MCT1	Monocarboxylate transporter 1
MVEC	Microvascular endothelial cell
NHDF	Normal human dermal fibroblasts
NO	Nitrous oxide
PBS	Phosphate-buffered saline
PDPN	Podoplanin
PECAM-1	Platelet endothelial cell adhesion molecule-1
PFA	Paraformaldehyde
SLO	Secondary lymphoid organ
SMC	Smooth muscle cell
vEC	Venous endothelial cell
VEGF	Vascular endothelial growth factor
VEGFR	Vascular endothelial growth factor receptor
VSMC	Vascular smooth muscle cells
VE-cadherin	Vascular endothelial cadherin
vWF	von Willebrand factor
Ti	Titanium
TiO_2	Titanium dioxide

Chapter 1 - Introduction

1.1 Endothelial cells

ECs are the cobblestone-like cells that line blood vessels and form the barrier between the blood supply and the surrounding tissue [1] [2]. Their apical surface is in direct contact with components of the blood system, while their basal surface is sat on the basal lamina – a specialised extracellular matrix (ECM) on which ECs lie. They are tightly packed together into a monolayer [3] of squamous epithelial-like cells, generally forming a continuum along blood vessels and the lymphatics (Figure 1.1). Nearly every tissue requires a blood supply and so ECs are exploited in large amounts, performing many functions required of a circulatory system. There is no doubt, then, that these cells form one of the largest organ systems in the animal body. The average human has around 1kg of ECs [4], a considerable mass since these cells are some of the thinnest in the body and only compose of a single sheet inside the circulatory system.

1.1.1– Endothelial cell structure

ECs are extremely thin cells relative to other cells in the body, at about 0.1-1 μm thick [5]. They have a diameter of roughly 10-100x this, generating flat, polygonal cells that are tightly packed to reflect their key function – to allow the selective passage of nutrients and metabolites through them [4]. The organisation and array of sub-cellular organelles within ECs is relatively simple. Organelles, including the endoplasmic reticulum and Golgi apparatus, are mostly situated around the nucleus and ECs also include a relatively larger concentration of pinocytic vesicles [5]. These are vesicles that are involved in the bulk transport of molecules from the extracellular space across the membrane by means of membrane invagination. ECs are unique in that they are the only cell type to contain Weibel-Palade bodies [6]. These are tubular organelles whose formation is driven by the constituent they secrete; von Willebrand factor (vWF) [6]. vWF has a vital role in haemostasis whereby it activates and subsequently adheres platelets to the endothelial lining to form a temporary blood clot as a prerequisite to thrombosis [7].

1.2 – Vessel composition

The role of vessels, in general, is to transfer fluid and fluid solute from one area of the body to another. Each type of vessel has a distinct function which is reflected in its molecular composition [8]. That aside, all vessels have a common feature: a smooth

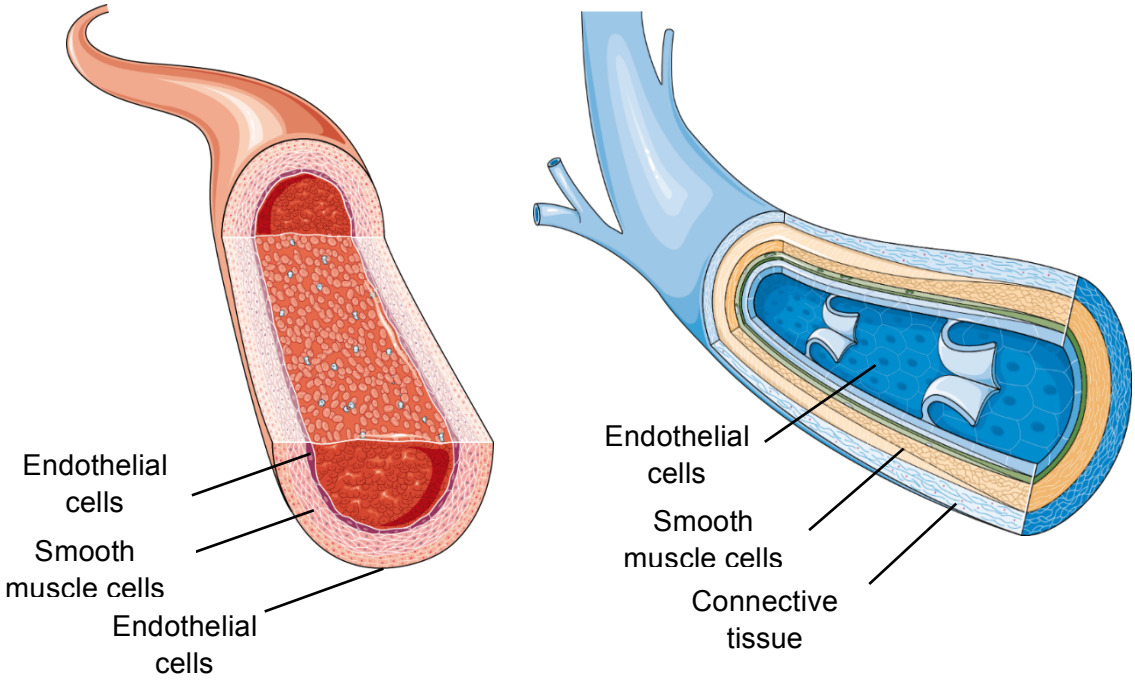

Figure 1.1 – **Endothelial cells form the lining of all blood vessels.** In Arteries (left) and veins (right), ECs form the lining of the blood vessel, separating the lumen of the vessel from the surrounding tissue. Smooth muscle cells form exterior to the endothelium which are then surrounded by connective tissue. Original image created using Smart Server Medical Art (https://smart.servier.com/).

monolayer of ECs [2] surrounded by an associated layer of connective tissue, called the basal lamina [8]. Both blood and lymphatic capillaries consist only of this single layer and associated basal lamina. In contrast, all the other vessel types contain additional layers of connective tissue, elastic fibres and smooth muscle cells (SMCs) [8] (Figure 1.2). A tight, coherent sheet of ECs is common to most vessels, maintained by high affinity interactions between intercellular monogenic cell adhesion molecules such as vascular endothelial cadherin (VE-cadherin) [9]. However, in the blood and lymphatic system, the capillary vessels are discontinuous [10]. They have intercellular clefts between their cell-cell junctions which allows for the passage of plasma proteins [11].

1.2.1– The circulatory system

As previously stated, different types of vasculature have distinct functions and hence their cellular compositions differ depending on their physiological role [8]. The blood system forms a continuous, closed circuit of hollow tubes around the body. It acts as a conduit for blood, which is pumped from the heart to every tissue in the body. Arteries carry blood away from the heart and generally carry oxygenated blood (Figure 1.2). They are all branches from the main artery, the aorta, with the exception of the pulmonary artery. The pulmonary artery differs from the rest of the body's arteries as it carries de-oxygenated blood. Blood is pumped at relatively high pressure out of the left ventricle of the heart though the aorta to all parts of the body [4]. The volume of tissue that needs to receive this oxygen rich blood is high, and so the heart must ensure a high pressure is maintained throughout the entirety of the arterial vessels. It does this by ventricular contraction, which traverses throughout the arteries. The pressure is relieved during ventricular relaxation. Arteries must have the capacity to withstand high pressure during systole and low pressure during diastole [4]. Arteries therefore must have thick walls with large amounts of elastic tissue to allow for stretch and recoil. Arteries have an endothelium sat on a basement membrane (tunica intima) that is surrounded by a thick layer of SMCs. These SMCs are sandwiched between two layers of elastic fibres (tunica media). The outer most layer is composed of connective tissue, called tunica externa (Figure 1.3). Their highly elastic properties, along with their large radii, allows for low resistance transport of blood around the body [11]. Low resistance in arteries is desirable to allow oxygenated blood to reach far reaching tissues.

The finest branches of the arterial tree are arterioles [11]. These carry oxygenated blood from arteries and pass it onto capillaries (Figure 1.2). Capillaries are phenotypically diverse, however in general they are composed of just a single cell layer

of ECs, along with a small amount of basal lamina and a few scattered pericytes [4,12] (Figure 1.3). Pericytes wrap themselves around the vessel and perform a variety of functions, mostly involving contraction of the vessel to regulate blood flow and vessel permeability [13,14]. The role of capillaries is to permeate extensive microscopic branches into tissues so that every cell in the body is around 100μm away from a capillary vessel [15]. This close proximity allows for the passage of oxygen and other nutrients across the endothelial lining and into the surrounding stroma before entering parenchymal tissue. Due to their thin vessel wall, blood pressure here must be lower to not rupture the capillary wall. Hence, arterioles are the major site of vascular resistance since they sit upstream of capillaries [11]. Arterioles, like arteries, have a characteristic tri-layer of vessel components; an intima of ECs sat on a basement membrane, a media layer of elastic fibres and SMCs, with collagen bundles, nerve endings and fibroblasts composing of the tunica externa layer [5] (Figure 1.3). These three layers interact in such a way that the radii of arterioles have plasticity. This allows for regulation of mean arterial pressure. Vasodilation of arterioles will increase the volume of the arteriole vessels and allow more blood to pass through them, at a lower pressure. Blood moves more slowly and hence has a longer time to passage solutes through the endothelium and into the surrounding tissue. This response is required during periods of exercise. Vasoconstriction of the SMCs will increase blood pressure due to lowering the radii of the arterioles. This flow resistance is altered via external signals such as metabolic factors, which affect the baseline level of contraction of SMC, known as the intrinsic tone [16]. These signals work by altering the Ca^{2+} within the cytoplasm of the SMCs and thus affecting the motion of their intrinsic myosin motor proteins and length of the actin microfilaments.

After its route through the capillary network, the blood will now be de-oxygenated as it has unloaded all its oxygen and nutrients to tissues on its route around the body. Here, it is collected into venules (Figure 1.2). These are microscopic vessels with the same cellular composition as arterioles however they have a much thinner layer of SMC [17]. The blood pressure here is very low and so additional valves and skeletal muscle contractions are needed to pump the blood to the veins.

Veins collect the de-oxygenated blood from the venules and take it back to the heart via the vena cava, the body's main vein [11]. The pressure difference between the veins and the right atrium, where the blood enters the heart from the venous system, is the driving force for venous return. The pressure is lower in the right atrium than in the veins and hence this gives the blood a potential energy to drive movement [11]. There needs to be very low resistance within the vessel to allow blood to easily flow to the heart.

Their vessel walls are therefore thinner and much more submissive than those of arteries and arterioles. They, too, are composed of an endothelial lining surrounded by elastic layers, smooth muscle layer and connective tissue however all these layers are comparatively thinner to allow for a wider lumen [11]. Once in the right atrium it passes through a tricuspid valve and is pumped into the right ventricle. It is now pumped to the lungs via the pulmonary artery to be re-oxygenated. Composing of a double circulatory system, the blood, having picked up oxygen at the lungs, is looped back to the left atrium at the heart via the pulmonary vein. This is the only vein that passages oxygenated blood. This blood is pumped into the left ventricle, where it is then forced out during ventricular systole.

1.2.2 – The lymphatic system

The lymphatic system is a unidirectional fluid transport system, similar to the circulatory system but carrying lymph fluid rather than blood. It is intimately linked to the circulatory and immune system [11], working in coordination with these two systems independently to achieve whole body homeostasis. It comprises a vascular tree, termed lymphatics, carrying lymph that has been absorbed from tissues and returns it to the circulatory system. The lymphatic system has three main purposes. Firstly, it balances fluid retention in tissues by absorbing excess interstitial fluid that has not been able to pass into the circulatory system across the capillary wall [11]. Secondly, it acts as a filter for the interstitial fluid that is absorbed from tissues. The lymph nodes, lymphatic organs connected to lymphatic vessels, contain immune cells, which are activated upon recognition of any pathogens present fluid passed through them. These immune cells have the capacity to secrete antibodies specific for that pathogen, which are passaged along the lymphatic vessels to the circulatory system and into tissues to help fight an infection [18]. The other function of the lymphatic system is to absorb fats from the small intestine [11].

Afferent lymph is collected by small lymphatic capillaries from interstitial spaces around cells in the body [18]. The capillary vessels merge and are collected in ducts, which lead onto afferent lymph trunks. These are akin to veins of the circulatory system [11]. Lymphatic trunks act as conduits, directing lymph flow towards lymph nodes, away from blood capillaries. The lymph passes through the lymph nodes and is filtered for pathogens. After passing through the lymph nodes, the lymph is now termed efferent lymph, and is drained back into the circulation through the subclavian veins via the thoracic duct and the right lymphatic duct [11] (Figure 1.4).

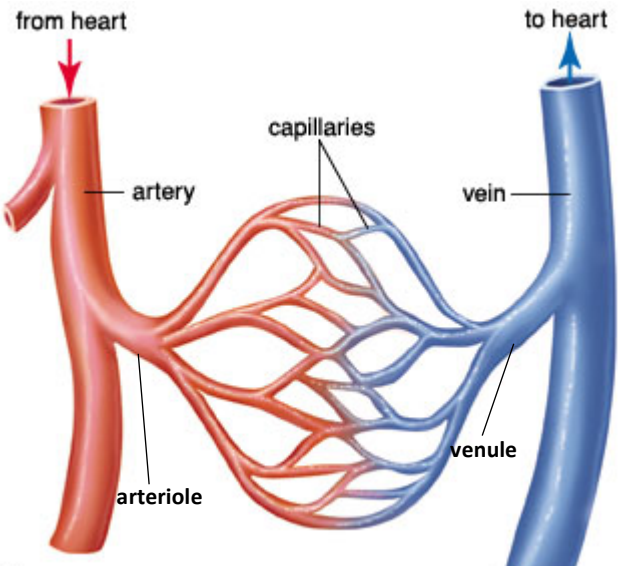

Figure 1.2 – Organisational hierarchy of the blood vasculature. Oxygenated blood flows away from the heart in arteries, the largest vessel type carrying oxygenated blood. Smaller vessels which branch away from these arteries are arterioles. These carry blood into tissues via capillaries, the smallest branches of the arterial tree. Blood here becomes deoxygenated as it diffuses into cells within tissues, and this blood emerges in venules. These are the most finite branches of the venous tree and adjoin to venules. These carry blood to the main branches, veins, which carry the blood towards the heart. Image adapted from Encyclopaedia Britannica.

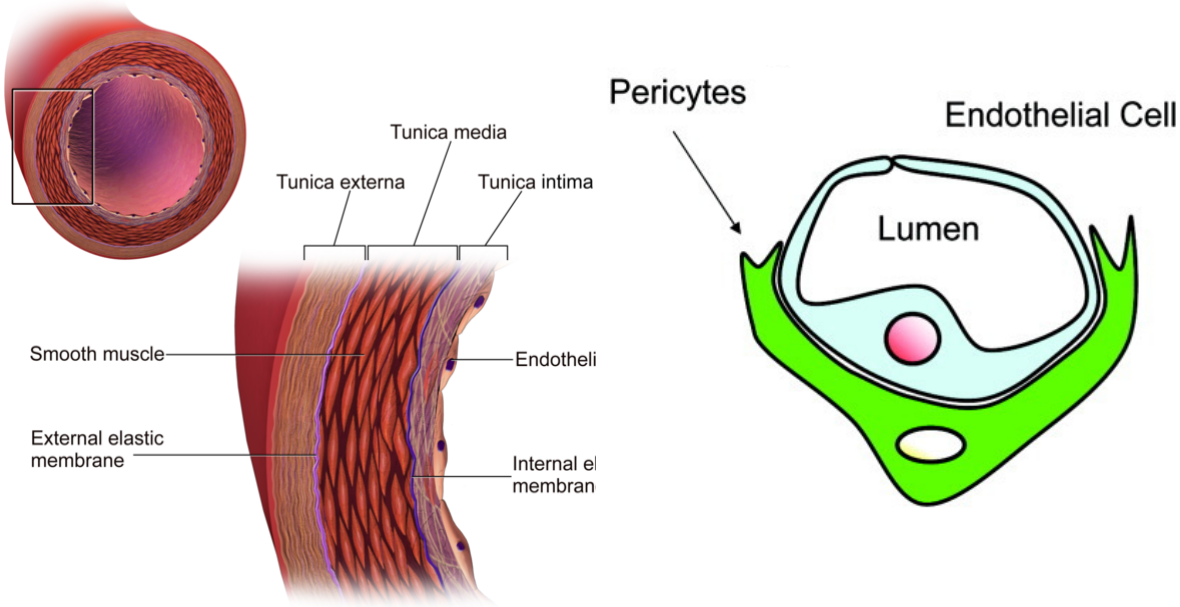

Figure 1.3 – Vessel composition of the blood vasculature. a) Larger vessels i.e. the arteries and veins, have multiple layers of elastic tissue separating the endothelium and its basal lamina from SMCs and the outer layer of fibrous tissue. This gives structural support and ability to contract and recoil. Smaller branches of these, the arterioles and venules, have the same trilaminar structure however these layers are relatively thinner. **b)** Capillaries have minimal layering outside of the EC and basal laminal layer, composing of some SMCs and pericytes. Images adapted from (a) medical gallery of Blausen Medical 2014 and (b) June Sung Lee [82]**.**

Lymphatic capillaries are analogous to continuous blood capillaries in that they are simply a monolayer of non-fenestrated ECs; however, they have a surrounding discontinuous basal lamina. Because of their thinness and connective tissue discontinuity, they have additional anchoring filaments within the vessel to prevent collapse [11]. These present parallel to the longitudinal axis of the lymphatic capillary wall and extend into the surrounding connective tissue. They offer the binding mechanism responsible for joining the lymphatic capillary wall to the connective tissue. Lymph vessels differ from blood capillaries in that they are blind at their distal end and the ECs overlap slightly [11,18]. The gaps perpendicular to the two overlapping ECs allows interstitial fluid to enter the conduit, which can only pass in one direction due to the closed distal end [18]. The capillaries join to collecting vessels, also known as trunks, via pre-collecting vessels. These pre-collecting vessels contain bicuspid valves at irregular intervals, differing from trunks which have similar valves at regularly spaced intervals [18]. This is due to pre-collecting vessels having a discontinuous EC lining, allowing interstitial fluid to enter the vessel. However, they differ from capillary lymphatics as they have SMC in their vessel wall to allow for propulsion of lymph forward [19]. This makes them functionally distinct from both capillary lymphatics and collecting lymphatics in that they both absorb fluids and propel it forwards. Trunks have a continuous EC lining and basal lamina, as well as a layer of smooth muscle cells and collagen fibres. They also contain regular spaced bicuspid valves to maintain the unidirectionality of the fluid flow [18]. Their walls are alike to that of blood vessels in that they are surrounded by one or more layers of SMC, capable of contracting to push the fluid in the anterograde direction, and collagen fibres [19]. The unit of vessel separating two bicuspid valves is called a lymphangion (Figure 1.5).

1.2.2.1 Lymphatic organs

The circulatory system is comprised of vessels, luminal fluid and an organ – the heart. So too does the lymphatics system. Here, lymphatic organs are classified as either primary or secondary organs [19]. The function of primary lymphoid organs is to generate lymphocytes and to allow for their maturation [18]. These organs include the bone marrow and the thymus. The role of the secondary tissue is for further maturation of these lymphocytes and to initiate a secondary immune response via B cell and T cell activation. The constituents of this secondary immune response include the spleen and the lymph nodes [18].

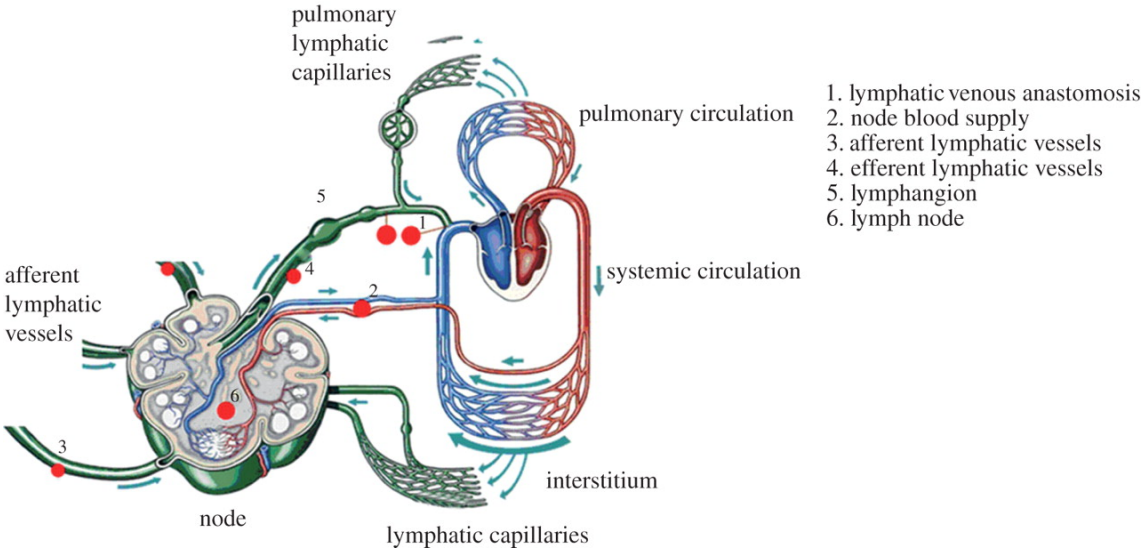

Figure 1.4 - The lymphatic system. Interstitial fluid from blood micro-vessels enters lymphatic capillaries to become lymph. This is pumped along afferent lymphatic vessels and converge at lymphatic trunks, also called collecting vessels. The lymph is directed towards lymph nodes, where it is screened for pathogens. An adaptive immune response ensues if pathogens are detected, and the lymph is passaged back into blood circulation via efferent lymphatic vessels leading to lymphatic ducts and the subclavian vein. Image taken from K. N. Margaris and R. A. Black [18].

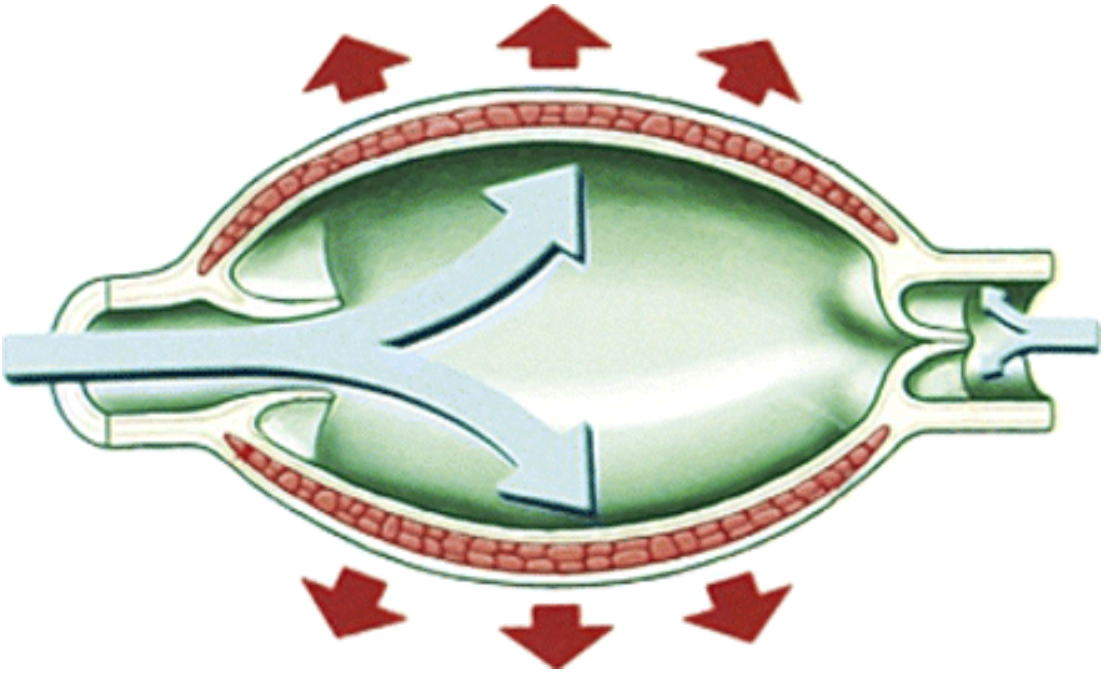

Figure 1.5 – A lymphangion. A contractile unit to propel lymph through lymphatic trunks towards lymph nodes. At either end of the lymphangion are bicuspid valves; these only open in one direction to maintain unidirectionality of lymph towards the lymph nodes and prevents backflow. Outside of the EC monolayer and basal lamina is a layer of SMC and collagen fibres that promote contraction of the unit. Image taken from K. N. Margaris and R. A. Black [18].

1.3 – Endothelial cell lineage

The endothelium is the first organ system to be developed in embryogenesis. Embryogenesis begins with a fertilised egg, the zygote. This zygote is thought of as totipotent [20]; it is a stem cell capable of replicating indefinitely and differentiating into any cell type in the adult human body. This embryonic tissue will go on to form the entirety of tissue in the adult body. As the zygote divides, its constituent cells begin to differentiate [20]. The cells facing the external environment express more epithelial characteristics and become the ectoderm germ cell line. Cells in the centre of the mass of cells forms the endoderm germ cell line, forming the gastro-intestinal tract and its appendages. Mesodermal cells, EC precursors [2], fill the space in between these two other germ line cells. This mesodermal embryonic tissue will go on to develop many internal organs such as the vascular system, skeleton, muscle and connective tissue [2].

On their route to becoming fully matured and specialised ECs, the mesodermal stem cells first differentiate into hemangioblasts at the primitive streak. The primitive streak defines the point at which all three germ cell lines are formed. These hemangioblasts have the potential to form both hematopoietic stem cells (HSCs) and EC precursor cells, angioblasts, respectively (Figure 1.6). To form ECs, the hemangioblasts are stimulated differently than when forming HSCs. These two stem cell lines are multipotent and can only go on to generate blood cells and ECs respectively [21]. The presence of this hemangioblast cell line was discovered nearly a century ago [21] as scientists discovered a simultaneous formation of HSCs and angioblasts at the primitive streak. This coupling was also observed in the equivalent structure in zebrafish, giving further justification to the presence of a common progenitor.

The molecular players involved in the specialisation of mesodermal stem cells into hemangioblasts and then into ECs has since been discovered. A number of growth factors and transcription factors have been identified which promote this differentiation. It seems FGF acts as the ‘time director’ [21], controlling the expression of other growth factors involved in hemangioblast formation. In addition, Runx1 is a transcription factor that acts as a master regulator, binding to DNA promotor regions and upregulating the expression of further hematopoietic transcription factors [21]. These transcription factors are themselves involved in the programming of the cell towards haematopoiesis, for instance upregulating genes for growth factor receptors. VEGF acts as a growth factor that directly influences the development of hemangioblasts. It binds to VEGF receptors present on the surface of mesodermal cells, inducing an intracellular signalling cascade and promoting the differentiation of mesodermal cells into hemangioblasts. Other players that directly promote this cellular differentiation are BMP4 and ZBP-89[21][12]

(Figure 1.6).

The fate of these hemangioblasts is decided via the Renin-angiotensin system. It acts as a switch in directing the differentiation of the hemangioblast either towards HSC or angioblasts. Angiotensin II type 1 binding to its receptor on hemangioblasts directs cell fate towards angioblasts, forming the different EC types. Conversely, Angiotensin II type 2 binding to its receptor directs hemangioblasts towards hematopoietic lineages [21]. Both cell lines are utilised during early development and in adult life, and so the relative progression down each pathway depends on the balance of molecular players of the renin-angiotensin system acting on each. If a cell reaches the angioblast stage, it has a decision whether to form one of three EC types. These different EC types fall within two different specialized vascular systems. These systems compose of blood vessels and lymphatic vasculature. These two systems have distinct functions and so their cellular composition must reflect this [21]; ECs in both systems are specialised. Lymphatic ECs (lECs) form the inner most layer of the lymphatic system, while venous ECs (vECs) and arterial ECs (aECs) provide the division between the blood and outer vessel layers in the blood vasculature.

The first and default status of ECs in vasculature development is vEC formation [12,21]. This EC status is maintained by low Notch signalling, achieved by the inhibition of arterial specific genes, including Notch. (Figure 1.6). In contrast, high Notch signalling, and therefore removal of Notch inhibition [22], upregulates aEC formation, diverging EC development away from vEC. Shh and VEGF signalling act upstream of Notch [22], upregulating its expression and hence maintaining a high amount of it in the developing organism. The final type of EC forms the inner lining of the entire lymphatic system; lECs. To direct angioblasts to lECs, Prox1, Sox18, Syk and SLP-76 are upregulated [22]. These ECs go on to form a distinct circulatory system that is mostly disconnected to the blood vasculature.

1.4 - Formation of vasculature during development

Vasculature development during embryogenesis involves three processes; vasculogenesis, angiogenesis and Lymphangiogenesis. Lymphangiogenesis provides all vascular routes for lymph to flow [23]. Angiogenesis and vasculogenesis, however, account for blood vasculature formation. Blood vasculature carries blood and its solutes, and these two formulative processes are clearly distinct from one another. Major break-throughs have been made in understanding the molecular details of both processes,

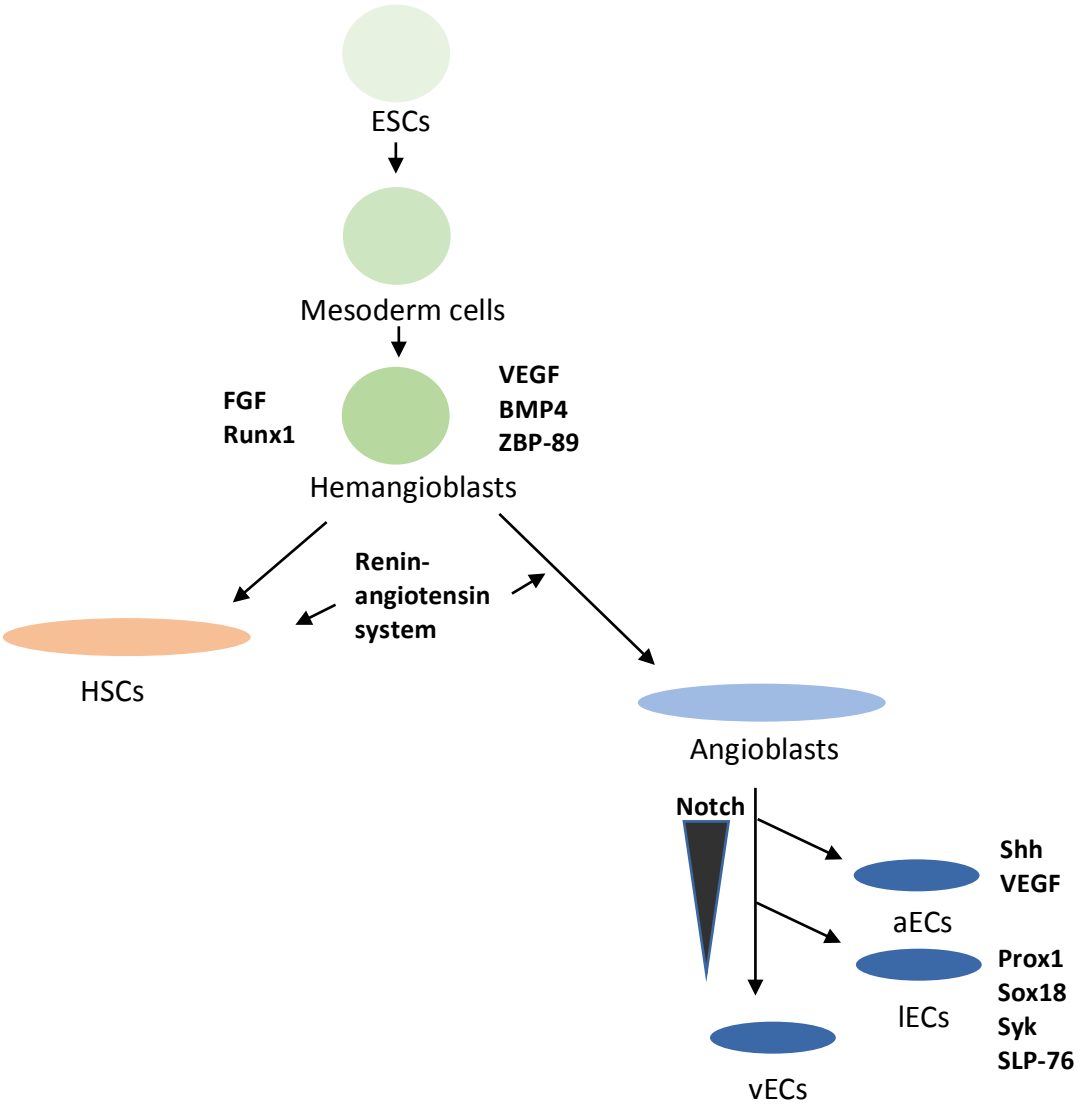

Figure 1.6 - Derivation of the different types of endothelial cells involved in vasculature development. Embryonic stem cells differentiate into the three germ line cells, of which the mesoderm cells go on to differentiate and form many of the internal organs of the body. Mesodermal stem cells are formed in the bone marrow, and then go on to specialise into hemangioblasts after mitogen stimulation. The fate of the hemangioblasts is decided by the renin-angiotensin system, which acts as a switch between HSC and angioblast generation. vECs are the default angioblast derived EC type, generated via relatively low Notch signalling. In contrast, high Notch signalling is maintained in angioblasts to become aECs. Shh and VEGF signalling promote angioblast differentiation into aECs by upregulating Notch signalling. Prox1 and Sox18 are upregulated during lymphatics development to generate vessels with lEC lined lumens. Syk tyrosine kinase and its adaptor, SLP-76, are the main players that promote lymphatics separation from the blood vasculature.

mostly brought about by studies carried out on ‘knock-out’ mice [9]. Vasculogenesis occurs developmentally prior to angiogenesis and is the *de novo* formation of blood vessels in an area previously devoid of vasculature [24]. It is driven by the aggregation of undifferentiated mesodermal cells, which then differentiate into ECs and form elongated tubes. Angiogenesis occurs after vasculogenesis begins, as it is the formation of blood vessels from existing vasculature. Its driving force is the proliferation and migration of ECs, forming elongated tubes [24], directed by a tip EC that has different characteristics to its follower cells. Lymphatic development has characteristics that overlap with vasculogenesis and angiogenesis; selected cells upregulate genes involved in ‘budding’ away from the source of lECs, directed by a mitotic stimulus towards mesenchymal tissue. In all cases of vessel formation, angioblasts are the precursor cells responsible for providing the entire populations of blood vessel ECs. These angioblasts will specialise into the three different types of EC, which undergo separate but distinct processes of development into tubules [25].

1.4.1 - Vasculogenesis

Vasculogenesis is the *de novo* formation of blood vessels and occurs during early embryonic development as well as in the adult [25]. The process of vasculogenesis begins with progenitor cells as described previously. Mesoderm germ cells cluster into aggregates called blood islands, embryonic versions of bone marrow [24], at the primitive streak at day 17 in humans [26]. After receiving secretory factors from the underlying endoderm [27], some of the mesodermal germ cells then segregate into hemangioblastic aggregates. Remaining undifferentiated, mesodermal cells then surround these aggregates, flattening against the core. The hemangioblastic core will then differentiate into primitive blood cells. The encapsulating undifferentiated mesodermal cells will differentiate into hemangioblasts and then angioblasts. In a secondary phase of vasculogenesis these angioblasts will become ECs during further differentiation, which are still surrounding the HSC aggregate [28]. This forms a spherical capillary. The third stage involves these ECs migrating and converging, fusing to form the 3D primary capillary plexus, the initial capillary network in the embryo. During fusion of the cellular plasma membranes, a hollow network emerges with a fluid filled lumen. This system continues to expand during embryogenesis by means of vasculogenesis, and angiogenesis [26]; the sprouting of new vessels from existing capillary vessels. Vessels formed by vasculogenesis will have no SMC layer, or associated pericyes and remains as a simple sheet of ECs for a considerable amount of

time before they form mature vessels [24].

During embryogenesis, vasculogenesis occurs in two distinct and independent sites. The primary site of vasculogenesis occurs in extraembryonic regions (Figure 1.7a). Hemangioblasts within the wall of the yolk sac, an extraembryonic membranous sac lined with endoderm with surrounding mesenchymal cells and derived from the mesoderm, give rise to blood island aggregates. The centre of these blood islands differentiates into blood cells and the exterior of the islands form ECs, which form the vasculature of the early embryo necessary to transport nutrients and metabolites between mother and embryo [28]. The secondary site of vasculogenesis occurs intra-embryonically (Figure 1.7b). Undifferentiated mesoderm germ cells from within the organs of the embryo differentiate into ECs after forming a hollow sphere, which form capillary networks via tubular fusing across the entire body. Hemangioblastic aggregates do not congress in the centre of these ECs.

Capillary fusing during vasculogenesis occurs in two mechanisms [28]. One process of lumen formation involves the intracellular vesicle fusion after ECs aggregation. These fused vesicles will then fuse with the plasma membrane at the point of cellular contact, forming a fluid filled lumen whose membrane is composed of plasma membranes from all cells in the cluster [28]. Another method involves the formation of intracellular lumina, formed from endocytosis of the plasma membrane, within each individual cell. The coalesced vesicles can then form a channel within the cell, and fusion with the tip of each cell will form a continuous lumen throughout the cells in contact with one another [28].

1.4.2 – Angiogenesis

Angiogenesis is a process that involves the growth of blood vessels from existing vasculature. Angiogenesis relies on the presence of existing ECs and hence provides a faster route to blood vessel formation than its partner process, vasculogenesis. It is heavily exploited during embryogenesis where vasculature must develop rapidly for nutrients to deliver to developing tissue, however there must be an initial stage of vasculogenesis to gain a vasculative foothold. Angiogenesis is the main process for vasculature maintenance, and its activity responds to the metabolic activity of the organism [20]. Energy supply to tissues must be equal to energy demand to reach a state of metabolic homeostasis. When the body's demands for nutrients and other components of the blood increases, such as when the body's mass increases, the vasculature must adapt accordingly and increase in volume [20]. During periods of lower

a

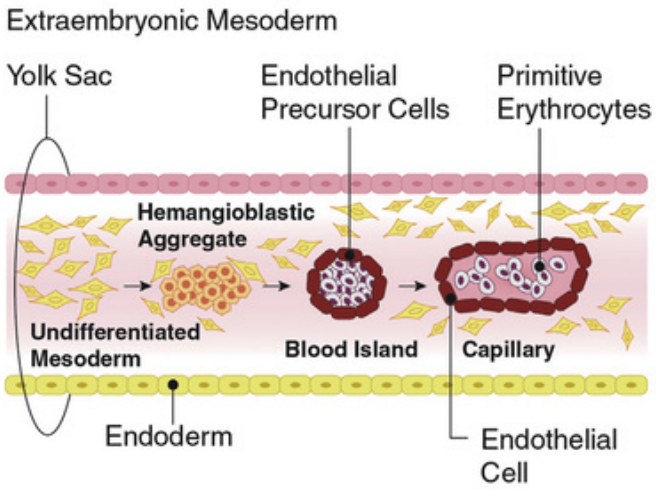

b

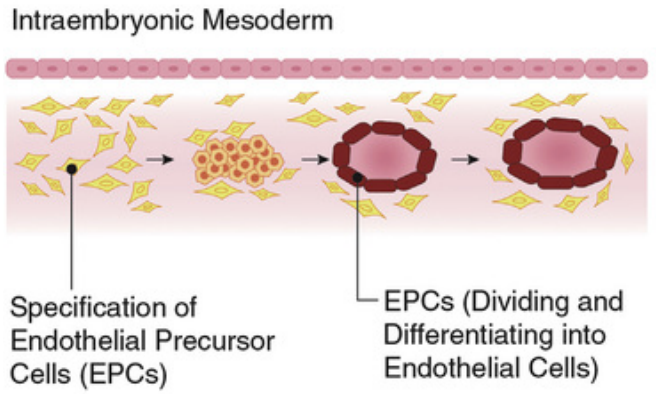

Figure 1.7 – Vasculogenesis. (a) Extraembryonic vasculogenesis begins in the wall of the yolk sac. Mesenchymal germ cells specialise into blood cell precursor cells, which cluster into blood islands. The cells on the aggregate exterior differentiate into endothelial precursor cells, whilst those cells in the core go on to form primitive blood cells. The EC cells proliferate and migrate, forming a capillary plexus. (b) Intraembryonic vasculogenesis involves a similar aggregation of mesodermal precursor cells but these all specialise into hollow tubes of ECs, with no formation of blood cells. This image is taken from J.M. DeSesso. 2006 [83].

metabolic activity, angiogenesis declines and so, too, does vascular density. This association between vascular density and metabolism is relevant to both health and disease.

The angiogenic activity of an organism depends on the balance of different secreted factors released from regions of tissue lacking in sufficient blood supply. Pro-angiogenic molecules will shift the balance in the favour of angiogenesis, whereas anti-angiogenic molecules will do the opposite. The major player in the up-regulation of angiogenesis is vascular endothelial growth factor-A (VEGF-A) [29]. Most frequently it is hypoxia that is the trigger for parenchymal cells, the functional cells of a tissue, to release VEGF-A [30]. VEGFs are potent soluble pro-angiogenic factors that act on ECs to induce an intracellular signalling response. As a result of this response, ECs migrate and align with the VEGF concentration gradient, which coordinates angiogenesis.

1.4.2.1 - Angiogenic factors

VEGF encompasses a seven-part family of molecules, each with a common VEGF homology domain [31]. This core has a cysteine knot motif, the cysteine residues contributing to intra- and intermolecular di-sulphide bonds that occur at one end of the four-stranded β-sheet VEGF monomer [31]. This dimerizes with another monomer to form an anti-parallel dimer [31]. The dimeric VEGF binds to one of three VEGF receptors (VEGFRs) present on ECs. VEGF-A is the best characterised member of the VEGF family. It can undergo alternate splicing to generate four alternate molecules [32], which can bind to heparan sulphate proteoglycans (HPSGs) in the ECM. These molecules have differing numbers of amino acids present after the signal sequence is cleaved from the main body. $VEGF_{189}$ and $VEGF_{206}$ bind to HPSGs via heparin-binding surfaces with high affinity [32]. Conversely, $VEGF_{121}$ lacks this heparin binding surface and hence cannot bind to HPSGs in the ECM. $VEGF_{165}$ has a heparin-binding surface but its affinity is not as high as $VEGF_{189}$ and $VEGF_{206}$.

Epidermal growth factor (EGF) and Transforming growth factor α (TGF-α) are also soluble pro-angiogenic factors. They act to induce proliferation of ECs and have shown to increase angiogenesis *in vivo* [33]. Both these molecules bind to the EGF receptor to induce a signalling response. This signalling response in a cancer cell has been shown to induce cell proliferation, angiogenesis and metastasis [33] giving a similar response to VEGF in these cells.

Anti-angiogenic factors are less well characterised than pro-angiogenic players. They are expressed in normal physiology to prevent excess blood vessel formation, which would be energy costly and unnecessary, and potentially tumourigenic.

Endostatin is a globular protein derived from collagen [34], found naturally in the body. It interferes with the cell cycle; disrupting intracellular signalling cascades resulting in cell cycle arrest and apoptosis [34]. Other factors which act in a similar manner are also fragments of naturally occurring physiological components. Angiostatin is a fragment of plasminogen, a pro-enzyme responsible for degrading inappropriate or old fibrin clots [35]. It is constitutively secreted by the liver in an inactive form [35], which activates on interaction with a fibrin clot. Both collagen and plasminogen are present in constant amounts in the body in normal physiology and so amounts of both the anti-angiogenic factors will be relatively constant. This maintains the balance between the pro- and anti-angiogenic states; angiogenesis only being upregulated when the balance of factors spills more towards the pro-angiogenic side.

1.4.2.2 - VEGF Receptors

VEGFRs are tyrosine kinases, each with seven immunoglobulin-like domains present in the extracellular region and a single pass transmembrane domain separating the extracellular region from the intracellular kinase domain [36]. Tyrosine kinases, on binding their substrate, hetero or homodimerize leading to the autophosphorylation of their C-terminus and the initiation of an intracellular signalling cascade. VEGFR-1 and VEGFR-2 are the predominate VEGFRs present on vascular ECs [31] and so are the most important VEGFRs in angiogenesis in later stages of an organism's development. Their molecular weights are 180 kDa and 210 kDa respectively. VEGFR-3 is expressed on vECs during embryonic development [31] and so is important for neovascularisation in early development. VEGFR-1 and VEGFR-2 are upregulated in tumour cells, as is VEGF [37]. VEGFR-2 interaction with VEGF is thought to be the main driving force for angiogenesis. Recent findings have suggested that VEGFR-1 and -2 are present in different amounts at the apical and basal surface of neural microvascular endothelial cells (MVECs) [38]. VEGFR1 having a greater distribution at the apical surface, and VEGFR2 present in greater amounts at the basal surface. This polarisation is the result of VEGFR-1 and -2 having distinct functions within their tissue microenvironment; VEGFR-1 induces a cytoprotective response and VEGFR-2 causes an increase in vascular permeability [38].

1.4.2.3 - Invasion and migration

The EC that senses the highest concentration of VEGF via its binding to VEGFRs on the EC (mainly VEGFR1 and -2) becomes the pioneering tip cell [32], and displays a relatively much greater number of VEGFRs on its surface [30] (Figure 1.8). These are presented on long filamentous projections from the plasma membrane called filopodia [39]. Intracellular cascades take place when VEGF-A binds its receptor, involving the secretion of large amounts of proteolytic enzymes from the filopodia important for digesting the surrounding stoma. The local concentration of VEGF-A is detected by the receptors, which can sense the gradient of VEGF and align itself to the area of highest concentration [30]. Integrins are presented along the filopodia membrane, which bind to the underlying substratum and generate traction. Contraction of acto-myosin fibres within the cell that are bound to these cell-ECM junctional complexes pulls the tip cell towards the stimulus. Cell-ECM contact complexes present at the rear of the cell must be endocytosed and recycled for the rear to be pulled up along with the front of the cell. The cell rolls over its integrin complexes generated at the leading edge of the cell and there is productive movement forward. Simultaneously, cells behind the tip cell proliferate as they follow the leader cell; they must retain their cell-cell junctions for a continuum of ECs to be created, which becomes the endothelial stalk. This tip-stalk morphology is dependent on Delta-Notch signalling; the activation of VEGFRs in the tip cell induces Delta-like-4 (Dll4) expression [39,40]. This cell bound factor then binds and activates notch receptors present on the cell membrane of stalk cells. This represses expression of VEGFR2 on the stalk cells, making them less responsive to the VEGF-A gradient and hence less migratory relative to the tip cell [39,40].

1.4.3 - Lymphatic system development

Lymphangiogenesis, lymphatics system development, occurs early on in embryogenesis and involves both angiogenesis and vasculogenesis [26]. Venous precursor cells in the embryo are the prerequisite for lymphatic development [41]. In a step-wise process and beginning with vECs, lECs are formed from the differentiation of vECs which then bud out to form lymph sacs. Lymph sacs are initial lymphatic structures from which the lymphatic vasculature stems from [42]. During development these sacs remodel into tubules, which permeate surrounding tissues and organs.

Early in embryonic development, PROX1 homeobox gene expression is upregulated in a subpopulation of vECs at the cardinal vein (CV) (Figure 1.9). PROX1 is

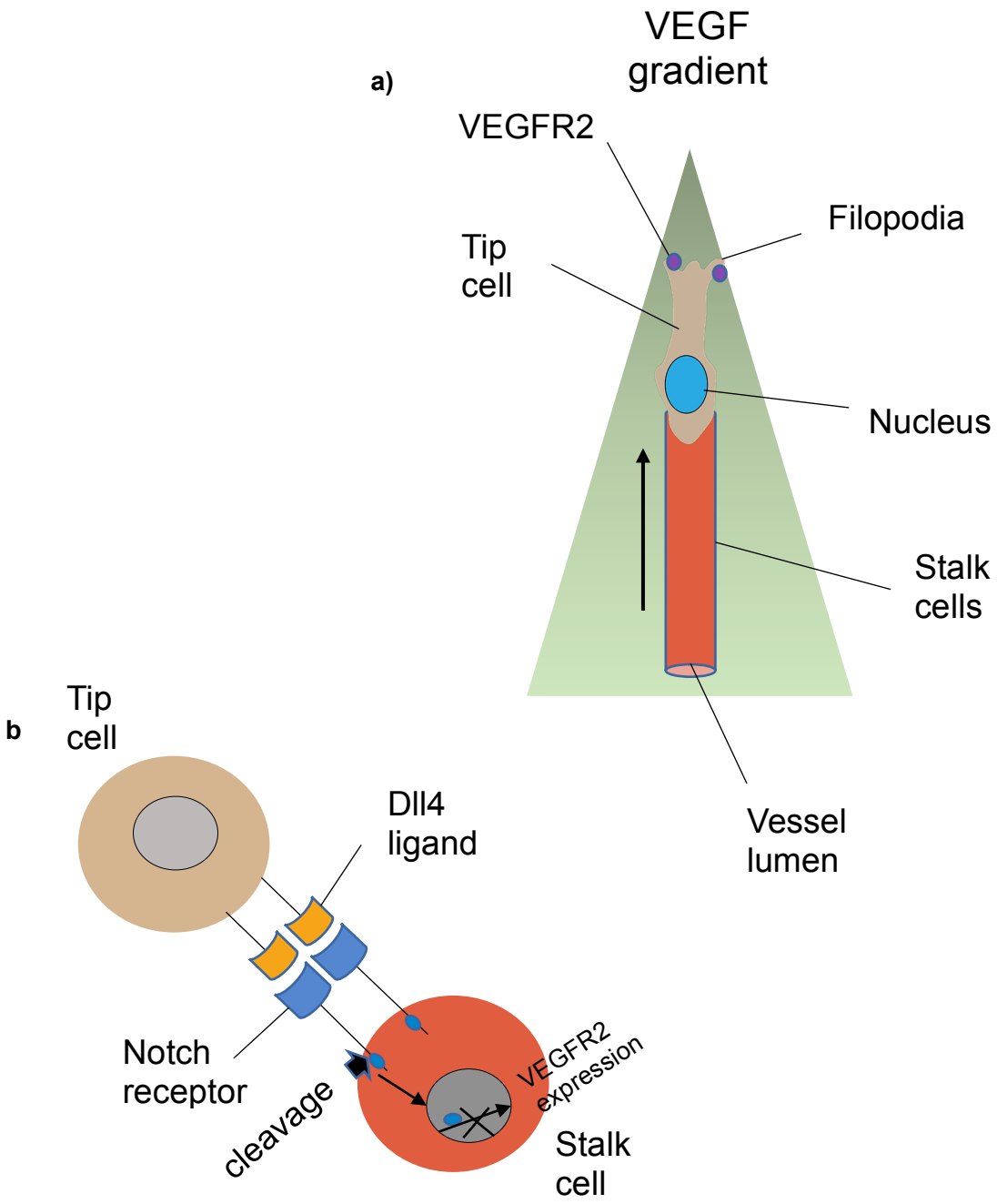

Figure 1.8 – Selection and auto-promotion of tip cell during angiogenesis. a) The tip cell migrates towards the area of highest VEGF-A concentration, complementing this gradient by expressing a higher concentration of VEGFR2s. Both concentrations are gradiented with low concentrations of VEGF-A accompanied by low concentrations of VEGFRs on the stalk cells. b) Tip cell selection replies upon Delta-Notch signalling. Activation of Notch receptors on stalk cells results in its proteolytic cleavage and release of its intracellular domain. This is transported to the nucleus and represses genes for VEGFR2, inhibiting tip cell characteristics.

a transcription factor heavily involved in lymphatics development and SOX18 and COUP-TFII, expressed by blood ECs at the CV, are responsible for Prox1 expression [41]. This is the commitment stage for vECs to become lECs, which now become lEC progenitors. PROX1 expressing ECs start to bud from the CV in a polarised manner [43]. Budding migration away from the CV requires mitogenic stimulation of the lEC progenitors. VEGF-C is expressed by mesenchymal tissue in a gradiented manner to bind to its receptor, VEGFR-3, present on the surface of the lEC progenitors. VEGFR-3 expression is maintained by PROX1, and binding of its ligand allows the alignment of lECs towards avascularised tissues. The interconnected budding of the lECs continues until they assemble together into lymph sacs. These sacs are intermediate structures and are the main source of lECs required to form the entire lymphatics system [41]. They are luminal structures with a monolayer of lECs, similar to structures formed during vasculogenesis. As with vasculogenesis, lumen formation occurs when intracellular vacuoles formed by endocytosis coalesce and form a channel through interconnected cells. During the formation of this structure, there is separation of the circulatory and lymphatic systems [43]. These lECs then proliferate and sprout away from the intermediate structure to form the entire lymphatic vasculature, utilising angiogenesis. lECs migrate towards mesenchymal tissues in a continuous fashion, the individual cells joined to each other via VE-cadherin adhesion junctions [41,44].

Not all lECs expressing PROX1 bud from the CV; a small subpopulation of cells does not express VEGFR-3 and hence are not migratory. These cells remain in place and form the connective lymphovenous valves between the lymph sacs and adjacent veins [41]. These valves are connective apertures and are continuous with the vECs of the vein, forming a double layer of lECs being present underneath a layer of lECs continuous with the lymph sac. They allow for a conduit of lymph to enter the blood stream via subclavian veins whilst preventing the reflux of blood into the lymphatics system [41]. The molecular mechanism of separation of the two vascular systems still remains unclear, however it is well established that platelet activation is a key stage in the process. Several molecular players have been shown to be involved in the activation and aggregation of platelets crucial for separation of the lymphatic and blood vasculatures, including podoplanin (PDPN) [41]. PDPN is expressed by budding lECs, suggesting a potential signalling route for vascular separation from lEC budding. Besides PDPN, Syk tyrosine kinase and its adaptor, SLP-76, are the main players that promote lymphatics separation from the blood vasculature and are expressed mainly by circulating haematopoietic cells [43].

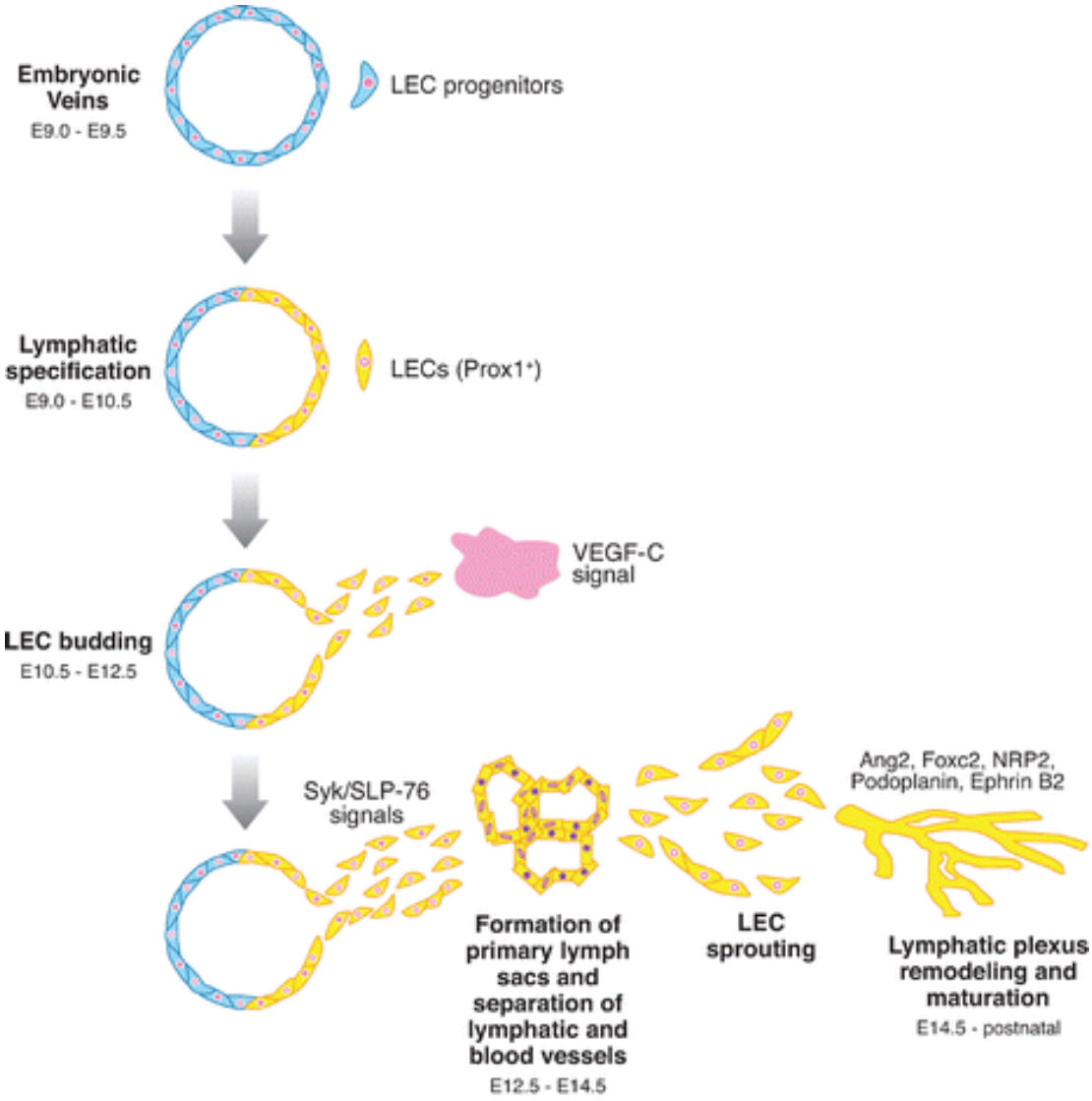
Embryonic Veins
E9.0 - E9.5
LEC progenitors
Lymphatic specification
E9.0 - E10.5
LECs (Prox1+)
LEC budding
E10.5 - E12.5
VEGF-C signal
Syk/SLP-76 signals
Formation of primary lymph sacs and separation of lymphatic and blood vessels
E12.5 - E14.5
LEC sprouting
Ang2, Foxc2, NRP2, Podoplanin, Ephrin B2
Lymphatic plexus remodeling and maturation
E14.5 - postnatal

lECs continue to proliferate and migrate, expanding the lymph sacs into the surrounding mesenchymal tissue. The lymphatic vasculature quickly expands throughout most of the developing embryo [43]. During maturation of this vasculature, the lECs must further differentiate into specialised lymphatic structures, such as collecting lymphatic vessels or lymphatic capillaries [41]. As embryonic development progresses, the lymphatic vasculature begins to express different gene products in a step-wise manner [43]. Collecting lymphatics downregulate their markers for lymphatic capillaries, namely PROX1, VEGFR-3 and LYVE1. They also upregulate genes to secrete ECM and induce SMC migration and proliferation to cover the vessels. Collecting lymphatic cells that form bicuspid valves however maintain their expression of PROX1. The interaction of ECM components with ECM receptors, such as fibronectin with integrin α9, contributes to the development of lymphatic vasculature. Similar to vasculogenesis and angiogenesis, additional guidance cues are needed as well as the VEGF family [43]. Sema3a, a neuronal axonal guidance protein, binds to the receptors Nrp1 and Plxna1 present on the collecting lymphatic vessels and lymphatic valves [43]. This is crucial for proper lymphatic vessel and valve development. In addition, ephrin signalling is required for vessel development and maturation. Ephrin B2 interaction with its Eph receptor on the lymphatic vessels stimulates specialisation of the vessels into collecting vessels [43].

1.5 – Endothelial cell functions

Primitive concepts of ECs were basic and underappreciated. The endothelium was merely seen as an inert lining of blood vessels, providing a protective and non-adherent barrier between the blood and surrounding tissue [4] that is involved in transport of substances across. Key observations taken in recent decades have shown that the endothelium lies at a hub of homeostasis [17], being involved in many key physiological processes. Serving as an interface between the blood and lymph and surrounding stroma, it controls the passage of substances between the two bodies. Thus, it controls the uptake of nutrients and disposal of waste products, as well as the initiation and regulation of inflammation [4]. The volume of luminal fluid passing through any particular area of the capillary network varies in accordance to physiological requirement, and these changes are brought about via vascular contraction or dilation. The endothelium behaves like a middle-man, controlling vascular tone in response to signalling factors present in the luminal fluid. If the endothelium is damaged or it detects damage to the

surrounding stroma, ECs are responsible for eliciting a blood coagulative response to avoid excessive blood loss from the circulation. Simultaneously, the tissue is induced into a state of repair before the blood clot is dissolves to return the vasculature to normal functioning. A new capillary network may be needed to complete tissue repair, which is intimately dependent on the detection of, and response to, various signalling molecules by ECs. Formation of the initial and dynamically changing vasculature network is also reliant on the action of ECs.

The microvasculature in different parts of the body are composed of organ-specific ECs, which have differentiated to become morphologically and physiologically distinct from one another [12]. Every organ in the body has its own unique functions, which are dynamic and versatile depending on both systemic and local environmental changes. Their vasculature must reflect this as they serve as the gatekeeper controlling organ microenvironments by forming an interface between the circulation and surrounding tissue. Their functions, therefore, differ depending on their organotypic micro-environment. The endothelium must be adaptable and responsive to the requirements of that particular organ [12]. In this way, they are responsible for many physiological functions, and their dysfunction is implicated in many pathologies.

1.5.1 - Transport of nutrients

The selective transport of molecules between the blood stream microvasculature and extravascular interstitium is reliant on the extent of the integrity of the endothelium. The continuous architecture of the endothelium, held together by tight junctions, generates a barrier-like function that exists ubiquitously in the human body [12]. While this is true for most vasculature, ECs in capillaries form three different types of endothelium, each with different functions.

Continuous non-fenestrated capillaries form a secure, fence-like sheet that only permits the diffusion of water, small solutes and lipid-soluble molecules across their endothelial lining [12] (Figure 1.10). Larger fluid components, such as plasma proteins and circulating cells, cannot pass through and remain in the blood stream. Larger components of the blood that are required by tissues to metabolise, such as amino acids, pass through the endothelial monolayer via transcytosis by selective transporters on the monolayer's cellular surfaces [4]. These are regulated by specific mediators such as insulin, nitric oxide (NO) and hypoxia induced factors, and the expression of these transporter molecules reflects the metabolic requirements of the subendothelial tissue. A specialised form of the continuous endothelium is the blood-brain barrier (BBB) in the

central nervous system (CNS) [12]. Neuronal cells do not have the capacity to replicate, and as a result are more vulnerable to pathogenic and other blood-borne toxins and fluctuations in blood constituents. The death of many cells in the CNS would be catastrophic to the health of an organism and could result in severe neurological diseases such as Alzheimer's disease. The micro-vasculature in this tissue must therefore tightly regulate the movement of ions, molecules and cells between the intra- and extra-vasculature regions. Capillaries in the CNS exclude pathogens, toxins, drugs and most other large molecules [12]. Aside from specialised tight intercellular junctions, ECs that make up the BBB have surrounding layers of pericytes and astrocytes [45]. Pericytes have long extensions of their cellular body which contact the abluminal surface of the capillary ECs at discrete points, however most of their body is embedded in the basal lamina surrounding the vessels. They contain contractile proteins, allowing for the regulation of the capillary diameter via cellular contractions/dilations [45]. Astrocytes are star-shaped glial cells that, among other functions, biochemically support the endothelium within the CNS. They promote barrier functioning of the BBB and make up a cellular link between the blood vessels and the electrochemistry of the neuronal system. They too have long polarised extensions that cover the blood vessel and pericyte fibrils. This coupling of the vasculature and CNS allows for vessel diameter regulation via contraction/dilation of the surrounding pericytes [45].

The intercellular tight junctions as well as surrounding cellular sheath around CNS capillaries that expel many molecules needed by neuronal cells means that extracellular transport systems are required. Highly specific transporters present on the EC plasma membrane import nutrients from the blood down their concentration gradient and traffic them into the CNS for cellular metabolism. These transporters are highly specific for their substrate, many of which are solutes. ECs in the CNS are highly enriched in glucose transporter 1 (GLUT1) at their apical surface, transporting glucose into the brain parenchyma from the blood [45]. Cerebral tissue is highly reliant on glucose as its source of ATP, relative to other sources of energy storage, and so this transporter is highly expressed on its micro-vasculature. Fulfilling 8-10% of the brain's energy requirements, lactate also plays a critical role in neuroenergetics [46]. It is able to enter the cerebrum via the monocarboxylate transporter 1 (MCT1), present at the apical cellular surface, which can traffic other monocarboxylates across. Lactate can be fully oxidised within brain cells during the TCA cycle after being converted to pyruvate by lactate dehydrogenase, generating 30-36 molecules of ATP [46]. During periods of hyperlacticaemia, such as during moderate to intense exercise, lactose may provide up to 25% of the ATP in cerebral cells [46]. The rate of lactose uptake and oxidation

increase, substituting for glucose uptake and oxidation so that it can be utilised to a higher extent in muscle cells. Transporters are also required to necessitate the traffic of amino acids across the BBB. LAT1 is responsible for the influx of large neutral amino acids [47], such as tryptophan and tyrosine, important for anabolic processes within the cell as well as catabolic metabolism during cellular starvation. Several pharmaceutical drugs are also substrates for this receptor [47], including L-DOPA, a precursor molecule to important neurotransmitters such as dopamine. L-DOPA is commonly used in the clinical treatment of Parkinson's disease. Drug delivery across the BBB is limited due to the tightly regulated cellular permeability, and so pharmaceutical drugs that complement luminal receptors are the main way of introducing a cerebral cellular response. In contrast, CAT1 transports cationic amino acids across the BBB into cerebral tissue. Other membrane receptors include the transferrin receptor and low-density receptor-related lipoprotein, among others. Receptors required for efflux of waste products generated from cellular metabolism are also apically localised in neural cells [45].

Fenestrated capillaries differ from continuous non-fenestrated capillaries in that they have intracellular pores joined by diaphragms [12] (Figure 1.10). The purpose of the diaphragm is to speed up the exchange of water and allow the passage of solutes that would not otherwise pass through a continuous capillary due to size restrictions. Small peptides can pass between the blood and interstitial fluid, making these vessels suitable to provide vasculature for tissues such as endocrine organs and the intestinal tract. Hormones enter the blood stream from endocrine glands to elicit systemic cellular responses. The extent of hormone secretion into the blood stream is partly controlled by the number of ECs and associated fenestrae. EC coverage is controlled by VEGF secretion, with VEGF binding to VEGFR2 and eliciting a signalling response that promotes EC proliferation and migration. VEGF, in turn, is upregulated in endocrine glands by hormones such as TSH, ACTH and FSH. These act to increase transcellular transport by increasing the number of ECs and intact fenestrae. Reducing the secretion of hormones into the blood stream involves low levels of stimulating hormones, reducing the number of ECs and fenestrae.

Sinusoidal capillaries have characteristic irregular shaped ECs and intracellular gaps with an incomplete basal lamina [12] (Figure 1.10). These gaps create conduits for cells and large molecules between the blood stream, lymph and interstitial fluid. Such access to vasculature lumen is utilised in an immune reaction, where an adequate response to infection relies on the production and secretion of immune cells. These cells are made in the bone marrow and mature in secondary lymphoid organs (SLO) [18]. To reach the area of pathogenic infection, these cells must be able to exit from SLOs via

efferent lymphoid vessels and enter capillaries via passing through the interstitial space. The open pores in the endothelial lining allows white blood cells, such as lymphocytes, to exit from the lymphatics and passively enter the circulatory system. Sinusoids are also present in the spleen, liver and several endocrine organs such as the pituitary gland. This type of capillary is involved in processes that require rapid physiological responses, as so it is the organisms best interest to have maximal exchange of components between the capillary lumen and surrounding interstitial fluid. The flow of blood to the sinusoids is slower, allowing a greater amount of time for fluid constituents to pass the EC barrier.

1.5.2 – Haemostasis

Maintenance of fluid, circulating blood around the blood vasculature is essential for normal physiological functioning. Blood must be fluid enough that it can be pumped around the body at an optimal rate that does not cause too much strain on the heart and vascular muscles. However, to prevent excess blood loss when a blood vessel is damaged, blood in the local environment must alter its viscosity and form a blood clot around the site of injury. This is haemostasis. In the normal physiological state, there is a careful balance of hypercoagulability and hypocoagulability in the blood [48]. Imbalances in this equilibrium results in pathological disorders. Some of these disorders are mainly caused by endothelium dysfunction; ECs, under normal physiological conditions, provide an antithrombotic surface to prevent inappropriate clot formation [4]. Inappropriate activation of the clotting cascade results in a thrombus (blood clot) which may block the vessel in which it was made. On the other hand, if the endothelium is deficient in a component of this same cascade, failure of coagulation may occur which makes blood loss a more likely and severe event [7].

The endothelium forms an interface between the blood and tissues. It is strategically located so that it can interact with components of the blood to regulate its haemostatic balance, while detecting loss to its own integrity. There are two main stages to haemostasis [7]. An initial plug is formed to quickly and temporarily block the site of endothelial lesion. This is made entirely of platelets – anucleate cell fragments that circulate inactive in the blood. These are activated on stimulation by components released by the damaged endothelium and adhere together and to the site of injury to form a plug. Secondary haemostasis serves to form a stable mesh of red blood cells and insoluble plasma proteins around the platelet plug, initiated by the conversion of soluble proteins into insoluble fibres.

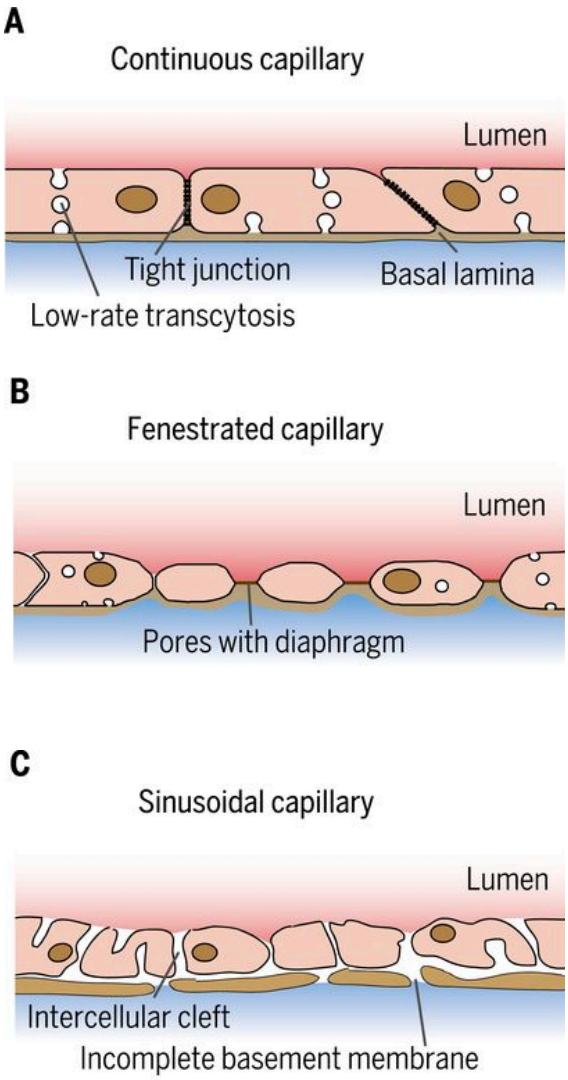

Figure 1.10 - Three major types of capillaries. (A) Continuous capillaries, mainly present at the BBB in the CNS, have tight cell-cell junctions and a continuous basal lamina to prevent the free passage of large molecules. Transport of anything that isn't water, small solutes or lipid soluble molecules can only pass though via regulated transcytosis. (B) Fenestrated capillaries have gaps in the EC monolayer, but which are covered with a diaphragm. There is still a continuous basal lamina and so there is not free passage of all molecules, however some peptides are able to cross these capillary networks. (C) Sinusoidal capillaries have complete intercellular clefts, made by intercellular gaps and a discontinuous basal lamina. This allows free passage of molecules, as occurs in the spleen to allow rapid movement of immune cells into the blood circulation. Image taken from H. G. Augustin and G. Y. Koh. 2018 [12].

1.5.2.1 - Primary haemostasis

Seconds after EC damage, platelets activate and begin to adhere together and to the site of damage [4]. Their activation relies upon stimulation of receptors on their surface. Collagen is the ligand for the GPVI receptor, present on the surface of platelets. However, as it exists in the subendothelial tissue, it is only available to bind upon subendothelial exposure during endothelial injury. The binding of collagen to GPVI activates the platelets, which undergo a morphological alteration from a small, disc-like shape to a more elongated shape with long, fibrillar membrane extensions. As well as changing their shape, the platelets expose integrins on their surface, which are able to bind to multiple ligands causing platelet aggregation and ECM adherence [49]. The most important integrin is αIIbβ3, which binds several subendoethelium components such as fibronectin, collagen, vitronectin and fibronectin as well as von Willebrand factor (vWF) [7]. This forms an expansion of platelet-platelet and platelet-endothelium adhesions [7]. Another receptor important for platelet activation is GPIb-IX-V, which binds to vWF via its GPIbα domain. vWF is a large multimeric adhesive glycoprotein complex that is stored in an immobilised manner in the cytosol of ECs, in organelles known as Weibel-Palade bodies (WPBs). It is also stored in this way in α-granules inside platelets themselves. vWF is stored as highly compact tubules, essential for physiological function of the factor [6]. On endothelial injury, these WPB expose vWF, which rapidly unfolds into ultralong strings that dock and bind to adhesive molecules on the endothelium and platelets. This forms a network of adhesions between platelets themselves and between platelets and the endothelium. Its release from α-granules is triggered by several agonists such as collagen and thrombin, revealed upon endothelial damage [6][7].

1.5.2.2 - Secondary haemostasis

This secondary process composes a complex, sequential activation of clotting factors present in the blood plasma [18]. These are serine proteases, synthesized in the liver, which circulate in the blood in an inactive form. An intact endothelium prevents the activation of these factors as it presents anti-coagulants on its surface. Thrombomodulin present on normal ECs binds to thrombin, and this complex binds to and activates protein C. Protein C acts as a serine protease, cleaving and inactivating crucial prothrombotic factors involved in clot formation. The binding of thrombin to thrombomodulin also acts to convert thrombin from a procoagulant to an anticoagulant

[11]. Furthermore, HPSGs on EC surfaces prevent platelet aggregation, stopping the progress of the initial platelet plug and hence the platform for secondary haemostasis. Heparin also stimulates the activation of antithrombin to inactivate any thrombin that is not in a complex with thrombomodulin [7]. In the event of exposure of the subendothelium to plasma components, prothrombotic plasma factors activate. Two pathways exist, one activated by factors intrinsic to the plasma and the other extrinsic, which result in the activation of factor X, converting prothrombin to thrombin [4]. Thrombin cleaves the soluble plasma protein fibrinogen to form insoluble fibrin. These polymerise to form long strands creating a mesh-like web of insoluble fibres that can trap cells and other blood constituents. The localised exposure of subendothelium ensures that both the extrinsic and intrinsic clotting pathways occur only at the site of endothelial damage [11]. When the endothelium has been fully repaired, it reverts back to an anticoagulatory state and further clotting is prevented. The original clot is dissipated by plasmin, activated from its zymogen plasminogen after exposure to blood clots, which degrades the fibrin mesh [11].

1.5.2.4 – Inflammation

Inflammation is a physiological response to injury caused by a multitude of agents and is part of the innate immune reaction [17]. This is a rapid response system, which uses non-specific methods of pathogen recognition. Inflammation has evolved in higher organisms to contain and eliminate the agents which caused the tissue damage and to remove any damaged and dead tissue. It also provides a route for regenerative agents to heal the region of injury and restore normal tissue architecture [49]. There are four main characteristics of inflammation; redness, heat, swelling and pain [17]. A fifth distinction is loss of function of the inflamed area, described later than the other characteristics and caused by spatial restrictions brought about by the swelling and/or pain preventing proper movement. These distinctions are the direct consequence of the inflammatory process. The main objective of inflammation is to increase blood flow to the area of injury to allow for mass movement of immune cells and agents across the endothelium and into the surrounding tissue. The endothelium is the interface between these immune cells and site of injury, and hence has a major role in the inflammatory process. All the cellular responses that occur during acute inflammation are the direct result of EC activation [49]. ECs serve to recruit leukocytes to the area of infection and regulate their behaviour and activity by releasing cytokines and growth factors. Adhesion molecules expressed on ECs allow the diapedesis of immune cells across the

endothelial lining and into the tissue to carry out their function [17].

Inflammation is first triggered directly through pathogen recognition by immune pattern recognition receptors (PRR), or indirectly by complement cascade activation. This is a system of plasma proteins which sequentially activate after immune interaction with a pathogen [50]. The resulting activated molecules, C3 and C5, are cleaved into C3a and C3b, and C5a and C5b respectively. C3a together with C5a activate a local inflammatory reaction via mast cell degranulation [11]. Conversely, mast cells can directly recognise pathogens using their PRRs, such as Toll-like receptors (TLRs), which evokes a signalling cascade resulting in their degranulation [51]. This degranulation releases cytokines such as TNF-α, CXCL10, IL-8, histamine as well as prostaglandins and leukotrienes [51]. These agents are released into the interstitial space, which act upon local ECs to upregulate the secretion of adhesion molecules to the apical surface.

The recognition of the site of extravasation by immune cells is brought about by these adhesion molecules, which act sequentially to mediate leukocyte contact and migration through the vascular wall [17] (Figure 1.11). These adhesion molecules are coordinated by several chemical mediators, such as chemokines, and are present to promote leukocyte rolling, tethering and capture prior to trans-migration through the EC wall. Initial tethering is brought about by members of the selectin family [17]. L-selectin is constitutively presented on almost all leukocytes, while E-selectin is presented on ECs and P-selectin on platelets and ECs only after cytokine stimulation. L-selectin binds to sulphated sialomucin groups [52] on the ECs during their routine vascular rolling, a process that enables chemokine detection. They have a glycocalyx rich in proteoglycans which tether these chemokines in place to allow their presentation to the rolling leukocytes. When EC's detect chemokine stimulation, they present P-selectin and/or E-selectin on their surface. These bind to P-selectin glycoprotein ligand-1 (PSGL-1) and E-selectin ligand-1 (ESL-1) respectively [52]. This is tighter binding than the initial interaction between L-selectin and EC glycoproteins and allows time for receptors on the surface of the leukocytes to sense chemokine gradients from ECs at the site of injury.

The interaction between the leukocyte and EC cell adhesion molecules, as well as presentation of chemokines to the leukocyte, causes activation of the leukocyte. LFA-1 and $\alpha_4\beta_1$ integrins on the surface of the leukocyte undergo a conformational change, from an inactive closed conformation to an open, active state displaying the ligand binding domain, the I domain [49]. This reaction is brought about by inside-out signalling where receptor-ligand binding triggers a signalling response inside the cell [50]. The

binding of integrins is much higher affinity than with selectins, and as a result the leukocytes are pulled towards the vascular endothelium much more tightly [52]. Activation of ECs by various chemokines also upregulates the expression of E-selectin, and ICAM-1 and VCAM-1. The latter are cell adhesion molecules, which bind complementary molecules on leukocyte membranes. Simultaneously, there is an increase in vascular leakiness brought about by contractions in EC actin filaments attached to tight and adherans junctional complexes [49]. This contraction is caused by the docking of neutrophils, via integrins, and pulls the cell-cell junctions away from each other, opening intracellular gaps and allowing plasma proteins and leukocytes to enter the interstitial fluid. The leukocytes are further directed through these inter-cellular gaps via platelet/EC adhesion molecule-1 (PECAM-1) [52], a protein present on ECs, leukocytes and platelets. It is evenly distributed on leukocyte cell membranes, but only at the lateral boarders of ECs to form cell-cell adhesives. Hence it is involved in guiding these leukocytes through the intercellular gaps during diapedesis. Once past the endothelial lining, leukocyte migration through the underlying stroma is reliant on matrix proteins binding to leukocyte adhesion molecules.

In the interstitial space, these immune cells destroy invading pathogens and clear away debris by means of phagocytosis [17]. They have chemokine receptors on their surface which detect a chemokine concentration gradient. These chemokines are released from damaged cells and hence guide the immune cells toward them [53]. Antibodies and complement can also cross the endothelial wall contained within blood plasma, helping to opsonise pathogens and enhance inflammation. The capacity for immune activity is greatly enhanced by vasodilation of the capillary network around the site of damage. This is brought about by histamine and prostaglandins, acting on SMCs surrounding blood vessels near the region of tissue damage. If the region is healed successfully and functionality is restored to the tissue, the inflammatory response diminishes as there is no further release of chemical mediators. However, if the abnormal conditions persist post the acute inflammatory response, the process persists and the repertoire of immune cells migrating to the tissue changes. Cells of the adaptive immune response replace leukocytes, including effector and memory T cells. If this response fails to clear the infection, inflammation persists, gaining a different set of characteristics than before [54]. The tissue enters a state of chronic inflammation in which there is continual tissue damage and repair, caused as a consequence of the elevated and prolonged inflammatory response [54].

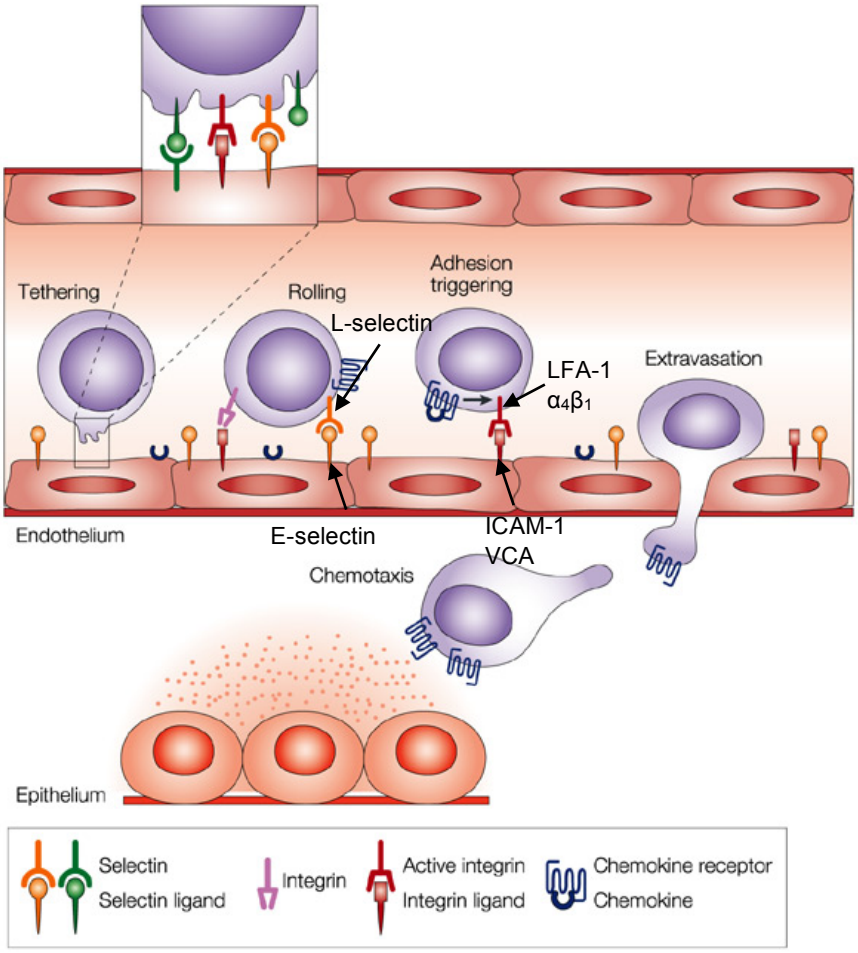

Figure 1.11 – Leukocyte extravasation. Pathogen detection results in mast cell degranulation and macrophage activation, leading to release of pro-inflammatory mediators. This activates ECs, which upregulate their expression of selectins on their luminal surface, which can bind their ligands that are constitutively present on the surface of neutrophils. This results in an intracellular signalling cascade within the neutrophil, resulting in a conformational change in their transmembrane integrins, which open into an active conformation. Activation of ECs by pro-inflammatory mediators upregulates expression of ICAM-1 and VCAM-1, which bind to LFA-1 and $\alpha_4\beta_1$ integrins respectively. This high affinity binding allows interaction between PECAM-1 on both the leukocyte and lateral EC surfaces, directing the leukocyte through the intercellular endothelium gaps and into the interstitial space. Cytokines released from the site of damage act as an attractive stimulus for migration of these translocated leukocytes, which then attempt to restore the tissue back to proper function. Image adapted from Kunkel and Butcher. 2003 [84].

1.6 – Endothelial cells in pathology

An average adult contains an endothelial surface of approximately 1 to 6 x 10^{13} cells that covers a surface area of approximately 1 to 7 m^2 [3]. It penetrates every organ and expands its vast network of vessels to reach every tissue, with every cell being a few microns away from vasculature. Its longest standing and primary role is maintaining a selectively permeable barrier between the blood/lymph and surrounding interstitial fluid. It also has roles in maintaining haemostatic homeostasis by means of balancing its antithrombotic and prothrombotic effects during normal physiology, tipping the balance towards a local prothrombotic response during endothelial injury. In addition to promoting local blood clotting at the site of injury, ECs will also induce inflammation in that area to clear any infections and heal the wound. Blood flow during injury and physiology is regulated by the endothelium via secretion of vasodilatory factors such as nitric oxide (NO) and prostacyclin, or by secretion of vasoconstrictive factors such as thromboxane and endothelin-1 [55] in response to various stimuli. Hence, ECs have a pivotal role in maintaining whole body homeostasis. Imbalances in EC responses leads to endothelial dysfunction, which contributes to the establishment and progression of many diseases. Having a pivotal role in inflammation, dysfunctional EC functioning leads to dysfunctional inflammatory responses. Chronic inflammation exacerbates fat deposition in artery vessel walls, leading to atherosclerosis. This will be the main focus of the role of the endothelium in disease, however it has roles in various other pathologies. These include hypertension, sepsis, thrombosis and cancer metastasis.

1.6.1 - Atherosclerosis

Atherosclerosis is a leading cause of mortality and morbidity in the developed world [56]. It is characterised by thickening of the intimal layer due to build-up of fatty plaques at focal points in large and medium-sized arteries [57]. These impinge on the vessel lumen, reducing the volume of blood able to pass, and may rupture causing acute vessel occlusion due to thrombosis [56]. This is responsible for pathologies such as myocardial infraction and stokes, causing vital organ ischaemic damage [58]. The extent of the damage caused by the disturbed blood flow to these organs depends of the magnitude and duration of the disruption in the blood supply [58].

The fatty plaques are composed of a central lipid core, composed of cholesterol and cholesterol esters [56], with an overlaying fibrous tissue cap, enclosed within the arterial endothelium [57]. The underlying molecular mechanism involves an imbalance in lipid metabolism and chronic inflammatory response at the arterial wall. This results in

an accumulation of oxidised lipid-laden macrophages (foam cells) which die via apoptosis and release their fatty deposits in the intima of the artery wall. The pools of oxidised lipids present as pathogens to the immune system, and so a low-grade inflammatory response is triggered. This activates ECs and vascular smooth muscle cells (VSMCs) which results in the bulk passage of immune cells across the endothelium and into the interstitial space. The SMCs take on a myofiboblast characteristic by the deposition of collagen and elastin after stimulation by growth factors [58]. This forms a fibrous cap on top of the lipid core, and repeated cycles of lipid deposition, inflammation, SMC proliferation and collagen deposition results in gradual increase of plaque volume and artery wall weakening [57]. This manifests into either chronic or acute vascular diseases.

Atherosclerosis pathogenesis is a two-stage process. First, the arterial wall is injured due to haemodynamic forces, chemical attack, mechanical denudation, immune complex deposition or diabetic hyperglycaemia [56,57]. The proceeding step is a response by the tissue to the injury that results in intimal thickening. There are regions of the cardiovascular system that are predisposed to atherosclerotic lesions. These organise into lesion-prone areas of the arterial tree [59]. These regions are characterised by the biomechanical forces acting on them, which translate into different transcriptomics resulting from the type of blood flow interacting with the area of vascular wall. It appears that atherosclerotic plaques form where blood vessels branch or curve. These regions have highly disturbed blood flow, with high oscillatory shear stress index. In contrast, unbranched arteries with uniform laminar shear stress are plaque resistant [59]. Uniform shear force results in the activation of nitric oxide synthase (eNOS), which catalyses the production of nitric oxide (NO) from L-arginine. NO in turn activates soluble guanylate cyclase in SMC, converting GTP to cGMP (Figure 1.12). cGMP activates a protein kinase and subsequent signalling cascade, resulting in a decrease in phosphorylation of myosin light chains and hence a decrease in the contraction of SMCs. This vasodilation lowers the pressure of blood flow in the artery and means there is a lower chance of arterial damage and hence inflammatory response. In addition, NO stabilises IκB, an inhibitor molecule for NFκB (Figure 1.12). NFκB is a transcription factor which mediates a pro-inflammatory cellular state. Hence, constitutive production of NO will stabilise IκB and maintain the EC in an anti-inflammatory state.

Inflammation that results from EC injury or regions of highly disturbed blood flow contributes to the initiation and progression of atherosclerosis. ECs upregulate cell adhesion molecules and undergo vasodilation and increased permeability. A thrombotic response is also activated as mast cells degranulate. This is a normal physiological

process as the body attempts to eliminate any infectious agents in the damaged tissue and initiate a repair process. However, prolonged injury due to high blood pressure, as well as low levels of NO in ECs with highly disturbed blood flow, will result in chronic inflammation. This increased blood flow and permeability of the vasculature will, as a consequence, increase the amounts of macromolecules such as low-density lipoprotein (LDL) that enter the tissue from the plasma [57]. LDL is a transport lipoprotein that carries cholesterol and other lipids in the blood and delivers the cholesterol to the liver and other tissue. LDL and its constituents can enter the sub-endothelium via intercellular pores (Figure 1.13). It is attracted by the negatively charged ECM, as it is itself positively charged. The accumulation of pools of LDL within the subendothelial matrix is greater when there are higher circulating levels of LDL in the plasma [56], hence diet has a large effect on the development of atherosclerosis. LDL retention in the sub-endothelium depends on interactions between the LDL carrier, apolipoprotein B (apoB), and the proteoglycan constituents of the matrix [60]. Once in the sub-endothelium, native LDL undergoes oxidation, among other modifications, by reactive oxygen species (ROS) produced from vascular cells. Oxidised-LDL (ox-LDL) is seen as 'foreign' to the body and triggers a pro-inflammatory response. ECs upregulate their expression of ICAM-1, VCAM-1, P-selectin, E-selectin and PECAM-1 in response to pro-inflammatory cytokines, which are presented on the cellular surface. The interaction of the selectins with carbohydrate ligands on the monocyte cell membrane mediates monocyte integrin expression. Heterotypic interaction of cell surface adhesion molecules between the monocytes (VLA-4) and ECs (ICAM-1, VCAM-1 and PECAM-1) is a prerequisite for monocyte diapedesis across the endothelial lining (Figure 1.13). Monocyte chemotactic protein-1 (MCP-1) and macrophage colony-stimulating factor (M-CSF) are secreted by ECs in response to ox-LDL [60]. These are released into the interstitial space and promote monocyte chemotaxis across the endothelium and their proliferation and differentiation into macrophages respectively.

Scavenger receptors present on the differentiated macrophages recognise a wide variety of ligands. They are multifunctional PRRs and are able to recognise and uptake oxidised-LDL, as well as cholesterol crystals cell debris etc [61]. Recognition of these ox-LDLs induces an inflammatory response by the macrophage, which releases more MCP-1 and hence further recruitment of monocytes. Activated macrophages also produce ROS which propagates further LDL oxidation [56]. In this positive feedback loop, macrophages begin to accumulate modified lipids in their cytosol and these cells cluster under the endothelial layer in the vessel. In time, these foam cells begin to die by apoptosis, spilling out their intracellular lipid stores into the extracellular space and

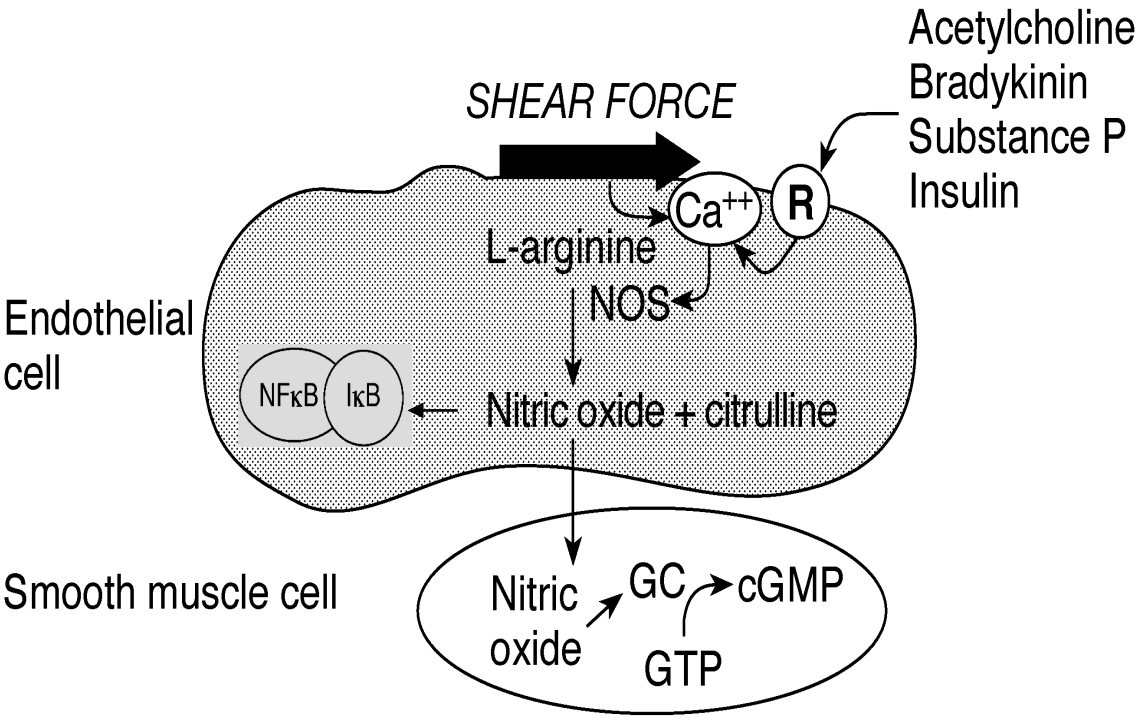

Figure 1.12 - Laminar flow (high shear force) results in the increased generation of NO. eNOS is activated by changes in intracellular Ca^{2+}, created by shear forces or receptor-mediated signalling. eNOS is an enzyme that catalyses the conversion of L-arginine to NO. Elevated NO levels, as with shear vascular force, stabilises NFκB due to NO binding to and stabilising its inhibitor molecule, IκB. NFκB cannot bind DNA to upregulate proinflammatory cytokine gene expression, hence a pro-inflammatory response is attenuated. NO also activates GC, converting GTP to cGMP, resulting in less phosphorylation of myosin light chains and subsequent reduction in SMC contraction. Adapted from Physiology of the endothelium. H. F. Galley and N. R. Webster [4].

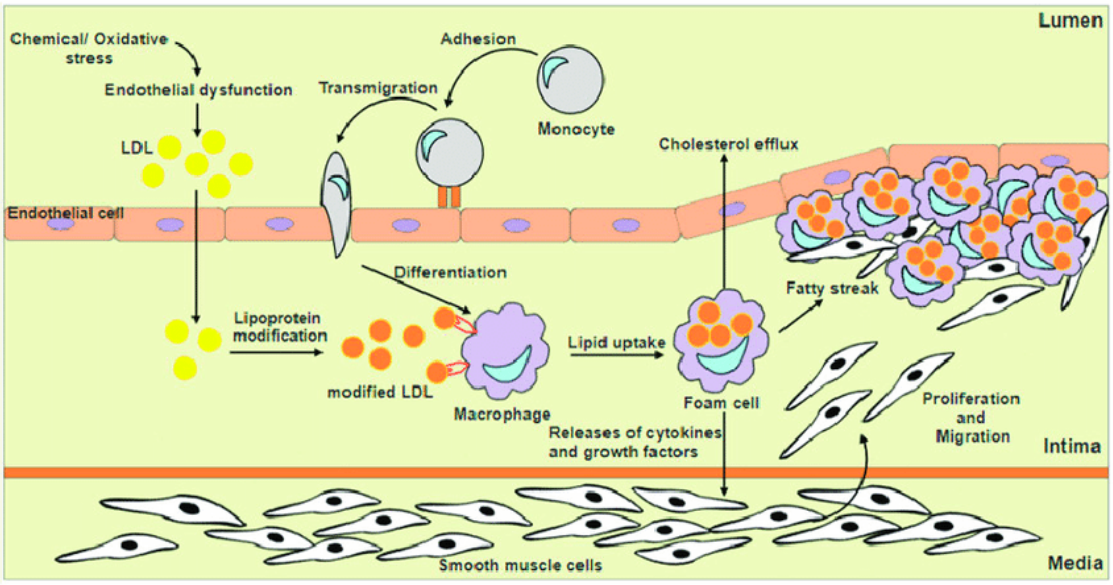

Figure 1.13 – Pathogenesis of atherosclerosis. LDL is able to cross the endothelium via intercellular pores. Once inside the interstitial space, LDL is oxidised and is recognised and taken up by macrophages via their scavenger receptors. Macrophages which have taken in ox-LDL become foam cells, fatty forms of macrophages which are indicative of atherosclerosis onset and progression. The recognition of ox-LDL in the sub-endothelium triggers an inflammatory response, which leads to further accumulation of macrophages in the interstitial space and foam cell formation. These foam cells die by apoptosis and release their intracellular lipids into a growing necrotic core beneath the plasma membrane. Cytokine stimulation of SMC contributes to their proliferation and migration to regions just below the endothelial lining. This SMC accumulation, together with the release of elastin, collagen and mucopolysaccharides by SMC, promotes thickening of the fibrous cap. Image from Bee Kee Ooi et al [85].

forming an ever-growing necrotic core. The prolonged activation of ECs together with macrophages, platelets and SMC will induce an adaptive immune response. T-helper cells enter the interstitial space via CAMs and interact with CD40 receptors via their CD40L (CD40 ligand) on their cell surface. This results in a signalling response within the cells, upregulating the expression and secretion of cytokines such as interferon-γ (IFN-γ) and metalloproteinases. IFN-γ promotes SMS proliferation, allowing SMSs to migrate and proliferate in-between the endothelium and lipid core. Other growth factors, such as platelet derived growth factor (PDGF) are secreted by macrophages and ECs to promote a chronic state of inflammation and these also induce SMC proliferation [56]. A chronic inflammatory state induces SMC to lay down elastin, collagen and mucopolysaccharides, contributing to the formation and stability of the fibrous cap [57].

1.6.1.1 - Clinicopathologic consequences of atherosclerosis

Atherosclerotic plaques develop over the lifetime of a patient, but symptoms only show when the luminal volume is reduced by 50-75% [57], or during an acute rupture or embolisation of the plaque. Expansion of the atheroma may impinge on blood flow to vital organs and tissues. This reduces oxygenated blood to regions downstream of the stenosis, which may not have clinical symptoms. At a tipping point, known as critical stenosis [56], the occlusion is so severe that demand for oxygenated blood exceeds supply and ischaemia of the affected tissues results. The patient will experience stable angina due to coronary ischaemia [57], which may occur at rest or during minimal exertion depending on the severity of the occlusion. Prolonged tissue ischaemia may also lead to atrophy of the affected tissue, which breaks down and dies by apoptosis. This may lead to organ failure, such as renal atrophy in atherosclerotic renal artery stenosis.

Acute pathologies due to atherosclerotic plaques occur due to plaque erosion or rupture, which activates a thrombotic response. The thrombus produced may lead to complete or partial vascular obstruction leading to tissue ischaemia [56]. Acute changes in plaques are usually more life threatening than chronic low-grade changes. The vulnerability of a plaque to rupture is more of a factor in the pathological effect of the coronary event, over the extent of the occlusion. Vulnerable plaques are more likely to have thin fibrous caps and larger numbers of foam cells and a large lipid core [56,60]. Fewer SMC is a large contributing factor to a vulnerable plaque, as they secrete collagen which stabilises the fibrous cap. Low relative numbers of SMC will secrete less collagen, causing plaque instability. Clusters of immune cells tips the balance of

collagen secretion and degradation towards that of degradation, thus destabilizing the mechanical integrity of the plaque. IFN-γ secreted by T-helper cells inhibits collagen secretion by SMC, and macrophages secrete various metalloproteinases that degrade ECM components. Plaque rupture usually occurs at the point of lesion, where the thrombus meets the atheroma. This area is rich in foam cells, suggesting that inflammatory factors may influence thrombosis [60].

Acute infections also increase risk of myocardial infarction and stroke, due inflammatory activation [60]. There are three different forms of clinical disease provoked by acute changes to plaques. An acute atherothrombotic occlusion occurs due to exposure of the sub-endothelium to the blood stream, leading to activation of the clotting cascade and formation of a thrombus. This may cause partial or total occlusion of the vessel. Total occlusion of the artery will lead to necrosis of downstream tissues caused by irreversible ischaemia, which may be fatal. Atherothrombosis in artery walls may, after degradation, result in detachment of small fragments of the thrombus. These then embolise in distal sites to the ruptured plaque, causing small infarctions in organs [57]. Weakening of the plaque due to inflammatory activity degrading ECM components can lead to atherosclerotic aneurysms. An aneurysm is a bulge in the blood vessel caused by dilation of the vessel. Sudden rupture of these leads to haemorrhage and high risk of fatality [57].

1.6.1.2 Preventative therapies

Drugs effective at lowering blood cholesterol concentrations and high blood pressure are used commonly in the clinic. Statins are the most widely used drug to lower cholesterol levels. They act to inhibit the hepatic enzyme responsible for intrinsic cholesterol production. This will result in a smaller lipid core beneath fibrous plaques and hence a more stable plaque. These are given to patients with hypercholesterolaemia and clinical symptoms of coronary heart disease. These symptomatic patients may also be taking a combination therapy of statins with aspirin. Aspirin is a platelet aggregation inhibitor and hence prevents a thrombotic response to plaque injury.

More invasive treatments to prevent and reverse cardiovascular disease include surgical procedures to remove atheromatous plaques and widen the lumen of the artery. Endarterectomy procedures ‘core out’ the fibrous plaque present in the subendothelial intima [56]. This dramatically reduces the patient’s risk of acute neurological events. To reduce the risk of coronary occlusion events, coronary angioplasty is performed. This is

a catheter-based procedure which mechanically widens the lumen of coronary arteries obscured by atherosclerotic plaques. This restores blood flow to the heart muscle and prevents ischaemia. This is a very common procedure with high initial success [62]. However, later complications such as restenosis may occur where SMC proliferation continues due to inflammation at the point of stent insertion [62]. This will eventually re-form the fibrous plaque over the fatty atheroma and render the surgery useless. The materials used in coronary stents must be flexible, supportive, capable of expansion, and biocompatible. Typically, foreign materials implanted into the human body results in trauma, inflammation, immune response and eventual healing and/or scarring. Materials that are not biocompatible can induce many complications, including cytotoxic chemical build-up and chronic inflammation. Titanium is the current metal used as a base for coronary stent instruments. It is inert and unlikely to evoke an inflammatory reaction.

1.6.1.3 - TiO_2 as a novel surface for coronary angioplasty

Coronary angioplasty, among other invasive procedures, utilises inert surfaces that are biocompatible with the human body. However, to avoid an immune reaction to the transplanted material, immunosuppressants are commonly used [63]. This reduction in the body's capacity to elicit an inflammatory response often leads to higher occurrences of bacterial infection at the site of transplantation [64]. Further to this, titanium medical implants are susceptible to microbial colonisation during transplantation [64]. These colonies expand within the host to form biofilms – chronic bacterial aggregates enclosed within a self-produced polysaccharide matrix [65]. These biofilms are resistant to antibiotics and the immune system, causing patients to develop prosthetic joint infections [66]. This, along with the induced immunosuppressed state of the patient, creates a favourable environment for these microbial aggregates which continue to replicate and maintain a state of chronic infection.

The number of these preventative procedures is increasing every year due to rising obesity and other health problems, and so too is the number of patients developing bacterial infections. With the continuous progression of antimicrobial resistance across global healthcare practices, there is a growing necessity for effective anti-microbial clinical devices. Novel contact-dependent physical approaches are hence being developed that aren't bias towards the killing of non-resistant strains of bacteria, nor do they exacerbate the antimicrobial resistance pandemic. Surface architecture and topology greatly affect the adherence and proliferative capacity of bacteria on a material surface, and hence on biofilm formation too [66]. In a paper by Professor Bo Su, a

Professor of biomedical materials at The University of Bristol, he describes the development of novel biomaterials with the potential for antimicrobial properties that would be suitable for surgical implants. Using a variety of chemical-physical techniques, nanostructured titanium (Ti) and titanium dioxide (TiO_2) surfaces are generated which mimic the surface of many naturally occurring antimicrobials [64]. Taking inspiration from nature, nanoscale pillar structures are generated and are composed of TiO_2 (Figure 1.14). These have been previously postulated to promote bacterial surface stretching and subsequent rupture between structures in contact with the microbial surface [66]. This bactericidal technique is known as contact killing. Using scanning electron microscopy (SEM), the morphology of E. coli and K. pneumoniae were observed when incubated on Ti and TiO_2 treated Ti surfaces. It appeared that the cell thickness was markedly reduced when incubated on TiO_2 nanostructured surface than when compared to the standard Ti flat surface. This was the result of loss of turgor pressure due to rupture of the cell membrane, resulting in a collapsed morphology and ultimately cell death. Fluorescence microscopy shows an increase in microbial cell death relative to cells which are alive when gram negative bacteria are incubated on the nanostructured surface.

This paper eludes to the antimicrobial effect of nanostructured surfaces for clinically applied materials. However, the response of physiological cells to these surfaces is also crucial in the efficacy and biocompatibility of the clinical implant. Cells must adhere, proliferate and differentiate properly to maintain a state of tissue homeostasis, avoiding excess cell proliferation (leading to hyperplasia and possibly tumour growth) and excess cell death (necrosis). Therefore, studies that show the response of physiological cells to the TiO_2 surface are required to establish the clinical relevance of the nanostructured surface.

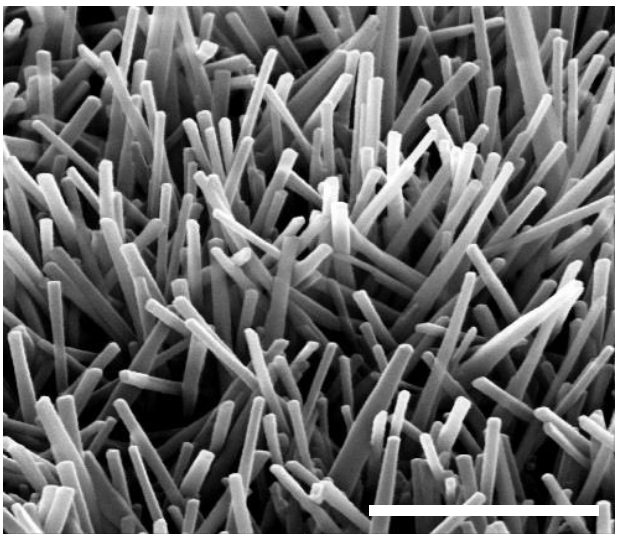

Figure 1.14 – SEM image of TiO_2 nanostructured surface. Ti alloy underwent thermal oxidation to obtain randomly oriented TiO2 nanostructures. The scale and topology of the nanoscale TiO_2 filaments promotes surface stretching and rupture of gram-negative bacteria. This contact killing property of the surface may have application in the clinic where chronic bacterial infections on clinical implants are common. This surface is generated and imaged by Professor Bo Su and colleagues, University of Bristol [64]. Scale bar shown = 1μm.

1.7 Aims & Objectives

Research into EC biology is in deficit to other well characterised cell types. Understanding fundamental endothelial cell biology is necessary to study endothelial functions in normal physiology. This study aimed to provide and optimise culture models for ECs and apply these techniques to more complex cellular assays.

Specifically, this study aimed to:

- Optimise the media used for HUVEC culture by analysing the proliferation of ECs in three different commercial formulations.
- Examine the growth of cells on different bioengineered surfaces, using surfaces with potential clinical applications
- Apply techniques of EC culture to develop a culture of zebrafish ECs
- Adapt an angiogenic co-culture protocol to a tumour angiogenic co-culture assay
- Optimise this protocol to gain best density of blood vessels for ease of vascular quantification
- Separately label HUVEC surface membrane proteins in order to detect for specific proteins on the apical and basolateral surface through proteomics

In addition to developing and optimising techniques for EC culture, this research project aimed to develop my own personal skills in cell culture in the lab.

CHAPTER 2 Materials and Methods

2.1 Materials

2.1.1 Cell culture

2.1.1.1 Mammalian cell lines

Cell Type	Source
HUVEC	Human Umbilical Vein Endothelial Cells Lonza, CC-2519
NHDF	Normal Human Dermal Fibroblasts Lonza, CC-2511
SW480	Colorectal adenocarcinoma Sourced from ATCC, CCL-228
SW480 overexpressing VEGF	Colorectal adenocarcinoma, stably transfected with VEGF by Mr. Haoche Wei. Sourced from ATCC, CCL-228

2.1.1.2 Zebrafish cells

Cell Type	Source
Fluorescent transgenic (Tg(fli1a:EGFP) zebrafish ECs	Freshly isolated by Mr. Aaron Scott, researcher at UoB. Refer to methods 2.2.1.7

2.1.1.3 Cell culture media

Media type	Source/composition
DMEM/F12	Dulbecco's modified Eagle's Medium Ham's F-12 nutrient mixture with 3150mg/L glucose, 0.55mg/L sodium pyruvate, L-glutamine and sodium bicarbonate (sigma-Aldrich D8062)
EBM-2	Endothelial Cell Basal Medium-2 Lonza, CC- 3156
EGM-2	Endothelial Cell Growth Medium-2 composed of EBM-2 + BulletKit, Lonza CC-4176
FBS	Fetal Bovine Solution. Sigma-Aldrich, F9665
Growth medium for SW480 spheroids	DMEM with 3150mg/L glucose, 0.55mg/L sodium pyruvate, L-glutamine and sodium bicarbonate (Sigma-Aldrich D8062) Supplemented with 10% (w/v) BSA, 10µg/ml and 10mg/ml penicillin and streptomycin (Sigma-Aldrich P4333)
Growth medium for transgenic zebrasfish ECs	EGM-2 supplemented with 100µg/ml Normocin (Thermo Fisher Scientific, NC9273499)

HIFA medium	EBM-2 plus Lonza BulletKit™ (CC-3162) supplemented with: 10ng/mL hr FGF/cf, R&D 233-FB-025 20ng/mL hr IGF/cf, R&D 8335-G1-200 4µL hydrocortisone (Lonza supplement) 10µL ascorbic acid (Lonza supplement) 10µL GA-1000 (gentamicin sulphate-Amphotericin, Lonza supplement)

2.1.1.4 Cell culture reagents

Reagent	Supplier
Fibronectin (FN) (0.1%)	Sigma-Aldrich, F0895
Gelatine (2%)	Sigma-Aldrich, G1393
Bovine type I Collagen (2.9mg/ml)	Sigma-Aldrich, 5074
Trypsin-EDTA (0.05%)	Thermo Fisher, 252-000-56
Trypsin neutralising media	Lonza, CC-5002

2.1.2 General solutions and buffers

Solution/buffer	Components
10x Phosphate-buffered saline (PBS)	27mM KCL, 1.4M NaCl, 15mM KH_2PO_4, 80nM Na_2HPO_4, pH 7.4.
10x Tris-buffered saline (TBS)	50mM Tris base 140mM NaCl pH 7.6

2.1.3 Immunofluorescence

2.1.3.1 Reagents

Reagent	Supplier
4`, 6-diamidino-2-phenylindole (DAPI)	Life technologies, D21490
1, 4-diazabicyclo[2.2.2]octane (DABCO)	Sigma-Aldrich, D2522
Mowiol 4-88	Calbiochem, 475904 Solution of Mowiol made up to compose of 2.5% (0.017g) 1,4-diazobicyclo-[2.2.2]-octane (DABCO, Sigma-Aldrich, D2522) with Mowiol, 4-88 (500µl)
Triton X-100 (0.2%)	Sigma-Aldrich, X100

Sodium borohydride	Sigma-Aldrich, 452882
Bovine Serum Albumin (BSA)	Sigma-Aldrich, A9647

2.1.3.2 Primary antibodies

Target	Type	Application/dilution	Supplier
VEGF Receptor 1	Rabbit pAb Goat pAb	WB- 1: 1000 IF- 1: 200	Cell signalling technology, 2893 R&D AF321
VEGF Receptor 2	Rabbit mAb Mouse mAb Rabbit pAb	WB- 1: 1000 IF- 1: 200 IF- 1: 200	Cell signalling technology, 2479 R&D mab3573 Abcam, Ab11939
Integrin α5	Mouse mAb	IF- 1: 200	BD Biosciences, 743109
VEGF	Mouse mAb	IF- 1: 200	R&D systems, MAB293
PECAM-1	Mouse mAb	IF- 1: 200	R&D, BBA7
α-tubulin	Mouse mAb	WB- 1:5000	Sigma-Aldrich, T9026
VE-cadherin	Rabbit pAb	IF- 1: 200	Abcam, ab33168
CD63	Mouse mAb	IF- 1: 200	Bio-Rad, MCA2142
Podocalyxin	Mouse mAb Mouse mAb	IF- 1: 200 IF- 1: 200	Santa Cruz Biotechnology, sc-23904 Santa Cruz Biotechnology, sc-23903
P-Glycoprotein	Mouse mAb	IF- 1: 200	Abcam, ab10333
ICAM-1	Mouse mAb	IF- 1: 200	Abcam, ab2213
Clathrin Heavy Chain	Mouse mAb	IF- 1: 200	BD Transduction Laboratories, 610383
Robo 4	Mouse mAb	IF- 1: 200	R&D, MAB2454
Flotillin 2	Rabbit pAb	IF- 1: 200	Abcam, ab96507
Caveolin-1	Mouse mAb	IF- 1: 200	BD Transduction Laboratories, 610406

2.1.3.3 Secondary antibodies

Target	Conjugation	Host species	Dilution	Supplier
Mouse IgG	HRP	Horse	1: 10,000	Cell signalling technology, 7076
Rabbit IgG	HRP	Goat	1: 10,000	Cell signalling technology, 7074
Mouse IgG	Alexa Fluor 488	Goat	1: 10,000	Thermo-Fisher, A-11001
Rabbit IgG	Alexa Fluor 488	Goat	1: 10,000	Thermo-Fisher, A-11008
Mouse IgG	Alexa Fluor 594	Goat	1: 10,000	Thermo-Fisher, A-11005
Rabbit IgG	Alexa Fluor 594	Goat	1: 10,000	Thermo-Fisher, A-11012
Goat IgG	Alexa Fluor 594	Donkey	1: 10,000	Thermo-Fisher, A-11058
Mouse IgG	Alkaline phosphatase	Rabbit	1: 10,000	Sigma-Aldrich, A1902

2.1.3.4 Fluorescent reagents

Alexa Fluor™ 488 and 594 labelled phalloidin was used at a dilution of 1:400 in BSA. Green and red CellTracker™ used from a stock solution made by 1,000x dilution of CellTracker™ in DMSO. All reagents bought from Molecular Probes (Life technologies).

2.1.4 ELISA

2.1.4.1 Reagents

Reagent	Source
Mouse anti-human VEGF capture antibody	R&D Systems, DY293B-05 (1.00 µg/mL)
Biotinylated goat anti-human VEGF detection antibody	R&D Systems, DY293B-05 (100 ng/mL)
Streptavidin-HRP	R&D Systems, DY293B-05 (40-fold dilution)
Recombinant human VEGF standard	R&D Systems, DY293B-05 (2000 pg/mL)
Wash buffer	0.05% Tween® 20 (Sigma-Aldrich P1379) in PBS, PH 7.2-7.4
Reagent Diluent	1% bovine serum albumin (BSA) in PBS, pH 7.2-7.4

O-phenylenediamine (OPD)	Sigma-Aldrich, P8287
Citrate phosphate buffer	0.1M citric acid, 0.1M Na_2HPO_4; pH 5.0

2.1.5 Immunohistochemistry

2.1.5.1 Reagents

Reagent	Supplier
0.3% (v/v) hydrogen peroxide	Sigma-Aldrich, H1009
BCIP/NBT	Sigma-Aldrich, B5655

2.1.6 Immunoprecipitation

2.1.6.1 Biotinylating solutions

Solution	Components
1x Tris-buffered saline (TBS)	Tris buffer (25mM) NaCl (0.15M) pH 7.2
Biotinylating solution	200mg/ml EZ-link sulfo-NHS-LC-biotin, Thermo Fisher, 21355
Lysis solution	NaCl (137mM) Tris buffer (20mM) EDTA (1mM) NP40 (0.5%) 1% (w/v) SDS DTT 1x protease inhibitor tablet pH 7.5
3x Laemmli sample buffer	186mM Tris-HCl 30% (v/v) glycerol 6% (w/v) SDS 1% (w/v) bromophenol blue 325mM DTT (45mg freshly added) pH 6.8

5.1.6.2 Biotinylating reagents

Reagent	Supplier

Ethylenediaminetetraacetic acid (EDTA)	Sigma-Aldrich, 1233508
Streptavidin beads	Thermo-Fisher, 11205D

5.1.7 Western blotting

5.1.7.1 Solutions

Solution/Buffer	Components
10x SDS-PAGE running buffer	192mM glycine 25mM Tris base 1.0% (w/v) SDS
1x Transfer buffer (high molecular weight)	192mM glycine 25mM Tris base
1x Transfer buffer (low molecular weight)	192mM glycine 25mM Tris base 10% (m/v) methanol
Blocking solution	5% (w/v) dry skimmed milk 1x TBS-T
10x TBS-Tween	10x TBS 0.1% Tween 20
2x Laemmli sample buffer	250mM Tris-HCL pH 6.8 2% (w/v) SDS 10% (v/v) glycerol 0.2% (w/v) bromophenol blue 20nM DTT

5.1.7.2 Reagents

Reagent	Supplier
Acrylamide:bisacrylamide (37.5:1, 30% (w/v) acrylamide	Bio-Rad, 161-0158
1M Tris-Cl, pH 8.8/6.8	Sigma-Aldrich, T1503
10% SDS	Fischer Scientific, 205-788-1
10% Ammonium persulfate (APS)	Bio-Rad, 161-0700
N, N,'N'-tetramethylethylenediamine (TEMED)	Bio-Rad, 161-0801
Immobilon-P polyvinyl fluoride (PVDF) membrane	Millipore, IPVH00010
Amersham Hyperfilm	GE Healthcare, 28-9068-44
Amersham ECL western blotting detection reagents	GE Healthcare, RPN2232
Streptavidin-HRP	R&D, DY998

2.2 Methods

2.2.1 Cell culture

All mammalian cells were incubated at 37°C in 5% (v/v) CO_2.

2.2.1.1 Coating of plastic culture dishes and plates

50µg/mL fibronectin in PBS was used to coat each well of a 6, 12 or 24-well plate and 10µg/mL in PBS used to coat a 10cm dish. Plates and dishes were left for 30 min at room temperature prior to the plating of ECs.

2.2.1.2 Coating of glass coverslips and titanium surfaces

To acid-washed 13mm coverslips or Ti and TiO_2 discs, 50µg/ml fibronectin, 30µg/ml type I collagen and 0.1% gelatine (triple coat) in PBS was added and all were incubated for 1 h at 37°C. For a single coat composed only of fibronectin, an aliquot of 500µg/ml fibronectin in PBS was added to the surface. ECs were seeded onto the coverslips after three washes with PBS.

2.2.1.3 Coating of Transwell

Prior to plating of HUVEC, the inside of Transwell with 0.4µm polyester pores were coated with 2.5µg/ml fibronectin, 2.5µg/ml gelatine and 50ng/ml collagen for at least 1 h at 37°C. The wells were then washed three times with PBS before seeding the HUVECs.

2.2.1.4 Culture of endothelial cells

HUVEC were cultured in EGM-2 solution in 10 cm dishes until a confluency of ~90% was reached. After aspirating the media, the HUVEC were washed twice with PBS before an aliquot of trypsin-EDTA (0.5ml for 6cm dish, 1ml for 10cm dish) was added. Incubation time at 37°C was dependent on how long it took for cell detachment; normally <2 min. 4x volume of trypsin aliquot of neutralising media composed of DMEM/F-12 with GA-1000 and 10% FBS was added to the dishes to inactivate the trypsin. The cells were counted using a haemocytometer and centrifuged at 1500rpm for 3 min. The pellet was resuspended in 4ml EGM-2 media. HUVEC were generally passaged at a ratio of 1:5 and were used for experiments between passage 2 and 6.

.

2.2.1.5 Culture of SW480 cells

SW480 were cultured in 10cm dishes DMEM/F12 solution until confluent. After aspirating the media, the SW480 were washed twice with PBS before a 500µl aliquot of trypsin/EDTA was added. The SW480 cells were incubated at 37°C until detached from the surface and then 4ml neutralising media added.

2.2.1.6 Culture of NHDF cells

NHDF cells were cultured in 10 cm dishes in DMEM/F12 until they reached 80-90% confluence (about 7 days). Media was refreshed every 48 h during this period. Cells were then passaged by aspirating the culture media, washing twice with PBS and addition of 1 ml trypsin-EDTA. Incubation allowed cells to detach from the plastic dish, and then cells were harvested in 4 ml DMEM/F12 culture media. NHDF generally passaged at a ratio of 1:5.

2.2.1.7 Isolation of zebrafish endothelial cells

20x pooled transgenic zebrafish larvae (3 dpf) were dissociated in 500 µl digestion buffer (described below) for 1 hour and 23 minutes in a Thermomixer set to 32 ^{0}C and 800 rotations per minute. 500 µl stopping buffer (described below) was added and mixed by pipetting. Samples were then centrifuged at 300 g with the supernatant being removed and the cell pellet resuspended in suspension medium (described below) – this was repeated to wash the cells. This solution was then passed through a 40 µm sterile filter before being centrifuged at 300 g and resuspended in 300 µl suspension medium and taken for FACS.

- **Perfusion Buffer** consists of 1X PBS plus 10 mM HEPES, 30 mM taurine and 5.5 mM glucose and was stored for up to three months at 4 ^{0}C. 49
- **Digestion Buffer** consists of perfusion buffer plus 0.25% Trypsin, 12.5 µM CaCl2 and 5 mg/ml Collagenase II and was freshly prepared on the morning of the experiment.
- **Stopping Buffer** consists of perfusion buffer plus 10% (vol/vol) FBS and 12.5 µM CaCl2 and was freshly prepared on the morning of the experiment.
- **Suspension Medium** consists of Leibovitz medium L-15 w/0.3mM glutamine plus 2% FBS, 0.8µM $CaCl_2$ supplemented with 50 U/mL penicillin and 0.05mg/mL streptomycin.

2.2.1.8 Culture of zebrafish endothelial cells

Zebrafish ECs were cultured in Lonza EGM-2 media supplemented with 100µg/ml Normocin at 28°C in 5% (v/v) CO_2.

2.2.2 Proliferation Assay

HUVEC were seeded on coated 12-well plates at $3x10^4$ cells/mL in freshly aliquoted PromoCell EGM-2 media. After cells had attached, the media was replaced with Lonza EGM-2 media, PromoCell EGM medium, or an aliquot of PromoCell EGM-2 medium that had been made and used before these experiments in the lab. HUVEC were harvested as described on section 2.2.1.4 and counted using a haemocytometer at 24, 48, 72, 96 and 118h after plating. Media was refreshed every 48h.

2.2.3 Immunofluorescence microscopy

Prior to immunofluorescence microscopy of cells, cells were fixed and stained with appropriate reagents. The confocal microscope used was a Leica SP5-AOBS. All images using a frame average of 4 and either 5x, 40x or 63x lens.

2.2.3.1 Preparing cells for immunofluorescence microscopy

To fix the cells, 4% paraformaldehyde was added and left to incubate for 15 min at room temperature to cross-link proteins within the cells. The cells were washed thrice with PBS and permeabilised with 0.2% (w/v) Triton X-100 in PBS for 5 min, before being washed with PBS three times. A further 5 min incubation was carried out with 0.1% (w/v) sodium borohydride. Cultures were washed thrice with PBS before an aliquot of primary antibody, diluted in 1% BSA, or phalloidin, diluted in PBS, was added to the cells for 1 h at room temperature. The cells were washed thrice in PBS before an aliquot of diluted secondary antibody was added (diluted in PBS) and incubated for 45 min in the dark at room temperature. After a 3x PBS wash was carried out to remove the secondary antibody, a 1:10,000 dilution of 1mg/ml DAPI was added and left for 45 min. Four PBS washes were done before the coverslips or other cell culture surfaces (titanium discs and Transwell membranes) were individually transferred to prepared

microscope slides. Excess PBS removed by blotting on clean paper towels. 10µl Mowiol mounting media was added to the cell culture surface and a 13mm coverslip placed top. An overnight period at room temperature was necessary for the Mowiol to set, after this the slides were kept in the dark at 4°C.

2.2.4 *In vitro* tumour angiogenesis co-culture assay

2.2.4.1 Preparation of methylcellulose solution

1.2g methylcellulose was added to 50ml of preheated (60°C) DMEM/F12 medium and placed on a magnetic stirrer for 20 min. 50ml of DMEM/F12 at 4°C was added to this solution which was mixed for a further 1-2 h at 4°C.

2.2.4.2 Formation and plating of SW480 spheroids

The DMEM/F12 solution was aspirated from the SW480 cell culture and the 10cm dish washed with PBS before trypsin-EDTA added. After <3 min incubation at 37°C 4ml neutralizing medium was added and the cells were distributed at [N° spheroids+10] *1000 into a 50ml polypropylene tube. Cells were suspended in [N° spheroids+10] *30µl methylcellulose stock solution. This was seeded in drops of 30µl onto the lid of an inverted tissue culture dish filled with 20ml PBS before being incubated at 37°C for around 6 days. Collection of the spheroids required the lid being flushed with 2ml PBS and capture of the spheroids into a microfuge tube. Spheroids were collected by centrifugation at 1200 rpm for 90 seconds and carefully removal of the supernatant. The cells were then resuspended in a solution of 30µl Matrigel and 70µl EGM-2 before being plated onto the co-culture. A 15 min incubation at 37°C was carried out before 400µl EGM-2 media was added and co-culture was left for 48 h at 37°C. At this point, the EGM-2 was refreshed and the plate incubated for a further 48 h before being fixed and stained.

2.2.4.3 *In vitro* co-culture of NHDF and HUVEC

NHDF were plated into 12-well plates in EGM-2 at $3x10^4$ cells/ml. Cells were incubated at 37°C/5% CO_2 for up to 7 days or until they had reached ~90% confluence. Media was refreshed every 48 h. HUVEC in 10cm dishes were cultured as normal (section 2.2.1.4), and a concentration of $6x10^4$ cells/ml were seeded onto the fibroblast covered 12-well plate.

2.2.4.4 Immunohistochemistry co-cultures for quantification

Immunohistochemistry was carried out to visualise the blood vessel formation in the *in vitro* tumour angiogenesis assay. The co-cultures were fixed using 4% PFA at 4° for 30 min. The wells were washed with formalin and further fixed in 4% PFA. The plate was kept at 4°C for 2 h before being washed twice with PBS. Each well was then incubated with 0.3% (v/v) hydrogen peroxide in methanol for 15 min at room temperature. Cells were washed 3 times with PBS before a 1 h incubation at 37°C with mouse anti-PECAM1 primary antibody diluted 1: 1,000 in 1% (w/v) BSA. An incubation with rabbit anti-mouse alkaline phosphatase-conjugated secondary antibody diluted 1:500 in 1% BSA for 1 h at 37°C was carried out after the primary antibody was removed and cells were washed four times with PBS. A six-time repeated wash with water was done immediately before freshly prepared BCIP/NBT substrate was added. BCIP/NBT was prepared by dissolving 1 tablet in 10ml ddH_2O and filtering through a 0.2µm pore filter. A 30 min incubation at 37°C was carried out to allow for adequate stain to develop. The wells were washed four times with ddH_2O and then stored at 4°C until imaging. Co-cultures were imaged by brightfield microscopy using a CCD camera attached to an Olympus CKX31 inverted microscope.

2.2.5 ELISA

A Quantikine Human VEGF Immunoassay kit was used to measure VEGF concentration in cell culture medium. All reagents used were warmed to room temperature prior to use and were reconstituted according to instructions as given by the manufacturer; R&D systems. A working concentration of 1 µg/mL was made of the capture antibody by diluting the contents of the vial in 1x PBS. 100µL of the stock solution was added to a 96-well plate. An air-tight seal was applied to the plate to prevent the evaporation of the antibody before being transferred to 4°C and left overnight. The capture antibody solution was aspirated before washing the plate 3 times with washing buffer (0.05% Tween-20 in PBS, pH 7.2-7.4). Washing buffer was removed at each stage by blotting the plate onto paper towels. Blocking the non-specific binding of detection antibody is crucial to get an accurate readout of VEGF levels, hence 300µl blocking buffer was added to each well (1% fatty acid free BSA in PBS pH 7.2-7.4, filtered) which was left to incubate at room temperature for 1 h. A further round of aspirating the solution followed by washing three times with washing buffer was completed. 100µL of the standard or sample solution was aliquoted into each well, the

standard being in appropriate dilutions to create a 7-point standard curve (2-fold dilution using blocking buffer starting at 2000pg/mL). The plate was sealed with an adhesive strip and left to incubate for 2 h at room temperature. Once its incubation was complete, the wells were aspirated and washed with washing buffer three times. A 100µL aliquot of the detection antibody was added to each well after dilution to its working concentration (100ng/mL). These plates were sealed again and left at room temperature for 2 h. The antibody solution was aspirated and washed three times with washing buffer post incubation. 100µL of a 40x dilution of streptavidin-HRP was added to each well and then the plate was covered and left at room temperature for 20 min, avoiding exposure to direct sunlight. The solution was aspirated and washed three times with washing buffer before 100µL of substrate solution was added. OPD was used as a water-soluble substrate for HRP, producing a yellow-orange colour detectable at 492nm. After 0.012% (v/v) hydrogen peroxide was added to 50mM citrate phosphate buffer (50nM citric acid, 100mM Na_2HPO_4; pH 5.0) OPD (0.8 mg/ml) was dissolved into the solution only immediately before adding to the wells. 100µl of this substrate solution was added to the wells, which were then incubated for 20 min in the dark, or until a yellow colour is seen. 50µl of the stopping solution, 2M H_2SO_4, was added to each well. Absorbance of each well was then measured at 492nm.

2.2.6 Immunoprecipitation

2.2.6.1 Biotinylation of HUVEC on Transwell

Prior to the addition of biotinylating reagent, $1x10^5$ HUVECs were seeded with EGM-2 onto Transwell coated with fibronectin, collagen and gelatine (see 2.2.1.3). 2.4x the volume of EGM-2 that was added to the top Transwell compartment was added to the compartment. After a 24 h incubation at 37°C, the Transwell were washed thrice with HIFA medium before 500µl HIFA was added to the inside of the wells and 1.3ml added to the outside. Cultures were incubated at 37°C for 48 h to reach confluency. If EDTA treated, 1mM EDTA was added to the apical surface of the cells, which were incubated at 37°C/5% CO_2 for 5 min. 5mg/mL sulfo-NHS-LC-biotin in HIFA was added to the apical or basal surface of the HUVEC on the Transwell.

2.2.6.2 Streptavidin immunoprecipitation

Biotinylated proteins were isolated using streptavidin coupled beads. Following their labelling, HUVEC were washed twice with TBS to remove excess biotinylation reagent. Lysis solution was added to the apical surface of the cells in the Transwells for 2 min. The cells were harvested by using a pipette to scrape and transfer lysate to microfuge tubes. If multiple wells were being used for one sample, lysis solution was transferred between wells before collection into microfuge tubes. Final aliquots were collected and kept on ice for 30 min. microfuge tubes were centrifuged at 4°C and 15000 x g for 12 min and supernatant containing the solubilized proteins collected and kept on ice.

Before use, streptavidin beads were pelleted via a three-time wash in lysis buffer and centrifugation at 1000 x g for 3 min at 4°C. Bead pellets were added to the sample solutions. These were then kept at 4°C with gentle agitation for 1 h before centrifugation at 1000 x g and 4°C for 3 min, discarding the supernatant. The samples were then washed again three times with lysis buffer with centrifugation at 1000 x g at 4°C for 3 min to remove non-biotinylated proteins. 3x Laemmli Sample buffer with 325mM DTT was added to the samples and the solutions left for 5 min at 95°C before being stored at -20°. Samples could then be analysed by SDS-PAGE and western blotting.

2.2.7 Sodium-dodecyl sulphate polyacrylamide gel electrophoresis (SDS-PAGE)

Proteins were analysed using SDS-PAGE and western blotting. After IP, 2x Laemmli sample buffer was loaded in equal volume to the samples, which allowed proteins in the sample to become reduced and denatured when heated to 95°C, which were then ran on hand-cast gels. A 10% separating gel was generally used, prepared using 10% (w/v) acrylamide/0.3% (w/v) bis-acrylamide, 0.1% SDS and 0.38M Tris-Cl (pH 8.8), 0.1% (w/v) ammonium persulphate (APS). The acrylamide could polymerise when 0.1% (v/v) TEMED was added just before pouring. Once set and levelled using 0.01% (w/v) SDS overlaid on top of the gel, stacking gel was prepared using 3.9% (w/v) acrylamide/0.1% bis-acrylamide, 0.1% SDS, 0.125M Tris-Cl (pH 6.8) and 0.05% APS. 0.1% TEMED was added just before pouring on top of the separating gel to allow polymerisation of the acrylamide. Once solidified, the wells were washed with 1x SDS-PAGE running buffer and the protein marker and samples were added. The cell was loaded with the gel and 1x SDS-PAGE running buffer and ran at 20mA for 20 min until the samples entered the lanes, and then a voltage of 150V applied for 60 min.

2.2.8 Western blotting

After their separation by SDS-PAGE electrophoresis, the protein samples on the gel were transferred onto an Immobilon-P polyvinyl fluoride (PVDF) membrane to allow their detection using antibodies or other high affinity binding methods. The gel was placed onto an activated PVDF membrane and this was then sandwiched between filter paper and fibre pads, both soaked in Western Transfer Buffer (WTB). The cassettes were loaded into Bio-Rad Mini Trans-Blot electrophoretic transfer cells which were filled with WTB, and proteins allowed to transfer at 270mA for 1 h at 4°C.

The transfer membrane was moved to a 5% (w/v) solution of dry skimmed milk powder diluted in PBS-Tween to prevent unspecific binding of primary antibody. After this the membrane was washed with 1xTBS-Tween and then incubated with primary antibody diluted in 1x TBS-Tween overnight at 4°C with gentle agitation. Excess antibody was removed by a three-time wash in TBS-Tween before the secondary-HRP antibody (diluted in TBS-Tween) was added for 1 h at room temperature. The membrane was again washed thrice with TBS-Tween prior to detection of the secondary antibody. Excess TBS-Tween was removed, and the membrane was soaked in enhanced chemiluminescence (ECL) detection reagents in a 1:1 mixture. The soaked membrane was covered in clingfilm and exposed to Hyperfilm for an amount of time depicted by the signal strength.

Chapter 3 Endothelial cell proliferation assays

3.1 Introduction

To study endothelial biology, it is useful to be able to culture ECs *in vitro*. Culturing ECs allows examination of their normal functions, but also allows for the study of pathological conditions. HUVECs are routinely used as model ECs and are prepared from the major vein of human umbilical cords. The main advantage from using this source is that the cells are easy to obtain, and as they are primary cells, they retain most of the properties of normal ECs far better than a cell line. Retaining their morphologically and physiologically unique properties is important for generating a cell culture that behaves in a biochemically similar way as an *in vivo* scenario. A major negative however, is that they have a limited life in culture before the cells begin to lose their distinct properties. The aim of the work in this first chapter was to learn the basic techniques of EC culture. While doing this, I also aimed to optimise and develop these techniques.

This work had three objectives:

1) To optimise the media used for HUVEC culture by analysing the proliferation of ECs in three different commercial formulations.
2) To examine the growth of cells on different bioengineered surfaces, using surfaces with potential clinical applications
3) To apply techniques of EC culture to develop a culture of zebrafish ECs

The number of, and reliance on, clinical applications based around *in vitro* models for angiogenesis is increasing and so it is growing more and more important to generate EC culture models.

3.2 Results

3.2.1 Optimisation of HUVEC culture

There are several different commercial sources of EC growth media. The lab usually uses Lonza EGM-2 as its primary EC culture formulation. There have been, however, recent problems with the supply of this media. The lab has since substituted Lonza EGM-2 with PromoCell EGM-2. However, HUVECs cultured in this media have recently had low proliferative rates. To assess possible alternatives, I analysed the proliferation of HUVEC in four different culture media. To do this, I calculated the number of cells present in each culture every 24h and observed trends in their growth. All three media

are composed of endothelial basal medium with additional supplements. The Lonza EGM-2 medium usually used by the lab contains the same supplements as the PromoCell EGM-2 medium, although these probably differ slightly in concentration. These supplements are refined, purified biochemical agents whose concentrations and activities will remain constant in every aliquot. PromoCell EGM, on the other hand, contains bovine pituitary extract, which contains crude versions of these components whose concentrations and activities will range depending on the aliquot. It will also contain undefined proteins present in the pituitary sample used, including bovine serum albumin (BSA). Two separate PromoCell EGM-2 were investigated; an aliquot of previously prepared EGM-2 that had caused low HUVEC proliferation (old PromoCell EGM-2), and an aliquot that was freshly prepared. This experiment seeded $3x10^4$ cells/mL into plates which were then cultured in each of the three different media. Every 24h the concentration of cells grown under the three different media was calculated. The rates of cell growth gave an indication of the best-suited media to HUVEC cell culture.

As shown in Figure 3.1, HUVEC cultured with Lonza EGM-2 media had greater proliferation than when using PromoCell EGM media (****$p \leq 0.0001$). This is to be expected, as EGM-2 culture media contain refined growth components whose concentrations reflect the requirements of HUVEC. EGM, however, contains crude components whose concentrations will not have been optimised for HUVEC growth and proliferation. Lonza EGM-2 media also gave greater proliferation than the freshly prepared PromoCell EGM-2 media (***$p \leq 0.001$). An anomaly occurred when HUVEC were cultured with an aliquot of PromoCell EGM-2 which had been suspended before this experiment. These HUVECs displayed no cell proliferation, and the number of cells declines within 24h after plating. By 72h there are no HUVEC surviving when incubated with this supply of PromoCell EGM-2 medium. It is likely that this supply of PromoCell EGM-2 did not contain all the growth components, or proper concentrations of these components, to support HUVEC growth and proliferation. HUVECs cultured in all four media show a likely decline in cell number at day 5. Thus, the optimal incubatory period is 4 days post seeding, after which the amount of growth components contained in the growth media begin to fall below that needed for cell survival and proliferation. HUVEC cultured with Lonza EGM-2 generally had the greatest observed cell proliferation at day 4 (max proliferation) and so this is the growth medium which should be used in all further HUVEC culture experiments in the lab.

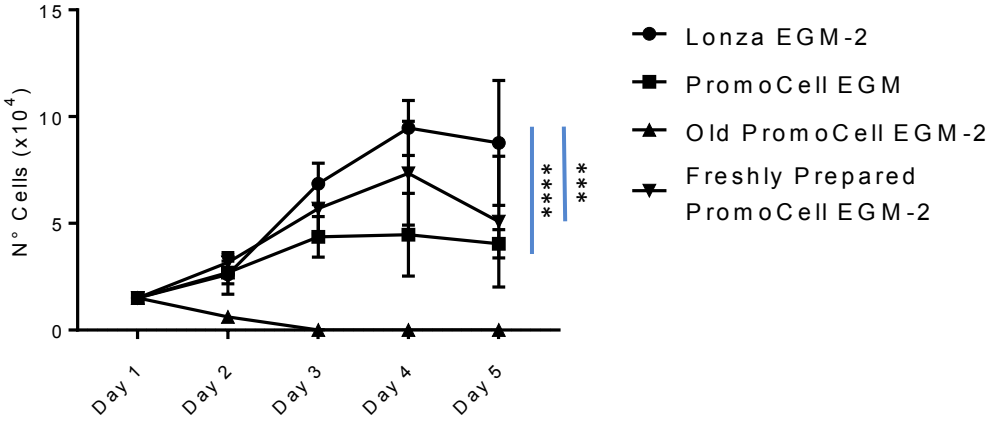

Figure 3.1 – Proliferation and survival of HUVEC differs when cultured in different culture media. ECs were seeded on coated 24-well plates at a concentration of $3x10^4$ cells/mL and cultured with Lonza EGM-2 (control) or PromoCell EGM, or with old or freshly aliquoted PromoCell EGM-2 media. Proliferation was analysed by counting fixed cells at 24, 48, 72, 96 and 118h after plating (days 1-5). Data shows the mean ± SEM of three experimental replicates. Statistical analysis was performed using a two-way ANOVA on all the data followed by a Tukey multiple comparison test on data obtained from day 4, ****p ≤ 0.0001 ***p ≤ 0.001

3.2.2 Confluency of HUVEC differs on different bioengineered surfaces

In cell culture, HUVECs are normally grown on either glass or plastic surfaces. In surgical implants such as stents that are placed in the coronary arteries of patients with atherosclerosis, the surface used is titanium (Ti). These biochemical surfaces need to be inert and anti-microbial so that they do not provoke an immune reaction and must also support the adherence and proliferation of the patient's ECs, which should ideally grow to cover the surface. Professor Bo Su, who works on the development of surfaces for biomedical applications, proposed titanium dioxide (TiO_2) as a potential surface for stenting [67]. This surface has a nanostructured architecture composed of filamentous protrusions with diameters of <50nm that repress the growth of bacteria by contact-dependent fission of bacterial surface membranes resulting in cell lysis and death [67]. The micro-structure has also been shown to increase the adherence and differentiation of physiological cells cultured on its surface by increasing the number of focal adhesion domains [68]. Specifically, it increases the number of phosphorylated focal adhesion kinase (pFAK) loci [68]. When phosphorylated, this kinase becomes activated and will initiate downstream signalling events promoting cell proliferation, survival, migration, invasion and angiogenesis.

I set out to study the culture of HUVEC on TiO_2 to ascertain the possibility of application of TiO_2 within this field. I used Ti and glass surfaces as controls, Ti not being modified by chemicophysical means and so representing a non-modified version of the TiO_2 surface that has a flat surface topology. It is also the surface currently used in prosthetic implant procedures in clinic. Glass is a good surface for HUVEC culture and is routinely used in the lab in cell culture assays. It was used to compare the efficacy of the TiO_2 and Ti surfaces for HUVEC culture. I seeded the HUVEC on the three different surfaces and then assessed their visual confluency after culture. Labelling their nuclei and actin cytoskeleton with DAPI and phalloidin respectively allowed the cells' confluency to be visualised using fluorescence microscopy.

Confluency of the cells was best achieved when HUVEC were cultured on glass coverslips (Figure 3.2) and when the surface was coated with fibronectin (FN), gelatine and collagen i.e. triple coat. The cell surfaces are in close contact with one another and appear as one monolayer. Cells grown on Ti are sparser than those grown on glass, with more gaps in the monolayer. Those HUVEC seeded onto TiO_2 formed islands of cells with gaps separating them from each other. The cells do not form a continuous monolayer with consistent cell-cell contacts and less cell spreading is observed. Furthermore, the control group where no coat was applied to the surface gave the least

confluent monolayer of HUVEC compared to the two coated surfaces. FN coating the surfaces allowed for somewhat confluent EC growth.

3.2.2.1 HUVEC cultured on TiO_2 surfaces exhibit markers of genetic instability

Whilst undergoing fluorescence microscopy analysis of the HUVEC grown on the three different biomaterials, markers for genetic instability were uncovered. Irregularities with the DAPI stained nuclei were seen. Some such irregularities were small pieces of DNA external to the main body of genetic information. There were additional thin bridges of DNA stretching from one nuclei to another across two separate cells. After inspection, these irregularities were determined to be micro-nuclei and chromatin bridges respectively (Figure 3.3). Both are caused by malfunctions in cellular division. Micro-nuclei are whole or fragmented chromosomes that fail to be incorporated into the nuclei of a daughter cell during cell division. Chromatin bridges are the result of end-end fusions of homologous chromosomes during metaphase, which fail to be resolved before interphase of the following cell cycle. Such features usually result in genetic alterations as the two daughter cells receive asymmetric genomes.

HUVEC cultured on the TiO_2 surface generally showed relatively more markers for genetic instability (Figure 3.4). HUVEC cultured on FN coated TiO_2, as well as HUVEC cultured on control TiO_2 , showed relatively greater amounts of micro-nuclei compared with corresponding coatings on glass or Ti (Figure 3.4a). However, HUVEC cultured on triple coated Ti showed a relatively greater percentage of micro-nuclei than HUVEC cultured on glass or Ti surface, and triple coated TiO_2.

In addition, TiO_2 generally gave a much greater percentage of chromatin bridges than the other two surfaces. As shown in Figure 3.4b, all three coated surfaces generated a higher percentage of chromatin bridges than any of the coatings on the other two surfaces. Aside from triple coated Ti, no chromatin bridges were observed in HUVEC cultured on glass and Ti surfaces.

The results acquired from this experiment cast doubt on the utility of TiO_2 as a surface for coronary angioplasty stenting, or indeed any other medical procedure where TiO_2 is used as a surface for cell growth. Because of this, I abandoned further research on these surfaces.

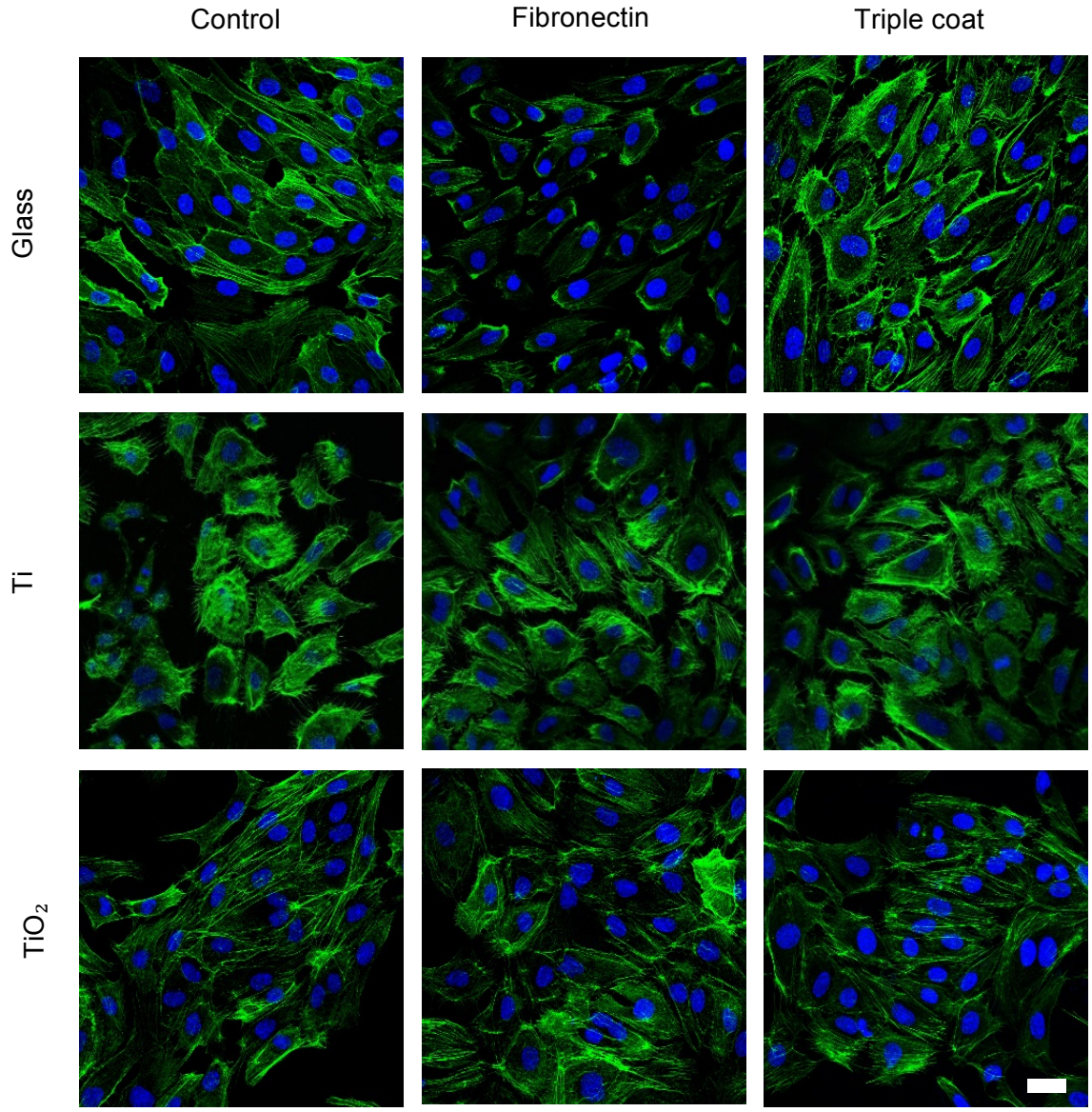

Figure 3.2 – Confluency of HUVEC depends on the surface and underlying substratum. HUVEC stained with DAPI and phalloidin to give visual indication of confluency and health of the cells. HUVEC were seeded on glass coverslips at a concentration of $6x10^4$ cells/mL and on Ti and TiO_2 surfaces at concentration of $2.6x10^5$ cells/mL before being cultured for 48h and then fixed and stained. (a) HUVEC seeded on glass coverslips developed into a confluent monolayer with cellular attachments. (b) HUVEC seeded on Ti surface gave moderately confluent monolayer of cells, however cellular junctions do not appear to have formed. (c) HUVEC seeded onto TiO_2 had a relatively low confluency, forming islands of cells rather than one continuous monolayer. (i) Control to compare the effect of using ECM components to coat the biomaterials. When no coat is applied, the cells struggle to form confluency. (ii) FN coated surfaces aid in allowing confluency, however the effect is greater with triple coated (FN, gelatine and collagen) surfaces (iii). Scale bar = 10um

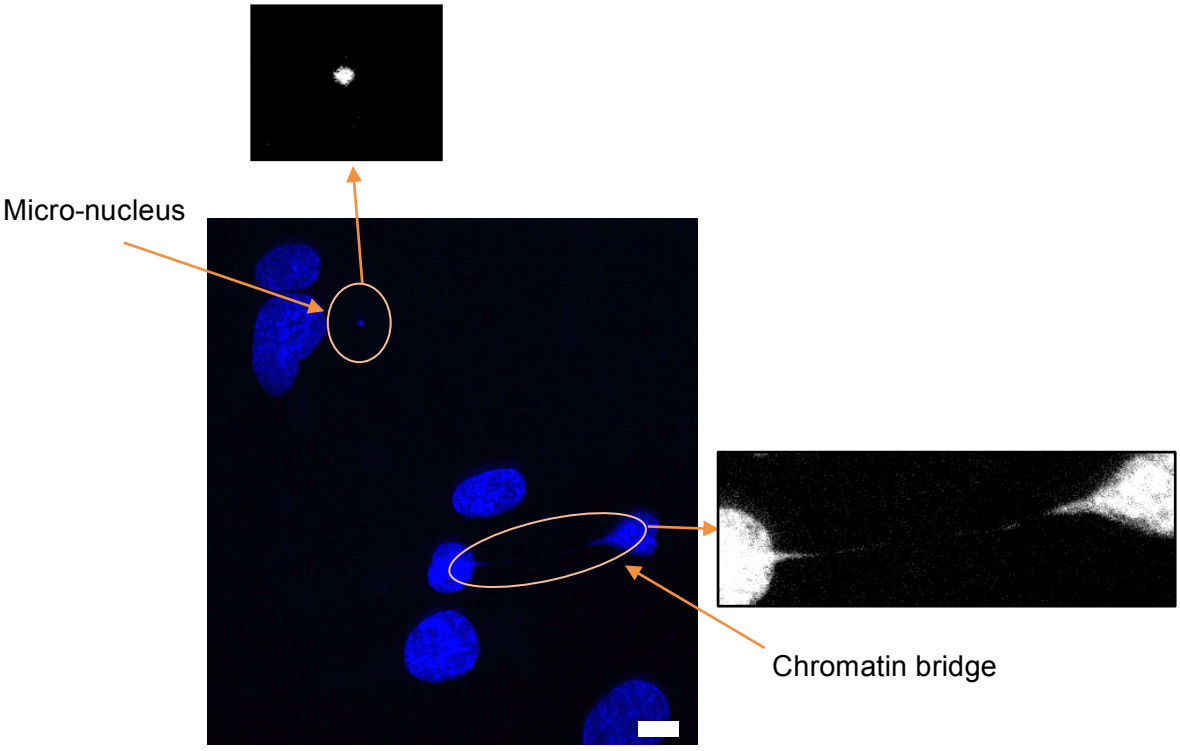

Figure 3.3 – HUVEC grown on TiO_2 display a greater number of micro-nuclei and chromatin bridges. HUVEC seeded onto TiO_2 biomaterial at $2x10^5$ cells/mL were fixed and DAPI stained after 48h. Confocal microscopy images reveal DNA that is surrounded by a nuclear envelope but external to the main body of nuclear material (micro-nuclei) and genetic linkages between two daughter cells exiting mitosis (chromatin bridges). The image taken above is from HUVEC cultured on FN coated TiO_2. Figure shows RGB channel for original image displaying both micronucleus and chromatin bridge. Also shown is single channel (blue) for both features, which have been enlarged for ease of visualisation. Scale bar = 10μm

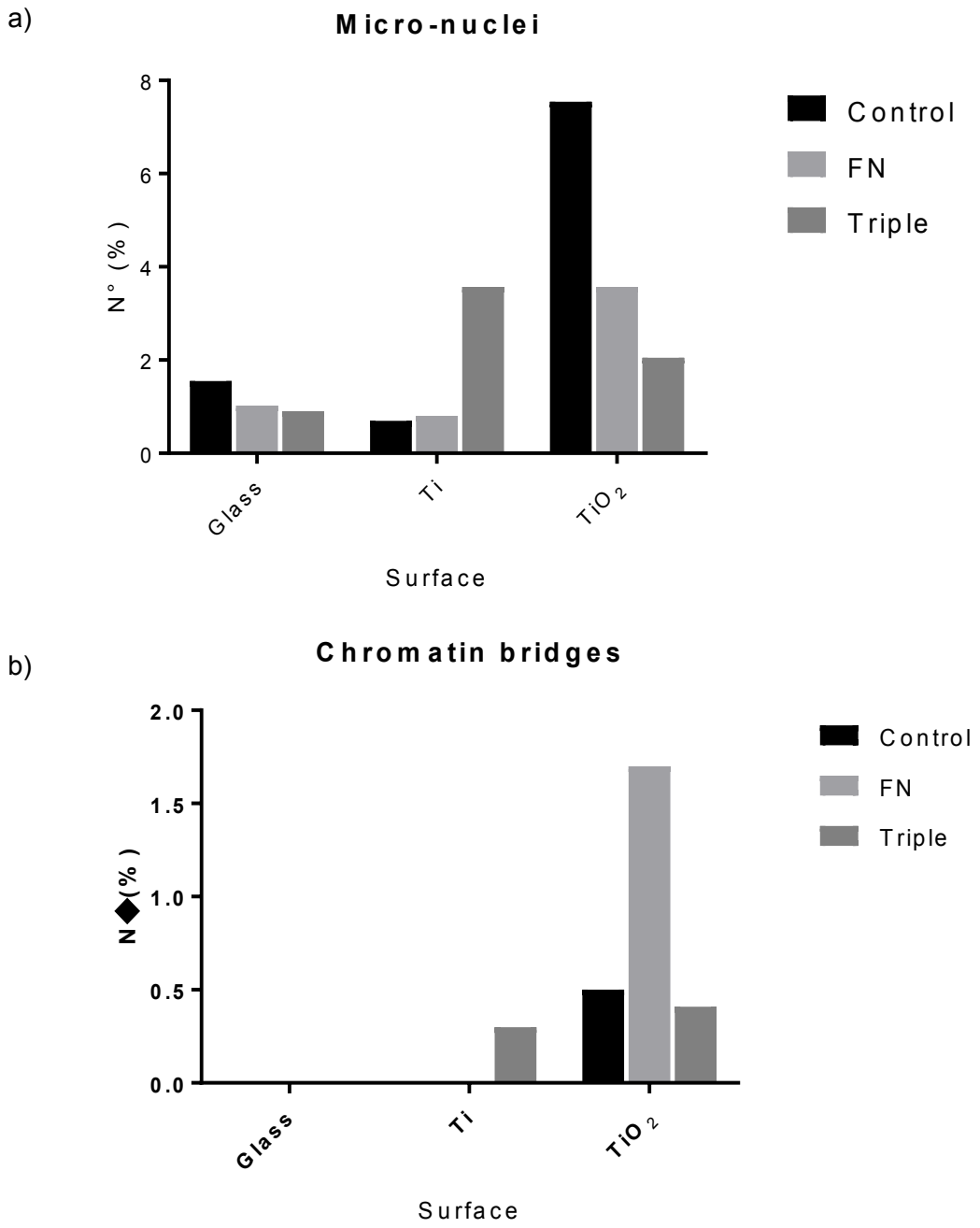

Figure 3.4 – Disparity of two genetic instability markers, micro-nuclei and chromatin bridges, across three biomaterials and surface coats. The number of cells and cells with genetic instability markers were counted on microscope slides using a widefield microscope. % micro-nuclei and % chromatin bridges were calculated using this data. Each surface was coated with either FN or a triple coat of FN, gelatine and collagen, or kept uncoated as a control. TiO_2 generally generated the greatest amount of genetic instability for both markers. Data shows % micro-nuclei/chromatin bridges across cells counted across 8 fields of view for each surface and coat.

3.2.3 An *In vitro* model for transgenic zebrafish larvae endothelial cells

The use of zebrafish as a model organism to understand human disease and physiology is increasing. Zebrafish are easier to genetically manipulate, inexpensive and suitable for larger scale genetic studies [69]. It is advantageous to use them as a model organism over a mammalian organism, such as a rat, as these have ethical, time scale and expense deficiencies.

Having an *in vivo* human model would be useful when modelling human physiology and disease. However, this is not possible due to ethical restraints. The use of human cells is therefore limited to *in vitro* models. In contrast, there are far fewer ethical restraints on making *in vivo* models using zebrafish. Further to this, their early development occurs externally, and zebrafish embryos are nearly transparent. This makes it possible to study their internal physiology and anatomy during early development using a low magnification microscope. These *in vivo* models are useful for studying processes and structures that occur in their physiological niche. *In vitro* models, however, would complement these as they are high throughput and simpler thus providing faster and more robust results that can form the basis of further *in vivo* studies. I therefore wanted to create an *in vitro* model for zebrafish EC culture. Complementing current zebrafish vasculature *in vivo* models would provide valuable information which could have clinical applications.

My research is based on the study of ECs taken from human sources. I therefore wanted to use this technical knowledge to develop a protocol for the culture of zebrafish ECs. To achieve this, I cultured fluorescent transgenic zebrafish larvae ECs that were labelled with Tg(fli1a:EGFP) marker on coated plastic plates and stained them with DAPI in order to count them. Fli1 is a strong promoter, which belongs to the ETS transcription factor family [70]. This family of proteins is critical for the development of the vasculature. It is therefore present in ECs across the entire vasculature, hence GFP is highly expressed in these cells providing a distinguishable marker for the endothelium. These transgenic ECs were obtained from zebrafish larvae at four days post fertilisation (dpf), and were cell sorted using fluorescence-activated cell sorting technique.

In particular, I focussed on the growth rate of zebrafish ECs in culture, and on optimising this protocol to obtain a useful concentration of ECs that could be used for further experimentation. It is known that HUVECs reach confluency when in cell culture medium at around 48h, and so I wanted to investigate whether the same was also true in zebrafish ECs. A growth curve experiment was set up to determine an optimum incubatory period to reach confluency. As shown in Figure 3.5, the zebrafish EC number

grew little if at all up to 48h. After this, the cell number begins to decline. Overall, there is no extensive zebrafish EC proliferation that would otherwise be seen in HUVEC cell culture.

To give visual representation of their confluency, zebrafish ECs were fixed and stained with DAPI (Figure 3.6). Preliminary cultures, using a 12-well plate, gave low confluency of the ECs (Figure 3.6a-c), the sparsity of the cells meant generally only single cells could be imaged. The cells in this experiment had an array of different morphologies which look dissimilar to that of normal ECs. ECs are usually elongated polygons, predominantly hexagonal. The five cells shown in Figure 3.6a-c possess large differences in morphology from one another. Figure 3.6a shows a cell with filamentous projections coming out from the main body of the cell, which suggests that it is a dendritic cell. Figure 3.6b shows a small, spherical cell with a large nucleus with a diameter of about 7-10μm, characteristic of a lymphocyte. The other cell in Figure 3.6b, and those in Figure 3.6c, have morphologies that is more characteristic of ECs. One of the cells in Figure 3.6c appears to be engulfing another cell or fragment of a cell. This is not a characterism of an EC, and so casts doubt regarding the purity of these sorted cells.

Secondary experiments using a 96-well plate gave higher concentrations of the seeded zebrafish ECs, and as a result a greater confluency. Despite achieving greater confluency, the zebrafish ECs did not form normal cell-cell junctions. Figure 3.6d+e shows that junctions form at regions of the plasma membrane that are relatively spaced out from one junction to the next. The main body of the cells are also more condensed than that seen characteristically in ECs. This gives a more fibrillar morphology of the cells, as region of the plasma membrane that form the cell-cell junctions must stretch further away from the cell body to form cellular connections. Despite the relative abnormality in the cellular junctions seen in these cells compared to normal ECs, their morphology is much more like that of normal ECs. Lastly, the cells grown in 12-well plates as shown in Figure 3.6a-c have a relatively greater diameter compared to the cells grown in 96-well plates as shown in Figure 3.6d+e. It appears that when zebrafish cells are grown in culture plates with a greater surface area, the greater the diameter of the cell.

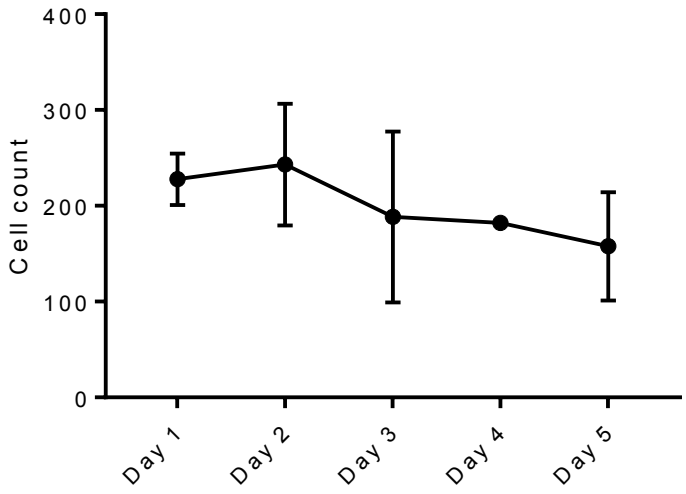

Figure 3.5 – Growth curve for zebrafish endothelial cells cultured over five consecutive days. Zebrafish ECs were cultured in a 96-well plate in Lonza EGM-2 media supplemented with Normocin and images of ECs were taken using a widefield imaging microscope. Fluorescent Tg(fli1a:EGFP) marker and DAPI staining allowed visualisation of the cells. Number of cells was counted in 3 random fields of view for each day. The number of cells was averaged across three measurements. The starting concentration of cells was $6x10^4$ cells/mL in 200µL EGM-2. Data shows mean ± SEM of three experimental replicates.

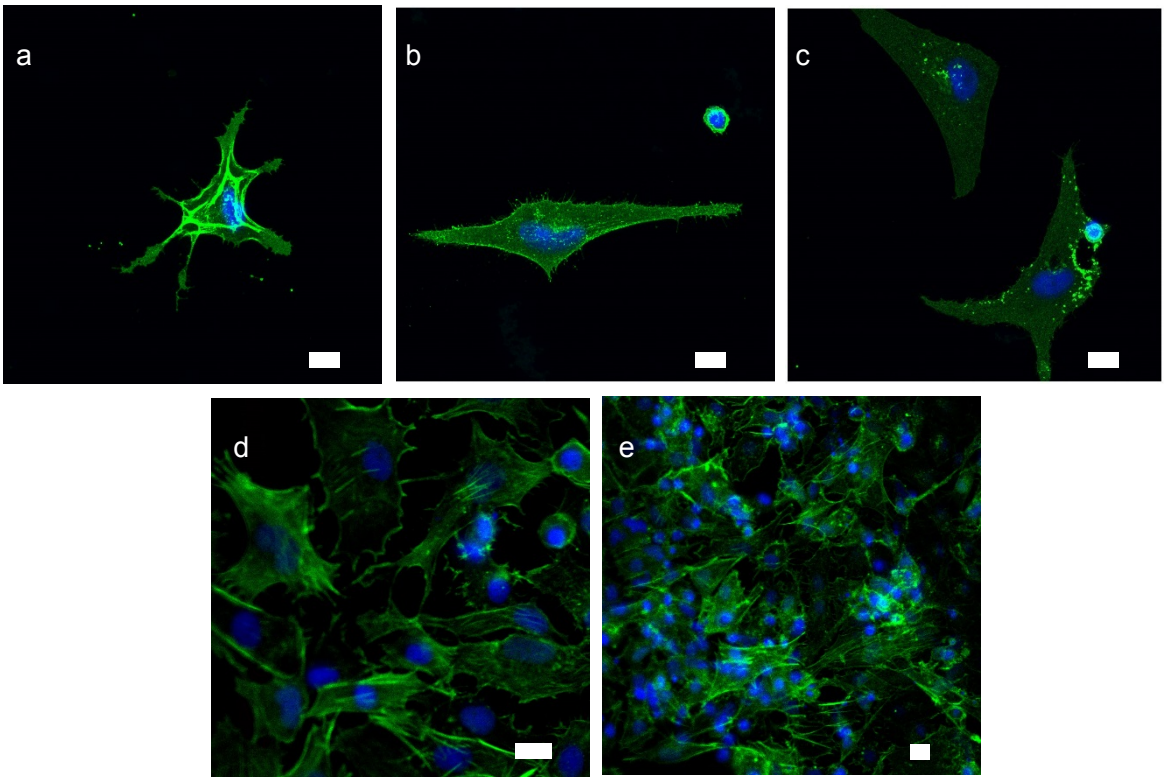

Figure 3.6 – Fluorescent transgenic (Tg(fli1a:EGFP) zebrafish sorted from whole larvae using FACS and cultured on coated plates. Representative confocal images for transgenic zebrafish with GFP driven expression by Fli1 EC promoter in as a cytosolic marker for endothelial cells. DAPI staining of nuclei carried out after fixation. (a-c) Individual zebrafish ECs in 12-well plate where cells lacked confluency. (d+e) ECs cultured in 96-well plate to greater confluency. ECs in d+e stained with phalloidin to visualise their actin filaments. Scale bars shown = 10μm.

1.3 Discussion

The findings from this set of data successfully determined that the HUVEC culture media that allows for the greatest cell proliferation and survival is Lonza EGM-2. This is the HUVEC growth medium that is normally used in the lab, whose supply has been discontinued. Until it is re-distributed, PromoCell EGM-2 should be used instead, as the HUVEC proliferation assay using this media had the second-best growth curve.

Once the correct media for proper HUVEC culture was established, further cell culture experiments could be carried out. Initially, the work on this chapter was based on research carried out by Professor Bo Su and colleagues [63]. They had proposed a novel surface for clinical applications that is biocompatible and has bacteriocidal properties. This surface, TiO_2, has nanopillar patterns which physically burst gram-negative bacteria that come into direct contact with the surface. Professor Su had observed a dramatic decrease in bacterial cell viability when gram negative bacteria were cultured on nanopatterned TiO_2 surfaces [67]. Further to this, Park et al investigated the capability of this surface to support physiological cells [68]. It was found that TiO_2 nanopillars support, rather than prevent, cell proliferation on their surface when nanotubes were spaced between 15-30nm apart. I wanted to determine whether HUVEC growth and proliferation could be supported on TiO_2 coated surfaces, using glass and Ti surfaces as controls. As shown in Figure 3.2, HUVEC achieved the best confluency when seeded on glass coverslips, with the worst confluency observed on TiO_2. Delineating the results from this experiment, it can be said that TiO_2 does not prevent HUVEC growth on its surface, however neither does it properly support HUVEC growth and proliferation.

In studying HUVEC culture on different surfaces, it was discovered that TiO_2 generated markers of genetic instability in the HUVECs. Interestingly, HUVEC cultured on TiO_2 displayed a considerably greater number of micro-nuclei and chromatin bridges, as a % of total nuclei, than HUVEC grown on glass and Ti surfaces (Figure 3.4). These genetic instability markers within cells have a high chance to manifest as genomic alterations, potentially leading to tumourigenesis. This, taken together with data from Figure 3.2, casts doubt on the use for TiO_2 in clinical applications. Its effect on HUVECs cultured on its surface needs to be investigated further to deduce all of its potentially hazardous cellular effects before it can be applied in a human.

One of the aims of the work in this chapter was to successfully develop a culture of zebrafish ECs. To be successful, this would involve the ECs attaching to the surface of the culture plate before proliferating and attaining enough cell survival to maintain the

culture for a number of days. Results from Figure 3.5 show that, when cultured in EGM-2 supplemented with Normocin, the transgenic zebrafish larvae ECs were successfully seeded, and maintained at a relatively stable concentration for around 48h. Normocin is an antimicrobial reagent, active against gram-positive and gram-negative bacteria, as well as against fungi. It was added to the EGM-2 cultured zebrafish ECs as initial conditions promoted the growth of fungi in the cell culture. Advanced contaminations with fungi cause increases in pH in the culture. This, together with competition for growth factors and other components required for cell viability and growth, causes a decline in cell number in the culture. Despite EGM-2 being supplemented with Normocin, the zebrafish EC number dropped after this point, suggesting that the cell culture conditions were not optimal for proliferation. Compared to HUVEC cell culture, the proliferation of these zebrafish ECs is much lower. EGM-2 is optimised for HUVEC cell culture, and so this may not provide the amounts and/or types of growth components necessary for rapid zebrafish EC proliferation due to differences in growth factor requirements across species. Fetal bovine serum (FBS) could be used to supplement the EGM-2 cell culture medium used; EGM-2 media used within the lab does not contain any serum, just purified growth factors and cytokines. FBS contains an array of crude growth factors and is more versatile for a variety of different cell culture applications. Reducing the surface: volume ratio of the culture plate from a 12-well to a 96-well plate improved the resulting confluency of the ECs and hence this optimised protocol has greater application for further experiments. Thus, this is a good starting point in producing a zebrafish EC culture protocol, however there is a lot of scope for optimisation, especially regarding optimising a culture medium.

Additionally, the morphologies of the zebrafish ECs, as shown in Figure 3.6a-c, do not conform to usual ECs. This suggests that cells other than ECs were sorted by FACS and cultured alongside cells containing the GFP marker. The Fli1 gene is present in all hematopoietic cell lineages, as well as in lung, heart and ovary tissue [50]. During site specific recombination of the Fli1:GFP construct there may have been incorporation into these other cell types. If these cells express GFP, they will be sorted as ECs by FACS and be included in the cell culture. Both dendritic cells and lymphocytes are a part of the hematopoietic cell lineage and so have the potential to gain the Fli1:GFP construct and become fluorescently labelled. A further method of cell sorting would be required to obtain a purer culture of zebrafish ECs.

Work in this chapter was intended to optimise various endothelial assays, but also to allow me to gain training in EC culture. By the end of this primary work, I was confident to continue to develop a more complicated assay.

Chapter 4 Adaptation of an *in vitro* angiogenesis assay to study tumour angiogenesis

4.1 Introduction

The development of several different *in vitro* co-culture assays has allowed two or more different cell types, either primary or cell line derived, to be cultured in concert. This level of cellular interaction means that their environment more closely resembles that of their physiological niche. The Mellor lab, where I am based, uses a well characterised co-culture assay to study angiogenesis [71]. The original assay combines primary endothelial cells (HUVECs) together with primary fibroblasts (NHDFs) in a 1:1 ratio simultaneously [72]. Over the course of 7-14 days the endothelial cells mature into tubules that form a dense network as a direct result of cellular interactions [71]. The interaction between these two cell types and that of the endothelial cells with the ECM is the driving force for blood vessel development. As occurs *in vivo*, the fibroblasts remodel the ECM into fibrillar collagen to support the tubulation of the ECs [73]. After a period of 5-10 days the co-culture will be a dense network of branching ECs – cellular branches extend into the X-Y plane and into the Z plane forming layers of capillary-like vessels that result in a 3D network [74].

My work with the Mellor lab involved the study of tumour angiogenesis. My goal was to adapt the co-culture assay used to study angiogenesis into one which investigates tumour angiogenesis. This adaptation uses 3D tumour cell spheroids and seeds them onto the well characterised co-culture assay once the co-culture becomes confluent. The 3D nature of the tumour cell clusters means that the tumour angiogenic effect is localised and the cancer cells are in an environment that closely resembles that *in vivo.* This assay can be used to quantitatively and visually assess the angiogenic effect of different tumours and hence give some indication of their aggressiveness.

This work had the following aims:

1. Form 3D spheroids of SW480 cell lines to recapitulate *in vivo* tumour architecture
2. Validate an SW480 cell line that has been virally transduced with VEGF
3. Adapt an angiogenic co-culture protocol to a tumour angiogenic co-culture assay
4. In doing so, optimise the protocol to gain best density of blood vessels for ease of quantification

4.2 Results

4.2.1 SW480 cancer cells can form 3D spheroids when combined with methylcellulose

The cancer cell line chosen was SW480, a colorectal adenocarcinoma line. This line was chosen for its growth pattern reproducibility in culture. The growth rate of these cells is relatively constant throughout the entire culture, meaning a similar number of SW480 cells are in each spheroid and so the angiogenic effect of each type of spheroid will be similar. SW480 cells are also at a relatively low stage of epithelial-mesenchymal transition and hence still maintain some E-cadherin junctions. In this experiment, some cell-cell contact is necessary to form multi-cellular spheroids where cells must directly bind one another and the ECM. The tumour stage was therefore picked to match the *in vitro* model.

Culturing cell lines in 3D allows for *in vivo* architectures to be generated, providing a platform for complex cellular interactions to occur. Several 3D cell culture protocols exist involving either scaffold-based 3D-models or scaffold free models (liquid based) [75]. In this experiment, I used scaffold-free systems as this promotes the endogenous production of ECM components and hence more closely resembles an *in vivo* scenario. By using the hanging drop method, multi-cellular SW480 aggregates form, mimicking their *in vivo* architecture. These so called spheroids [75] are composed of several hundred cancer cells which aggregate into clusters at the apex of a drop of media suspended on the lid of a tissue culture dish (Figure 4.1). As shown (Figure 4.1a) the SW480 cells form viscous droplets when combined with methylcellulose that can be cultured by the hanging-drop method when inverted in a tissue culture dish lid. These spheroids vary in size (Figure 4.1b) and become dispersed evenly within the methylcellulose. Methylcellulose, a derivative of cellulose, was chosen for its high viscosity when dissolved in water, which allows for the localised clumping of the cancer cells.

4.2.1.1 Validation of the SW480 V cell line

Jimmy Wei, a PhD researcher within my lab, created a stable SW480 cell line that overexpresses VEGF (SW480 V). High VEGF levels have a close association with high blood vessel density at the site of a tumour, and poor disease prognosis. I set out to validate the SW480 V cell line by comparing the secretion of VEGF from SW480 V and

a

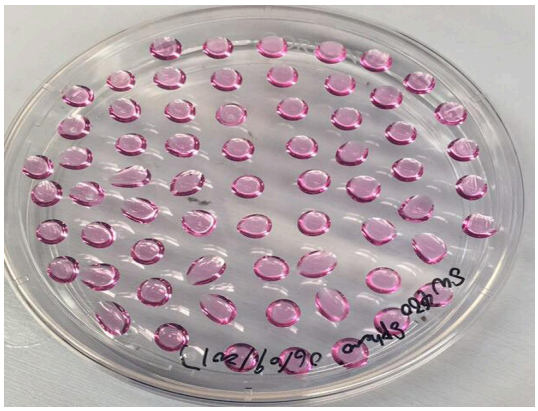

b

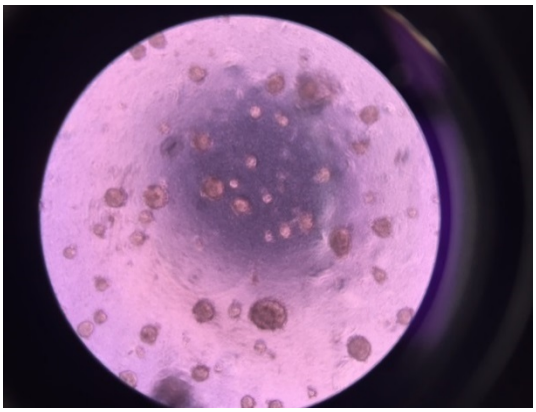

Figure 4.1. Images of the hanging-drop method for cell culture. (a) 30µl droplets of methylcellulose plated onto the lid of a petri dish, each containing roughly 1000 SW480 cells. The lid is inverted above 20mL PBS and incubated at 37°C/5% CO_2. (b) Multi-cellular aggregates of SW480 cells present at the apex of a droplet of methylcellulose. Images taken by light microscopy.

the SW480 parental cell line (SW480 P). In order to do this, I carried out an ELISA to quantitatively measure the amount of VEGF in the medium from SW480 V and P cell cultures.

By first constructing a standard curve, validation of the relationship between absorbance and VEGF concentration could be deduced. Using a recombinant standard VEGF solution, I found that the curve had a positive correlation, with each point following the curve closely (Figure 4.2a). Interestingly, I found that SW480 P secretes little or no VEGF (Figure 4.2b). This does not follow the general assumption that tumour cells upregulate VEGF production. SW480 V secretes relatively much more VEGF than SW480 P, with concentrations in the medium at around 80 pg/mL ($P<0.01$). The average VEGF concentration in peripheral venous plasma, with samples taken from 2833 patients totally a wide variety of cancer types, is 328 pg/ml [76]. The SW480 cell line obtained is likely to have lost some of its tumour properties during passaging and so its capacity to express and secrete VEGF will have declined.

The average VEGF concentration was calculated for both cell lines (Figure 4.2b). To determine how homologous the expression of VEGF was from each cell line, I carried out an immunofluorescence protocol. SW480 P had no visible expression of VEGF (Figure 4.3a) shown by the lack of green signal that would have been generated by the Alexa Fluor® 488-conjugated secondary antibody. Conversely, SW480 V produces VEGF in much greater amounts (Figure 4.2+4.3b). The staining shows signal in vesicles around the nucleus and in areas beneath the cell. The latter suggests that this VEGF is being secreted and subsequently trapped by components of the ECM. Since the VEGF signal is relatively evenly dispersed across all the cells, they must all be secreting VEGF and have therefore been successfully transduced by the lentivirus.

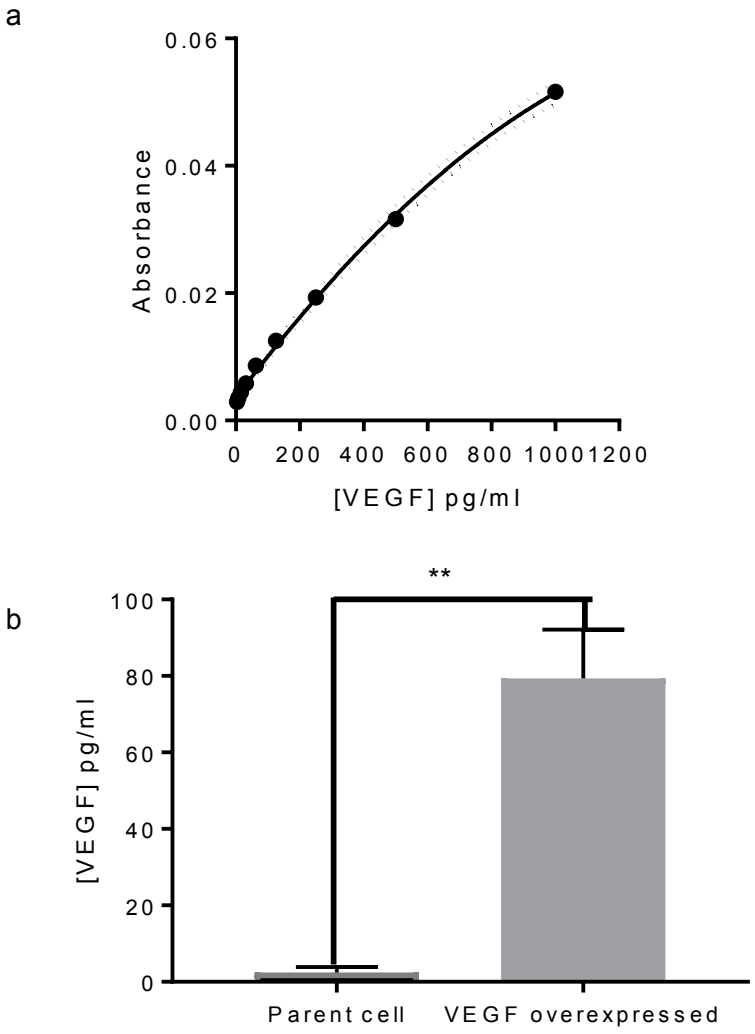

Figure 4.2 – Concentration of VEGF secreted from SW480 P and SW480 V cells. SW480 V secretes significantly higher amounts of VEGF compared to SW480 P when ELISA was performed to quantitatively measure VEGF concentration. (a) A two-fold serial dilution of standard VEGF solution was made to create a 7-point curve, showing the association between VEGF concentration and absorbance at 492nm. (b) Average [VEGF] secreted by SW480 V + P was calculated using the standard curve and A492nm values. Samples were taken from both cell lines, seeded at concentrations of $1x10^5$ cells/ml for 48 hrs, by collection of medium. SW480 V secreted more VEGF than the parental cell line. Statistical analysis was performed using a Student's t-test, **P<0.01. Data are means +/- SEM of three experimental replicates.

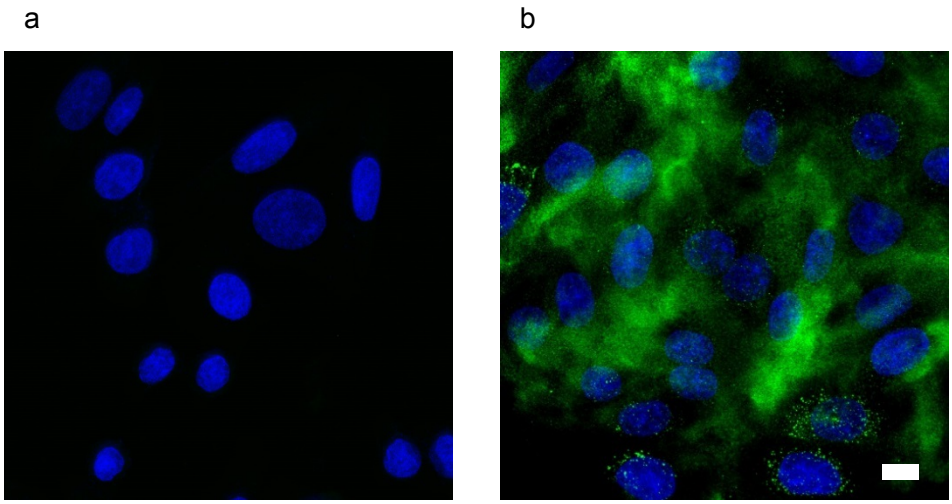

Figure 4.3 – VEGF immunofluorescence staining of SW480 P and SW480 V cells. SW480 P and SW480 V cells were seeded onto coverslips at a concentration of $1x10^5$ cells/ml. Cells were exposed to DAPI and anti-human VEGF antibody with compatible fluorescently labelled secondary antibody to stain for nuclei and VEGF secretions respectively. Cells were imaged by confocal microscopy to visualise their locations. (a) SW480 parental cell line shows only DAPI staining. (b) SW480 V shows DAPI staining and staining for both vesicular VEGF and VEGF 'clouds'. Scale bar shown = 10μm.

4.2.2 Adaptation and optimisation of the tumour angiogenesis assay

As already discussed, there is a well-established protocol for the co-culture of NHDF and HUVEC (angiogenesis assay). Here, I am building on the adaptation of this protocol, integrating 3D tumour spheroids into the co-culture. This tumour angiogenesis assay gave quantitative data as to whether SW480 V promoted angiogenesis, relative to SW480 P. There had, however, been difficulties in determining whether there was a directionality of the blood vessels that was caused by the SW480 spheroids. The density of the blood vessels had to be optimal for the assay for blood vessel directionality to be distinguished. They must not be too dense, as there is a high chance that the SW480 spheroids would be seeded directly onto vasculature. This would give no indication as to whether the blood vessels are responding to the spheroid or not as there would be little or no movement away from the spheroid. If the blood vessels are too sparse however, they may be at too great a distance away from the spheroids that they cannot respond to the VEGF gradient. It would also be hard to tell if the direction the blood vessels are growing towards is due to the spheroids, or due to chance alone. The density is dependent on the incubation period of the co-culture after HUVEC and tumour spheroids have been seeded. I therefore set up a time course experiment whereby the incubation times for these two events in the co-culture differed, resulting in four different alternates.

Qualitative analysis of the co-cultures once they had been fixed and stained for PECAM-1 revealed that the best time to seed the spheroids was +1 day after the HUVEC were seeded. Once the spheroids were seeded onto the co-culture, day 4 was found to be the optimal day to fix and stain the co-culture. This was the best amount of time for vascular growth to be able to determine any directional influence by the spheroids. Figure 4.5a+b shows an example of an assay with this time course. The density of blood vessels is great enough that it is possible to tell if vascular branching is directed towards the spheroid that hasn't occurred by chance alone. It is not too dense that it is likely the spheroids will be seeded directly onto the blood vessels that make it difficult to quantify the number of branches. The spheroids have become embedded within the co-culture, with blood vessels growing above the plane of the spheroids. As shown in Figure 4.5a, SW480 P spheroids typically have less branching of blood vessels towards them that are also less dense. In comparison, SW480 V have a greater number of and more densely branching vessels towards the spheroids, as shown in Figure 4.5b. These are typical images taken of the co-cultures containing the two lines of SW480 cell. Due to the amount of time is takes for a co-culture to be established after

initial seeding of the NHDFs, I did not have enough time during my MRes to achieve n=3 for each different time course. I could not therefore perform any quantitative or statistical analysis on the data sets.

a b

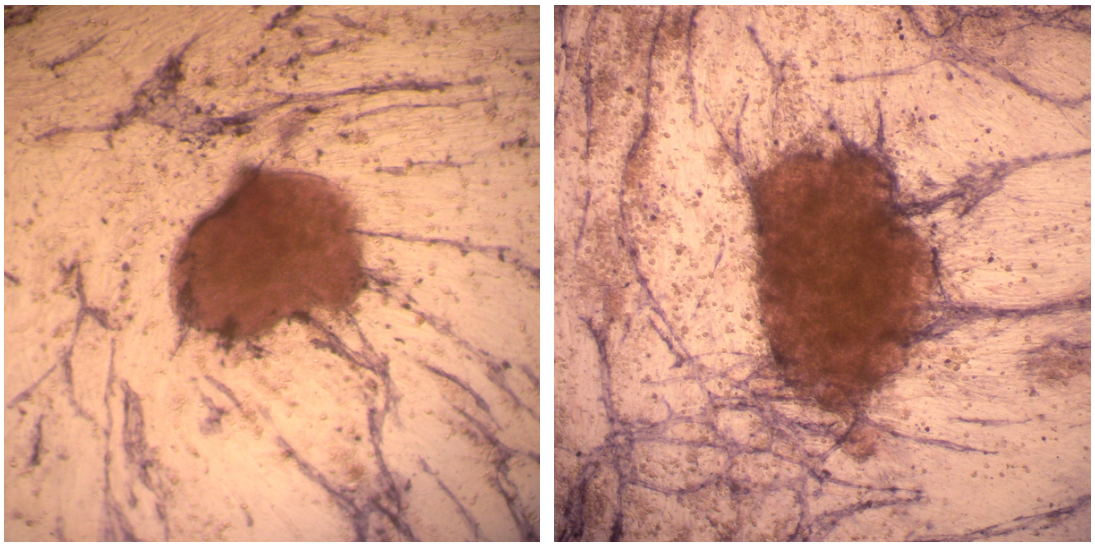

Figure 4.4 – *In vitro* tumour angiogenesis assay. NHDF and HUVEC were co-cultured at concentrations of $3x10^4$ cells/mL and $6x10^4$ cells/mL in 12-well plates respectively until confluent and then SW480 P (a) and SW480 V (b) spheroids were seeded. An optimum time to seed the spheroids after the HUVEC were seeded was +1 day. Images were taken once the cells were fixed and stained with anti-PECAM-1 on day 4. (a) An SW480 P spheroid in co-culture with PECAM-1 stained vasculature. Fewer blood vessels have branches growing towards the spheroid. (b) SW480 V in co-culture, vasculature is PECAM-1 stained. More blood vessels have branches growing toward the spheroid and there is a higher density of vasculature.

4.3 Discussion

The results from this chapter are encouraging, however without quantification or statistical analysis of the blood vessel growth towards the spheroids, no conclusion can be made as to the effect of VEGF. It is well established that VEGF is a pro-angiogenic factor, and its expression is upregulated in a number of cancer cell lines. The effect of upregulating VEGF in SW480 cells on blood vasculature was examined. This upregulation of $VEGF_{165}$ in SW480 cells, a stable cell line created by Jimmy Wei, was first validated using an immunofluorescence assay. As shown in Figure 4.2, the stable cell line overexpressing VEGF produces a greater amount of VEGF than its parent cell line. The immunofluorescence captured in Figure 4.3 shows the VEGF being secreted in vesicles. The clouds of Alexa Fluor 488 signal that exist apart from the vesicular VEGF suggest that the VEGF is being tethered outside of the cell, most probably by the ECM. Indeed, $VEGF_{189}$ and$_{296}$ isoforms have previously shown to localise to the ECM [77] and so $VEGF_{165}$ would probably follow the same secretion pathway. This immobilisation of the VEGF will create a local gradient to the SW480 cells, with a high relative concentration close to the SW480 V that decreases in concentration as distance from the SW480 V lengthens. $VEGF_{165}$ has moderate tethering to the ECM and so it will have a gradually declining concentration gradient. This VEGF inclination allows ECs to migrate towards the VEGF secreting cells, responding to this growth factor binding to their VEGF receptors and initiating intracellular signalling events leading to forward movement. In tumour physiology, this promotes angiogenesis towards the cancer cells. Since this VEGF is trapped in the ECM it was not collected in the cell medium and hence would not have been included in the ELISA [VEGF]. Thus, the true concentration of VEGF secreted by the SW480 V cell line would be greater than that calculated by the ELISA. *In vivo*, VEGF receptors are saturated at ~10ng/mL. The ELISA conducted using the SW480 P and V samples showed that SW480 V secrete ~1/100 of this. However, the ELISA used medium taken from SW480 V and SW480 P cells in culture, which would combine all the VEGF secreted by the cells in the culture dish and is assumed to be evenly spread throughout all the cells. In practice, VEGF secretions form SW480 cells will be more localised, allowing for a gradient of VEGF to be established.

As shown in Figure 4.1, these SW480 cell lines were able to be encapsulated into droplets composed of methylcellulose. Using the hanging droplet method of cell suspension, the SW480 cells were evenly distributed within the droplets. This clustering of SW480 cells localises their secretions. Hence, the local concentration of VEGF around the spheroids will be greater than that found by the ELISA. The effect of this localised VEGF on blood vessel growth was then examined in EC and NHDF co-culture.

An *in vitro* tumour angiogenesis assay was set up to investigate the effect of both SW480 cell lines on blood vessel growth. A co-culture was established between NHDFs and ECs until blood vessels reached maturity. After SW480 spheroids were seeded and finished their incubatory period, changes in the vasculature were observed. Results from this assay suggest to a potential link between VEGF secretion by SW480 cells and the local growth of blood vessels. Figure 4.5 shows the density and general directionality of blood vessels surrounding randomly chosen spheroids of SW480 V and SW480 P tumour cells. The co-culture containing SW480 P cells has visibly a lower density of blood vessels surrounding the spheroid than the co-culture with SW480 V cells. These spheroids in figure 4.5 were chosen at random for each co-culture, and so the outcome of each can be presumed to follow a general trend for each of the cell lines. However, as discussed, there can be no conclusive remark on whether VEGF secreted from SW480 spheroids has an effect on blood vessel growth due to the lack of experimental replicates for each time course. This is a preliminary experiment requiring further co-culture repeats using the time-course suggested by this chapter. Quantitative analysis should then be carried out to assess statistical significance between SW480 P and SW480 V on blood vasculature growth.

Chapter 5 Surface protein labelling of HUVEC

5.1 Introduction

All types of cell have an underlying cell polarity. One aspect of their cellular polarity is the distribution of surface membrane proteins. Membrane proteins provide the characteristic functioning of a particular type and region of membrane. The type of protein and its relative amount in a membrane controls the biochemical activity in that region. For instance, the inner mitochondrial membrane functions to generate ATP using an electrochemical gradient by being endowed with transmembrane ATPase [78]. This allows the inner mitochondrial membrane to have a distinct function that is different to other organelles. Certain membrane proteins have an asymmetric distribution, being present in greater amounts at the apical or basolateral surface of the cell. Conversely, they may be non-polarised and be equally distributed at either surface. Transport proteins are present within the membrane separating two compartments. The presence of these carriers at the membrane allows selective transport across this particular membrane [79]. For instance, GLUT-4 is present at the apical surface of adipocytes and striated muscle cells. Here, it allows the facilitated diffusion of glucose down its concentration gradient from interstitial fluid and into the cytoplasm of adipocytes and muscle cells [80]. Due to the fluidity within cell membranes, cells have methods of restricting lateral diffusion of membrane proteins to maintain membrane protein distribution. Tight junctions are a specialised type of adherence complex that hold cells together at their lateral surface to create a tight, continuous layer of cells [2]. As these tight junctions are transmembrane, they also serve as a molecular fence to prevent the lateral movement of surface proteins within the membrane of the cell.

Determining the polarity of membrane proteins within different cell types is an ongoing challenge. Epithelial cell surface protein polarity has been studied in detail and so there exists an in-depth list of proteins whose surface distribution has been determined. Contrastingly, there is much less known about the polarity of ECs. Recent research has elucidated, however, the polarity of two membrane proteins present within neural microvascular ECs (MVECs) [38]. The polarised receptor distribution of VEGFR1 and VEGFR2 allows for distinct signalling responses to VEGF-A, an isoform of VEGF that is present in both luminal and abluminal tissue. It was proposed that the response of VEGFR1, present predominantly at the apical surface of MVECs, to VEGF-A is one of cytoprotection. VEGFR2, which is predominantly abluminal, binds to VEGF-A and initiates a response to induce increased cell permeability. This research suggests that there is further scope for determining EC surface membrane protein polarity.

The aim of the work in this chapter was to further investigate the polarity of membrane proteins in HUVECs. I aimed to separately label its surface membrane proteins in order to detect for specific proteins on the apical and basolateral surface. To validate this method of surface protein labelling, I used immunofluorescence to directly stain for proteins at the apical and basolateral surface of HUVEC and compared the results of this with that obtained from the surface protein label.

5.2 Results

5.2.1 Production of a confluent, polarised HUVEC monolayer

When cells are cultured on surfaces, they adhere to this surface via adhesion complexes present at their basal surface. Thus, reagents cannot gain access to this surface of the cells. Adding labelling reagents to the culture medium will mainly label the apical surface. To resolve this issue, Transwell membrane inserts were used. These are permeable devices that support cell culture on their surfaces and allows for passive transport of molecules through to reach the basal surfaces of the cells. They allow small molecules to enter through the 0.4μm polyester membrane pores, and then reach the basal surfaces of the cell culture. The separation of solutions at the apical and basolateral surfaces of the cells seeded onto the Transwell, together with its permeability, allows these two surfaces to be separately labelled.

For the two surfaces of the cells to be separately labelled, there must be stable cell-cell junctions with no gaps in the monolayer. The confluent monolayer reduces the likelihood of the biotinylating reagent being able to diffuse through the cell monolayer and incorrectly labelling the opposite surface of the cells. A protocol was developed, by researchers in my lab, to support the culture of HUVEC on Transwell inserts to form a confluent monolayer. This involved the seeding of HUVEC onto the transwells in EGM-2 and after a 24 h incubation replacing this media with HIFA medium. I carried out this protocol and visualised the cells on the Transwell inserts to assess their confluency. To do this, I stained the HUVEC tight junctions and adherens junctions with ZO-1 and VE-cadherin respectively. I also counterstained the cells with DAPI to visualise their nuclei. As shown in Figure 5.1, a confluent monolayer of HUVEC was achieved and hence there was a barrier preventing any reagent labelling a surface that wasn't intended.

5.2.2 VEGFR1 is apically polarised within HUVEC membranes and becomes cleaved when EDTA is added

Little is known about the polarity of surface proteins in ECs. In addition to this, it is not yet fully understood how to biotinylate the apical and basal surfaces of these cells separately. Hence, until a protocol is developed and validated that biotinylates both surfaces of the cells separately, we cannot gain conclusive evidence regarding the polarity of endothelial surface proteins. I decided to validate a method of HUVEC biotinylation by staining for surface proteins after the cells had either been apically or basolaterally biotinylated, whose polarity within HUVEC membranes has already been deduced.

Previous research showed VEGFR1 to be apically localised, and VEGFR2 basally, within neural MVECs [38] (Figure 5.2). These set off distinct signalling cascades within the EC to carry out separate functions. I hypothesised that there, too, would be polarisation of other surface proteins in HUVEC cells. To assess the polarity of these two surface proteins within HUVEC, Hudson et al used sulfo-NHS-LC biotin to label surface proteins on cells cultured on Transwells. It had been well established that basal biotinylation is relatively much weaker than apical biotinylation. So, Hudson and colleagues incubated EDTA as well as the biotinylation reagent at the apical surface to biotinylate both surfaces of the HUVEC. EDTA is a chelating reagent which binds divalent metal ions and inactivates cell-cell junctional complexes, creating gaps in between cells. It therefore allows access to the basal surface of the cells. So, the biotinylation reagent can label both the apical and basal cell surface. Relative distributions of surface proteins can be deduced at the apical and basolateral surfaces of cells from western blotting. Exposure of the apical surface of cells to either labelling reagent or labelling reagent with EDTA allows labelling of the apical or both apical and basolateral surfaces respectively. Looking at the relative thickness of bands on a western blot for both these two conditions reveals relative distributions of surface proteins.

Staining with VEGFR1 antibody confirmed that VEGFR1 is apically localised (Figure 5.4). There was a band present at ~120KDa with no EDTA added, possibly representing isoform 1 (150KDa) which ran incorrectly on the gel. EDTA treated HUVEC did not show this band. Instead, these treated cells generated two smaller bands at ~60 and ~68 KDa which suggests a cleavage event has taken place on the receptor, due to the addition of EDTA. VEGFR2 was below the level of detection in this assay (Figure 5.4).

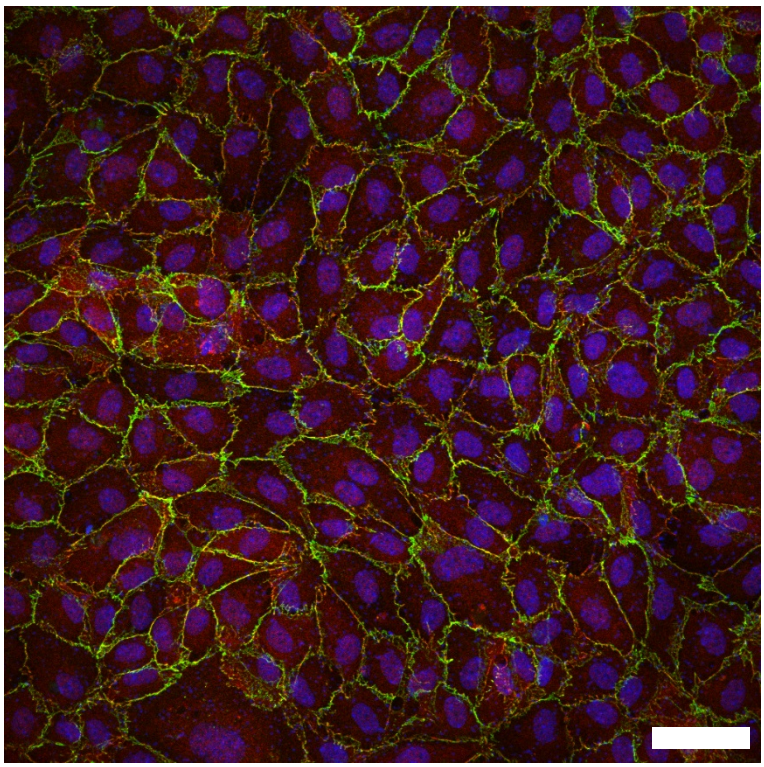

Figure 5.1 – HUVEC cultured on Transwell insert forms confluent monolayer. HUVECs were seeded at concentration of $2x10^5$ cells/mL on a Transwell membrane insert. After a 72hr incubation, cells were fixed and stained with ZO-1 (red), VE-cadherin (green) and DAPI (blue). Cells were imaged by confocal microscopy at low magnification to get an impression of their confluency. Scale bar = 50μm.

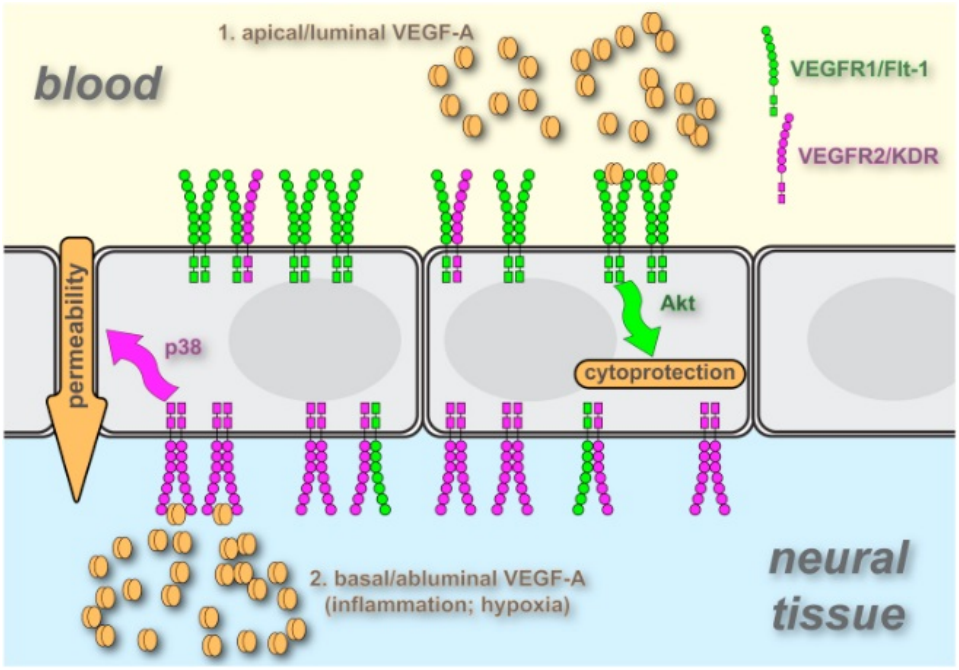

Figure 5.2 – Hypothesised distribution of VEGFR1 and -R2 in neural microvascular endothelial cells (MVECs). Hudson et al conducted several *in vivo* and *in vitro* experiments on neural MVECs and found that vascular permeability was only increased when VEGF-A was added to the basal surface of the cells. There was a reduction in the amount of junctional claudin 5 (Cldn5), an integral component of cell-cell tight junction complexes, when added basally, indicating the loss of such cellular junctions and hence an increase in paracellular permeability. A cytoprotective response was only seen when apical VEGF-A bound to VEGFR1, eluding to its presence predominantly at the apical membrane. Diagram taken from Hudson et al, 2014 [38]**.**

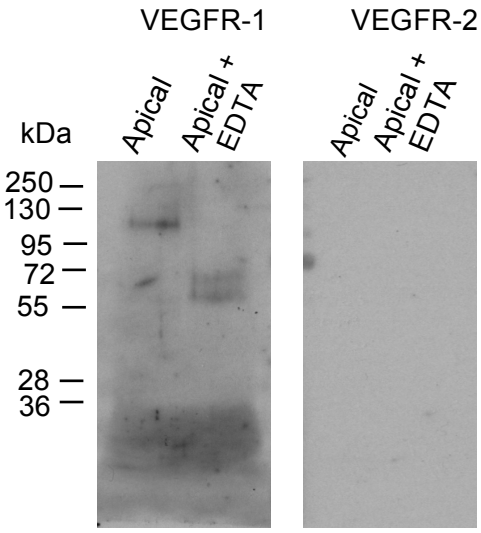

Figure 5.3 – Western blot of VEGFR-1 and -2 with and without EDTA added apically. 5mg/mL sulfo-NHS-LC-biotin was incubated with HUVEC, seeded at $2x10^5$ cells/mL on Transwells, for 30 mins at 37°C. HUVEC incubated with 1mM EDTA shown by lanes labelled apical + EDTA. Lysis medium ran on western blot and stained for VEGFR-1 and -2. VEGFR-1 is present at the apical surface of HUVEC shown by band at ~120kDa. The addition of EDTA generates two smaller bands, which could resemble two regions of a cleaved VEGFR1 monomer. The event which causes two smaller bands to be produced when EDTA is added occurs either intercellularly or extracellularly. It cannot be determined if VEGFR-1 is present at the basolateral surface of the HUVECs. No VEGFR-2 signal detected, possibly due to insufficient amounts of protein present in the sample.

5.2.3 Biotinylation reagent can label the apical and basolateral surfaces of HUVEC without the need for EDTA

As shown, EDTA cleaved VEGFR-1 and hence we cannot deduce from this method its basolateral polarity. This outcome is worrying, as using EDTA may give a false positive result for a protein when this sample is applied to mass spectrometry. I set about to assess the plausibility of being able to efficiently biotinylate the apical and basolateral surfaces without the use of EDTA. 5mg/mL sulfo-NHS-LC-biotin was added to both the top and bottom compartments of the Transwell, and its ability to label to the apical and basolateral surfaces of the HUVEC was studied via fluorescence microscopy.

Immunostaining showed that the biotinylating reagent can label the apical and basolateral cellular surfaces (Figure 5.4). Sulfo-NHS-LC-biotin, added apically, labels the apical and basolateral surfaces of the HUVEC. The streptavidin Alexa Fluor™ 594 signal can be seen at the top and bottom of the cell in relatively equal amounts. In contrast, when added to the bottom Transwell compartment, it preferentially labels the basolateral surface of the HUVEC. The biotin label is relatively evenly distributed, reflecting the fact that it modifies primary amine groups on cell surface proteins. These include lysine, a relatively abundant amino acid, and amino-termini of polypeptides, which occur on every protein. There is a strong fluorescent signal at the basolateral surface of the cells when basally biotinylated; the ECM is protein dense hence it binds to biotin and may give the appearance that the biotin is binding to the basal surface of the HUVEC. In either case, the biotinylating reagent has been able to reach the primary amine groups by diffusing through the Transwell membrane.

The mean pixel intensities taken at the top and bottom of the cells in the images gives an indication of how strong the streptavidin Alexa Fluor™ 594 signal is and hence a comparison of the amount of biotinylating reagent present at each of these surfaces. ECs are very thin, to carry out their specialised functions, and hence fluorescence signals at the apical and basal surfaces of these cells are difficult to resolve. Here, I analysed the relative pixel intensities at the top and bottom of the nucleus as this is the widest section through the cell. When Sulfo-NHS-LC-biotin was added to the top and bottom compartments of the Transwell, greater mean Alexa Fluor™ 594 signals were obtained from the apical and basal surfaces of the cells respectively (Figure 5.5). This shows that the biotinylating reagent preferentially labels HUVEC surface proteins which face the compartment that the label was added to. Indeed, when added to the basal surface of the cells (bottom Transwell compartment) the mean pixel intensity, averaged across five points on the confocal image, for the basal surface of the cell membrane

was 74.03. Comparing this to the mean signal intensity at the apical surface, calculated as 35.48, shows that this is more than twice as large. When added apically (top Transwell compartment) the biotinylating reagent labels more proteins at the apical side of the HUVEC, as the mean pixel intensity here was 64.8, compared to 59.47 at the basal side. However, these averages are very similar and so we cannot deduce that, when added apically, the sulfo-NHS-LC-biotin preferentially labels the apical surface over the basal surface. The similarity with which the biotin label modifies the apical and basal surfaces when added to the top Transwell compartment is a cause for concern; when apically biotinylated surface proteins are taken away for proteomic analysis, this will be a mix of relatively similar amounts of apical and basal surface proteins. Thus, the polarity of such proteins will be incorrectly determined.

5.2.4 Biotinylation at the apical surface is more efficient than at the basal surface

Biotinylation is possible at both the apical and basal surfaces of HUVEC on Transwells (Figure 5.4). However, previous studies have shown that this process is relatively less efficient at the basal surface of the cells on Transwells than the apical surface [81]. I wanted to conduct an experiment to determine the ability of a reagent to label the apical surface relative to basal surface of HUVECs grown on Transwell inserts. To do this, I added sulfo-NHS-LC-biotin at the same concentration to the apical and basal surface of the HUVECs on Transwells. Due to evidence of poor basal surface labelling, I labelled the basal surfaces of samples with increasing concentrations of sulfo-NHS-LC-biotin. Samples were taken after the cells were lysed and analysed by western blotting. This protocol assumes that there are similar amounts of total protein at the apical and basal surfaces of cells.

As shown, when 5mg/mL sulfo-NHS-LC-biotin is added apically this results in a greater relative amount of total protein being labelled then when the same concentration is added basally (Figure 5.6). This is consistent with findings from previous papers [81]. The efficiency of biotinylation at the basal surface increases when increasing amounts of biotinylating reagent are added to the HIFA medium. This efficiency never reached that of the sample that was apically labelled despite being in 2x and 4x greater concentrations respectively. Thus, I found it is much more difficult to label proteins present on the basal surface of cells on a porous membrane even when the amount of label was increased up to 4x greater.

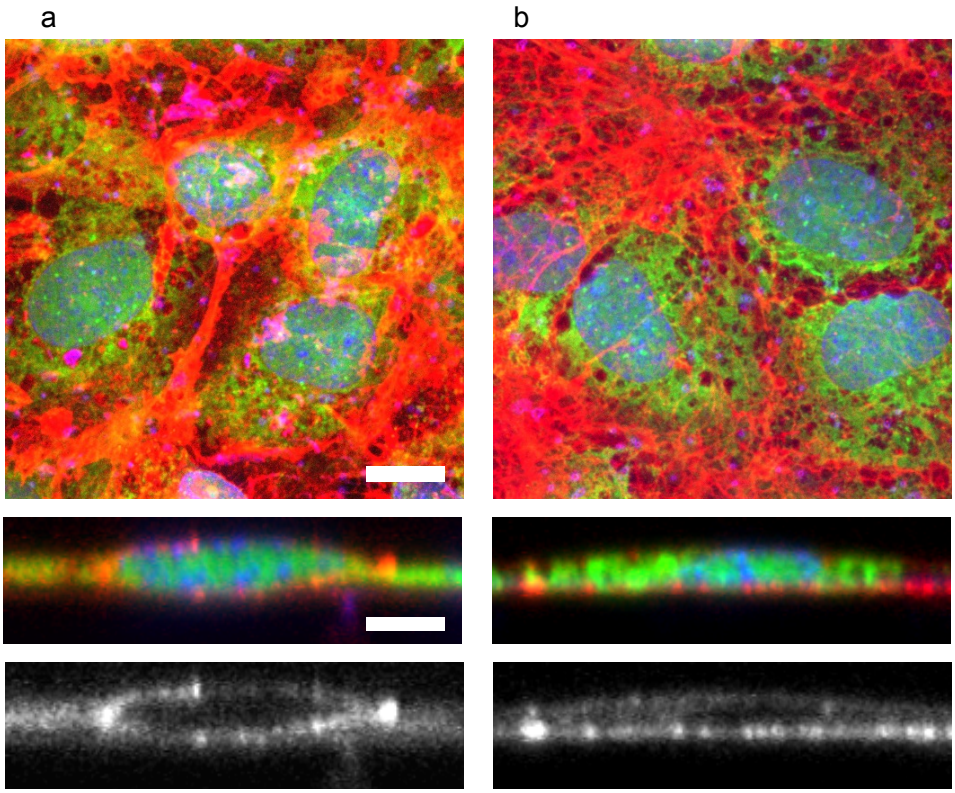

Figure 5.4 – Apical and basolateral HUVEC surface membrane proteins are able to be labelled when reagent added apically or basolaterally, respectively. HUVEC cultured at $2x10^5$ cells/mL on Transwell inserts and incubated for 30 mins at 37°C with a green CellTracker™ and a) 0.2mg/ml sulfo-NHS-LC-biotin added to the apical surface of HUVEC and b) 0.4mg/ml sulfo-NHS-LC-biotin added to the basal surface of HUVEC. Cells were then fixed and stained with DAPI (blue) and streptavidin Alexa Fluor™ 594 (red). XYZ projections through apically and basally biotinylated HUVEC are shown. Scale bar = 10µm.

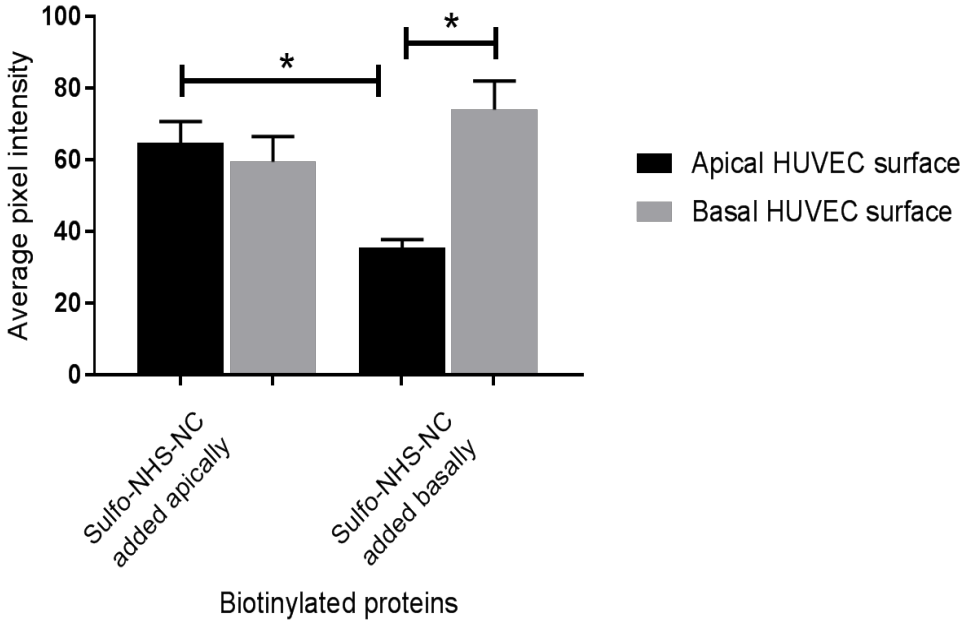

Figure 5.5 – Graph showing the mean pixel intensities of labelled HUVEC apical and basal surfaces. Mean pixel intensities were averaged at each surface across 5 cell nuclei on each fluorescence confocal image. Sulfo-NHS-LC-biotin was added to the apical and basal surfaces of HUVEC, and the mean pixel intensities of streptavidin Alexa Fluor™ 594 calculated at each surface. This equates to the amount of biotin label present at each surface when label added apically and basally to the cells. Statistical analysis was performed using a 1-way ANOVA on all the data followed by a Tukey multiple comparison test on data obtained from day 4, *$p \leq 0.05$. The bar graph shows the mean ± SEM of five experimental replicates.

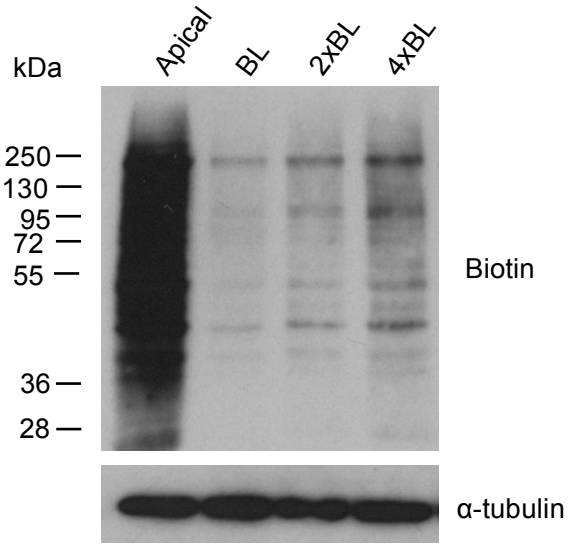

Figure 5.6 – Biotinylation of the apical surface is greater than the basal surface of HUVEC. HUVEC seeded at $2x10^5$ cells/mL on 0.4µm Transwells and biotinylated from either apical (Apical) or basolateral (BL) surface of Transwell. 5mg/mL sulfo-NHS-LC-biotin added to the top Transwell compartment and proteins at the apical surface of the HUVEC were very efficiently labelled. Basal surfaces biotinylated via addition of 1x, 2x and 4x the amount of sulfo-NHS-LC-biotin that is added apically, added to the bottom compartment of the Transwell. Increasing the concentration of sulfo-NHS-LC-biotin increases basal biotinylation. After solubilization, the labelled proteins were separated by SDS PAGE and subjected to Western blot analysis.

5.2.5 Optimising labelling at the apical surface of HUVEC

As shown in figure 5.7, the ability of sulfo-NHS-LC-biotin to label the apical surface proteins of HUVEC is greater than basal surface proteins. Even though greater total proteins can be labelled at the apical surface, in labelling the apical surface proteins some basal surface proteins are also labelled (Figure 5.5). For separate proteomic analysis of proteins at the apical and basal surfaces of the cell, these two surfaces must be labelled independently. To increase the relative labelling of apical compared to basal surface proteins, the amount of time the biotinylation reagent is incubated with the apical surface of the HUVEC on Transwells was reduced. The effect of this is twofold; there is less time for the labelling reagent to pass through any leaks in the monolayer, and less time for apical surface proteins to be endocytosed and recycled to the basal surface of the cell before fixation and hence lost from the apical surface of the cell. Previous western blots were the result of a 30 min incubation at 37°C. Here, the biotinylation is carried out over a time course of 30 min (Figure 5.8).

Western blot analysis revealed that total biotinylation increases over time (Figure 5.7a). The amount of biotinylated protein, however, saturates by 20 min. A 5 min incubation resulted in minimal protein being labelled. It is important here to assess relative biotinylation reagent labelling at the apical and basal surface of the HUVECs at each time point. Immunofluorescence using Alexa Fluor™ 594 streptavidin was carried out to visualise the localisation of biotin on the HUVEC surface membrane (Figure 5.8b). Image analysis of the confocal IF images showed a greater relative amount of streptavidin 594 signal at the apical surface than the basal surface during 5, 10 and 20 min incubations. It appears that relative apical to basal surface labelling increases when the incubatory period is reduced. Quantification of these images was required for justification of these analysis. Average pixel intensities were taken of streptavidin 594 signal at the apical and basal surface of the HUVEC, taken either side of the nuclei of five different cells for each time-point. A mean average pixel intensity for each of the apical and basal surfaces allowed a ratio of apical to basal labelling to be calculated for each time-point (Figure 5.7b). 5 and 10 min incubations with the biotinylation reagent gave greater apical than basal labelling. Incubations longer than this reduced the apical binding efficiency relative to basal surface binding, with a 30 min incubation having greater basal than apical binding. A 10 min incubation gave the greatest ratio of apical/basal labelling, at 1.62. Therefore, reducing the incubatory period generally increases apical to basal labelling. However, 1.62x greater labelling at the apical surface than the basal surface, when the labelling reagent is added apically, indicates that this surface has not been labelled in isolation.

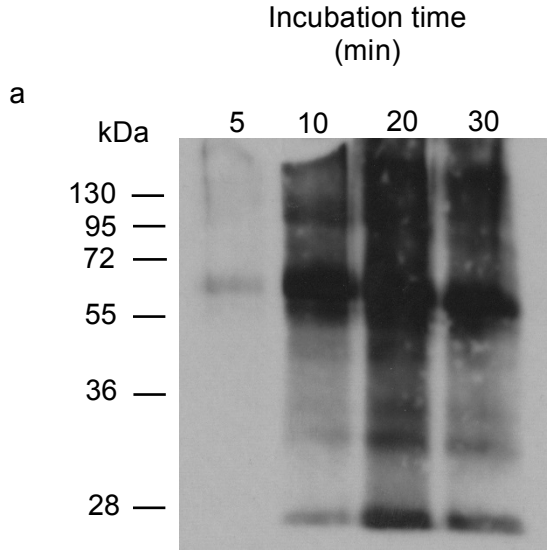

Figure 5.7a – The amount of surface biotinylation increases with increasing incubation time. HUVEC seeded at $2x10^5$ cells/mL on Transwells were incubated with 5mg/mL sulfo-NHS-LC-biotin, added apically, at 37°C. Increments in incubation time shown, with intervals of 5, 10, 20 and 30 mins. Minimal protein is labelled when biotin reagent incubated on Transwell for 5 mins. The amount of total protein labelled increases substantially at incubation time of 10 min. 20 min is the saturation point for biotinylation of proteins by sulfo-NHS-LC-biotin, as it is the time-point with the greatest amount of total protein.

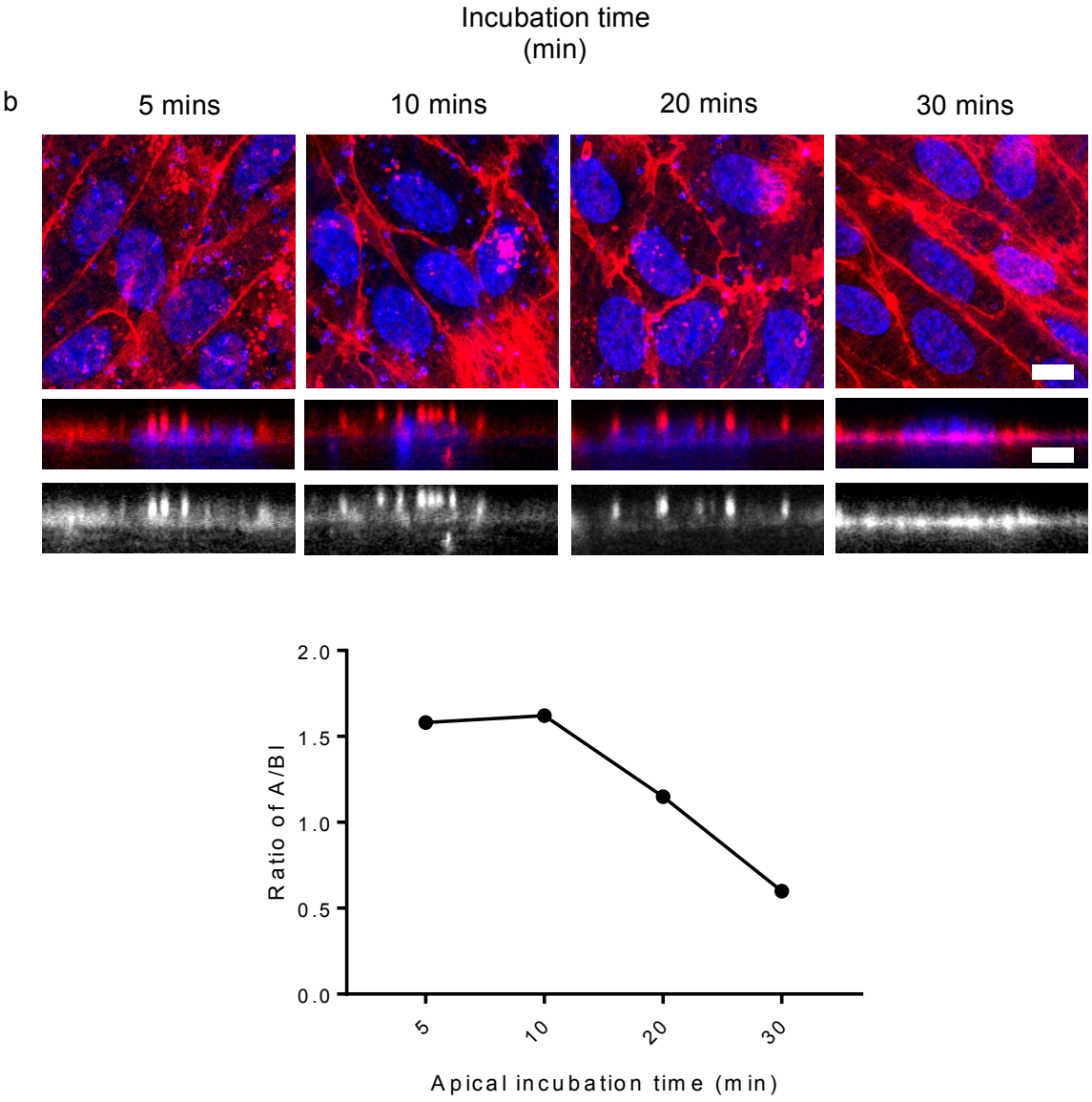

Figure 5.7b – The relative apical to basal surface labelling declines with increasing incubation time. HUVEC seeded at 2x10⁵ cells/mL on Transwells incubated with 5mg/mL sulfo-NHS-LC-biotin, added apically, at 37°C. Increments in incubation time shown, with intervals of 5, 10, 20 and 30 mins. After a 5 min incubation, 1.58x more apical proteins are biotinylated than proteins at the basal surface. At 10 min this rises slightly, however after this time the ratio of apical/basolateral surface protein labelling declines. The most promising relative binding is at 10 min, at 1.62x A/Bl. Scale bar = 10μm.

5.2.6 Incubating HUVEC with biotinylating reagent at 0°C does not increase relative apical binding

As shown in Figure 5.7, reducing the amount of time that the biotinylating reagent was incubated with the apical surface of HUVEC was effective at increasing the relative amount of label at the apical surface than the basolateral. However, there is still some degree of basolateral surface labelling and so this method is only partly effective at increasing apical labelling independently from basolateral labelling. The same experimental procedure was repeated at 0°C in an attempt to label the apical surface in isolation. At 0°C, cellular processes slow down as the metabolism of the cell declines. As a result, cellular trafficking slows, and so less biotinylated apical surface proteins will be endocytosed and taken to the basolateral surface when compared to the same experiment carried out at 37°C.

Immunofluorescence confocal microscopy suggests that HUVEC incubated with biotinylation reagent at 0°C for 5 and 10 min gave equal or greater biotin binding at the apical surface compared with the basal (Figure 5.8a). This is demonstrated by similar or more streptavidin 594 staining at the apical relative to the basolateral HUVEC surface. After 10 min, more proteins at the basal surface than the apical surface were biotinylated. Quantification of surface labelling using image analysis software showed that there was similar or more apical surface binding relative to basal at 5 and 10 min incubations (Figure 5.8b). However, these ratios are lower than the corresponding time points at 37°C. 20 and 30 min incubations gave greater amounts of biotin labelling at the basal surface than the apical. Again, these ratios are lower than the corresponding values for HUVEC at 37°C, hence cold experimental conditions do not increase the relative amount of label present at the apical surface of HUVEC compared to basolateral surfaces. Lower apical/basolateral label ratios for corresponding HUVEC incubations at 0° compared to HUVEC at 37° suggests an increase in label, and hence apical surface protein, being transferred to basolateral surfaces. Under cold cellular conditions, cell-cell junctions can become ‘leaky’ as tight junctions detach and cells ‘round up’. This allows the biotin reagent to pass through intercellular gaps and become exposed to the basolateral surface. However, lower magnification images taken of the HUVEC cultured on Transwells (Figure 5.1) shows that they form confluent monolayers of cells with no visible gaps. This creates uncertainty as to how the label is reaching the basolateral layer. From these previous experiments, it is clear that labelling the apical surface in isolation from the basolateral surface is very difficult. Label repeatedly reaches the basolateral surface, even when intracellular trafficking is slowed.

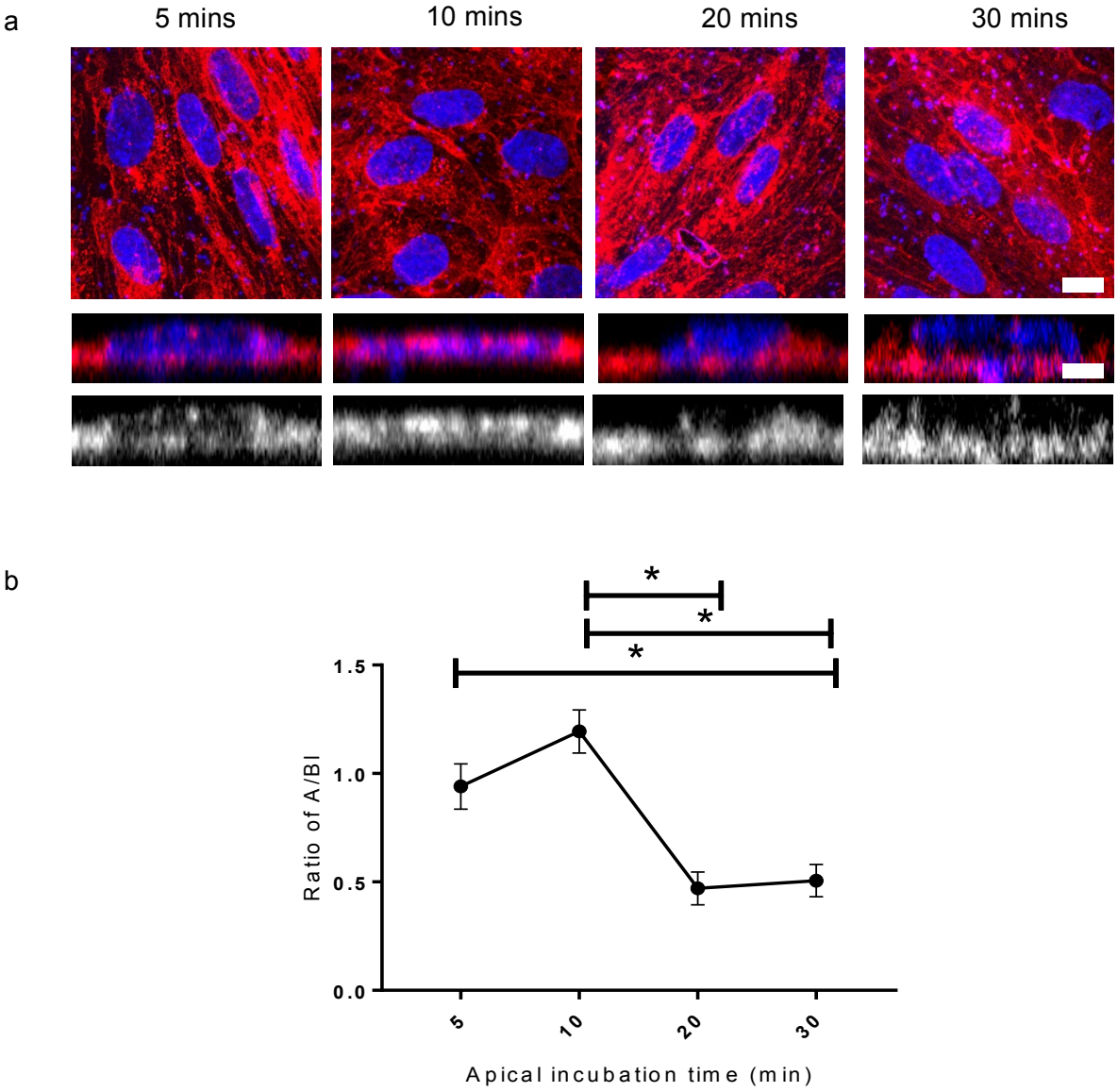

Figure 5.8 – Incubating HUVEC with biotinylation reagent at 0°C gives lower relative apical to basal surface protein labelling when compared to warm conditions (37°C). HUVECs seeded at seeded at 2x10^5 cells/mL on Transwells on ice were incubated with 5mg/mL cold sulfo-NHS-LC-biotin, added apically. Increments in incubation time shown, with intervals of 5, 10, 20 and 30 mins. Immunofluorescence at each time-point shown, with quantitative data representative of the ratio of apical/basal streptavidin 594 signal. 5 min cold incubation with the labelling reagent gave almost equal labelling at the apical and basolateral surfaces of the cells. The binding efficiency of the biotinylation reagent was greatest at 10 min cold incubation, however time points after this gave greater basal binding efficiency. Relative apical to basolateral surface labelling at each time-point lower than corresponding time-points at 37°C. Scale bar = 10μm. Statistical analysis was performed using a 1-way ANOVA on all the data followed by a Tukey multiple comparison test on data obtained from day 4, *$p \leq 0.05$. The graph shows the mean ± SEM of five experimental replicates.

5.2.7 Immunofluorescence is an effective method of directly imaging and quantifying surface protein polarities

In order to observe how reliable the method of apical or apical and basolateral surface biotinylation is, a method to directly image proteins at the apical and basolateral surface was developed in parallel. Direct methods to visualise surface proteins do not require the addition of labelling reagent. Using a direct method, the fluorophore will simply bind to a surface protein via a primary and secondary antibody. It is a more reliable method of identifying surface proteins and can be used as a cross-reference when deciding the validity of using biotin to label surface proteins in isolation.

This alternate method involves labelling HUVEC with immunofluorescent antibodies that are specific for surface proteins to be identified. These proteins can then be detected via confocal microscopy and their polarisation deduced via analysis of the fluorescence signal present at each surface domain. XY as well as XYZ images were captured, with z-stacks taken with intervals of 0.13μm to obtain a z-projection of around 80 stacks. The polarity of proteins on the HUVEC surface membranes were deduced by image analysis software of the confocal images. The mean pixel intensity of the secondary antibody 594nm signal was compared at the apical and basal surfaces of the cells to deduce the relative antibody binding at these two surfaces. The challenge here is that HUVEC cells are extremely thin, and so it is difficult to differentiate signals at the apical surface of the cells from signals at the basal surface. To get around this issue, these average pixel intensities were taken from regions at the apical and basal regions of the nuclei at the HUVEC surface membrane, as this is the widest point within a cell.

This method, however, is relatively low throughput and is costly, and also relies on the antibodies being effective. Ideally, this experimental procedure would only be established to validate HUVEC surface protein biotinylation. However, as previously demonstrated it is not possible to label apical or basolateral surface proteins in isolation. Determining the surface proteome of HUVECs therefore relies on this direct immunofluorescent method of protein identification.

Immunofluorescence microscopy of HUVEC surface proteins is likely to give reliable results as surface proteins remain immobile at the time of protein staining. To validate this method of protein labelling, strong markers of the apical and basolateral surfaces need to be stained and identified. Due to their cellular function, these proteins will be localised to either the apical or basolateral surface of HUVEC specifically. Staining for these will provide critical indication as to whether the use of fluorophore conjugated antibodies will give valid proteomics data for other surface proteins.

Integrin α5 and ICAM-1 primary antibodies were used in the initial immunostaining

procedure as these are highly established HUVEC surface proteins. Based on their function, integrin α5 is likely to have a polar distribution at the basolateral surface membrane. This protein is one monomer of a heterodimer constituting a cell adhesion glycoprotein (integrin) that binds to fibronectin within the ECM. This binding aids in cell adhesion to the ECM and in intracellular signalling transduction from the ECM to promote survival, proliferation, growth and differentiation. ECM is situated at the basolateral surface of ECs and hence this is where the integrin α5 will be primarily localised. ICAM-1 is a cell adhesion molecule. ICAM-1 binds to LFA-1, an integrin present on immune cell surface membranes, and provides initial binding that brings the immune cell in close proximity to the endothelium. Once at the endothelium, firmer binding, which is more characteristic of an immune reaction, takes place between integrins present on the immune cell and the endothelium. This promotes diapedesis of the immune cell across the endothelium and into the underlying tissue where it acts to clear infection and repair damage. I hypothesised that ICAM-1 would be expressed principally at the apical surface of HUVEC, so that it can be exposed to immune cells within the blood. ICAM-1 is constitutively expressed, albeit at a low level, in ECs and immune cells. When inflammation if triggered, expression of ICAM-1 is dramatically increased on both sets of cells. This promotes an immune response large enough to control any infection or damage within an area of tissue. I was therefore interested in confirming the polar distribution of these two proteins within HUVECs, giving validation to this technique of protein labelling.

For this initial screen using integrin α5 and ICAM-1 primary antibodies, permeable Transwells were used as a surface to culture HUVECs. These provide a better surface to obtain a confluent monolayer of cells, essential for maintenance of surface protein polarity. They also better mimic the physiological environment and so the architecture of the cells will be as close to that as in normal physiology as possible. Figure 5.9a shows that, indeed, integrin α5 is present predominantly at the basolateral surface of HUVEC and ICAM-1 is situated mostly at the apical surface. Moreover, integrin α5 appears to form fibrillar structures. This is characteristic of α5β1 integrins, heterodimers of α5 and β1 subunits. Fibronectin binding to the α5 subunit of the integrin promotes α5β1 oligomerisation and fibril formation. Figure 8a shows only one HUVEC expressing ICAM-1. Under normal conditions, this protein is not expressed in high enough amounts to be detected by immunofluorescence. There will have had to be some form of stimulation for this cell to upregulate its ICAM-1 expression and trafficking to the apical surface for this signal to be detected. Quantification of the immunofluorescence data for integrin α5 and ICAM-1 confirms their opposing polar distribution. The ratio of mean

pixel intensity for integrin α5 at the apical and basolateral HUVEC surfaces is 0.73, which falls below 1, hence there is a greater amount of integrin α5 present at the basolateral surface of the cell than the apical. Contrastingly, ICAM-1 has an apical to basolateral ratio of greater than 1, at 1.68. ICAM-1 is present more at the apical surface than the basolateral surface. The ICAM-1 signal ratio SEM is relatively greater than the SEM for integrin α5, its average ratio fluctuating across the 3 sets of repeats to a greater extent.

5.2.8 HUVEC cultured on coverslips reproduce membrane surface protein polarity as that seen on Transwells

As shown previously in Figure 5.9, integrin α5 and ICAM-1 display polar distribution on HUVEC surface membranes when HUVECs are cultured on Tranwells. To scale up this screen, HUVECs cultured on coverslips were investigated. Coverslips allow greater reproducibility of results, and it is easier to culture cells on this surface relative to Transwells. I was interested in reproducing the results from the initial Transwell experiment outlined above, so again I did a screen for integrin α5 and ICAM-1. This was to validate that the use of coverslips for HUVEC culture generates the same surface protein polarity as with Transwells.

HUVEC were seeded on coverslips and grown until confluency and then prepared for immunofluorescence as appropriate. Again, confocal images were taken of XY and XYZ sections of the stained HUVEC, and average pixel intensities at the apical and basolateral surfaces deduced. Figure 5.10 shows that each protein displays a similar staining pattern to that generated on the HUVEC grown on Transwells. integrin α5 shows more staining at the basolateral surface, which arranges into extracellular fibrils concurrent with that seen on Transwells. ICAM-1 shows apical surface localisation as seen on Transwells. In addition, the ratio of apical: basolateral signal follows the same pattern as previous; integrin α5 generates a ratio of 0.60 and ICAM-1 a ratio of 2.81. Again, ICAM-1 displays a substantially greater amount of fluctuation regarding mean relative intensities. These are promising results as they reproduce the results and patterns of antibody staining as seen using HUVEC on Transwells. From this, it can be deduced that coverslips can be used as a higher throughput method of protein screening.

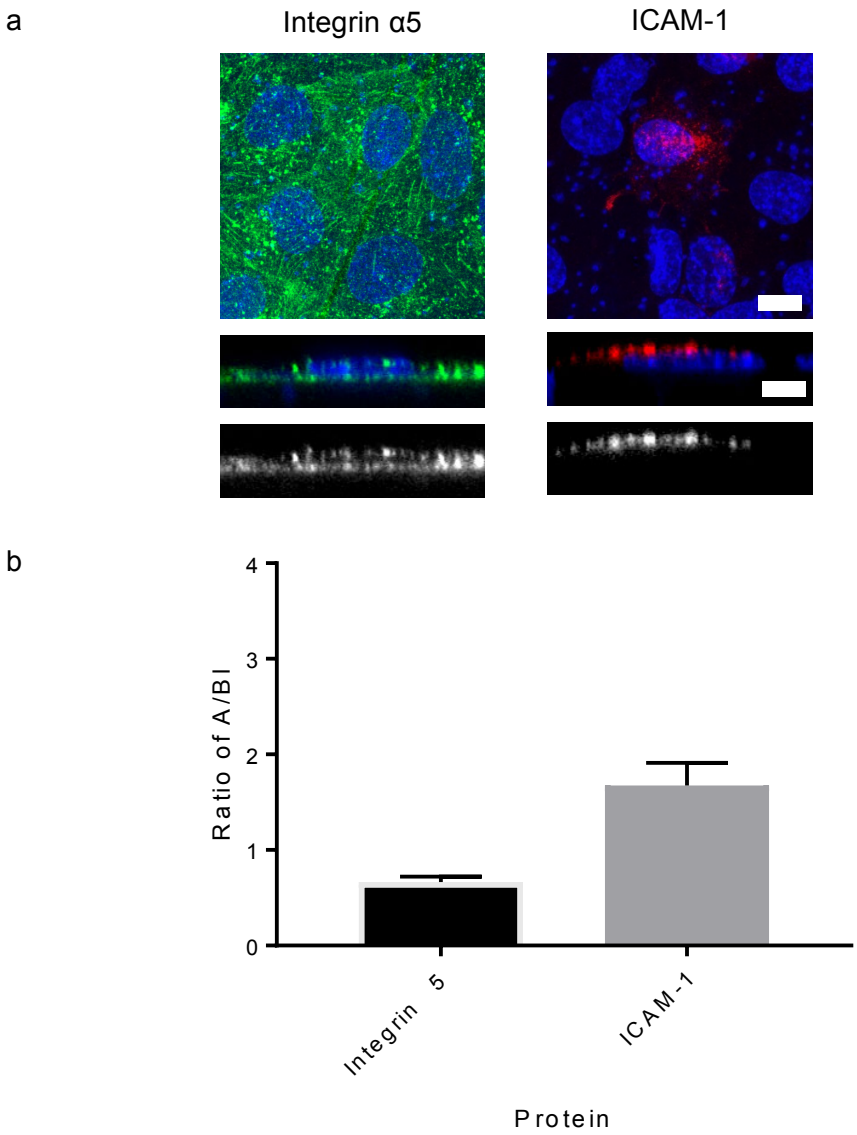

Figure 5.9 – Integrin α5 is basolaterally polarised and ICAM-1 is apically polarised in HUVEC grown on Transwells. HUVECs were cultured on Transwells at $2x10^5$ cells/mL and then fixed and stained with DAPI (blue) and for integrin α5 (green) and ICAM-1 (red). a) XY and XYZ images were captured using confocal microscopy. The polarity of both these proteins can clearly be seen from above and below the nucleus (DAPI stained to see thickest part of cell). b) The ratios of apical: basaolateral pixel intensities were deduced from the XYZ images using imaging software. The bar graph shows the mean ± SEM of three experimental repeats for integrin α5 and ICAM-1; n=3. Scale bar = 10μm.

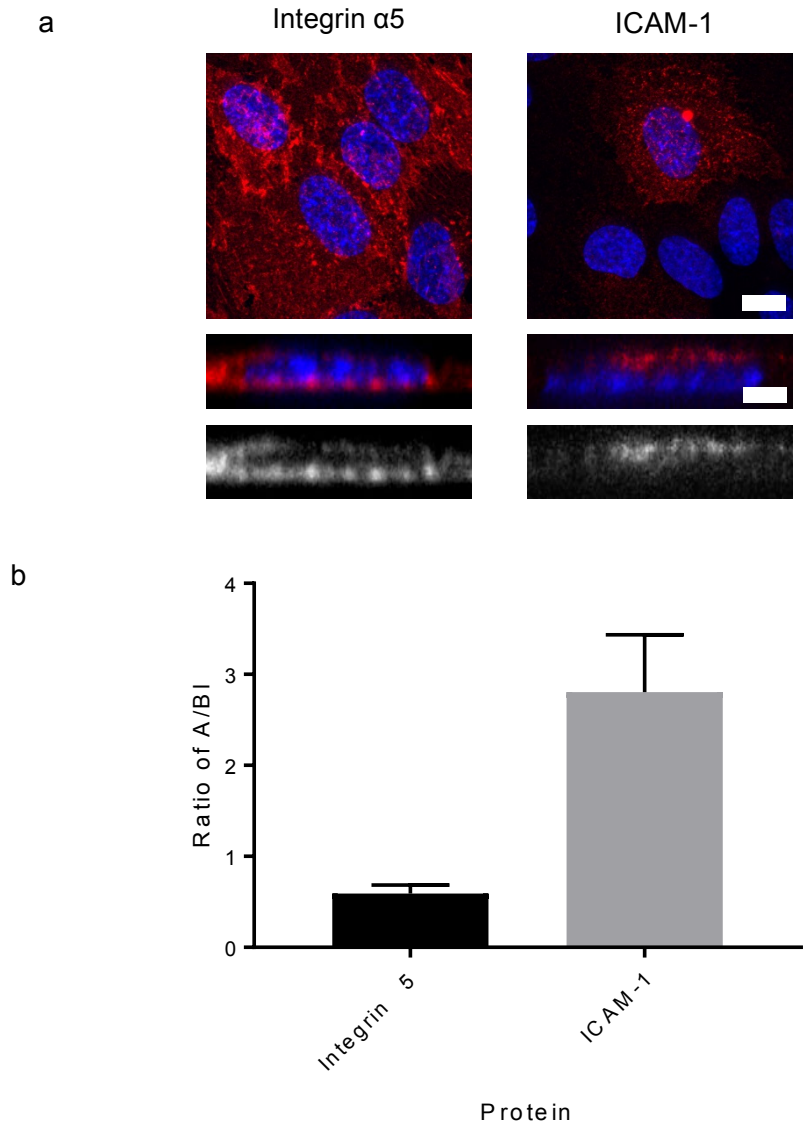

Figure 5.10 – Integrin α5 is basolaterally polarised and ICAM-1 is apically polarised in HUVEC grown on coverslips. HUVECs were cultured on glass coverslips at $6x10^4$ cells/mL and then fixed and stained with DAPI (blue) and for ICAM-1 and integrin α5 (red). a) XY and XYZ images were captured using confocal microscopy. The polarity of both these proteins can clearly be seen from above and below the nucleus (DAPI stained to see thickest part of cell). b) The ratios of apical: basaolateral pixel intensities were deduced from the XYZ images using imaging software. The bar graph shows the mean ± SEM of three independent experiments for integrin α5 and ICAM-1; n=3. Scale bar = 10μm.

5.2.9 Some HUVEC surface proteins show a propensity for either the apical or basolateral surface of HUVEC grown on coverslips

As shown from Figures 5.9 and 5.10, integrin α5 and ICAM-1 show polarity within surface membranes of HUVEC grown on coverslips and Transwells. The reproducible data generated from both experiments allows for the use of coverslips as a surface for HUVEC culture and staining. To further the proteomics data generated from previous HUVEC staining, I was interested in determining the polarity of a number of other membrane proteins known to be on HUVEC surface membranes. I began by staining for VEGFR-1 and VEGFR-2, as it has been suggested in a paper published by N. Hudson and colleagues [38] that VEGFR-1 shows apical polarity and VEGFR2 basolateral in neural MVECs. This paper proposes this apicobasal distribution due differential apicobasal VEGF signalling seen at vascular blood-neuronal barriers. I was interested if this distribution applies to HUVEC as well as MVECs.

Using the immunofluorescence protocol described above, HUVECs were stained with VEGFR-1 and VEGFR-2 primary antibodies. After incubation with a fluorophore-conjugated secondary antibody and DAPI, the HUVECs were imaged under a confocal microscope. Both VEGFR-1 and VEGFR-2 gave strong signals that could be detected and imaged. Figure 5.11 shows the distribution of VEGFR-1 and VEGFR-2 in HUVEC grown on coverslips. An issue with clarity arose with the staining for VEGFR-1, however it is evident from these XYZ images that VEGFR-1 is relatively non-polarised. Its apical: basolateral ratio is 0.84, a value close to 1, indicative that it is present both and the apical and basolateral surface of the HUVEC in almost equal amounts. VEGFR-1 looks to be concentrated in the Golgi apparatus, positioned around the circumference of the nucleus. It is therefore not positioned directly above and below the nucleus at the surface membrane. Occupying a more lateral position from the nucleus within the cytoplasm, the signal is not included in the measurements taken from the apical and basolateral surfaces. It may therefore have the appearance from the XYZ images of being non-polar in surface membranes, but this might be caused by signal originating from the Golgi. Contrasting to VEGFR1, VEGFR2 has a polar distribution. From the XYZ images in Figure 5.11, it is clear that VEGFR2 is present in greater amounts at the basolateral surface of HUVEC. Indeed, the ratio of apical/basolateral signalling is 0.56 meaning that there is nearly twice as much VEGFR2 present at the basolateral surface than the apical. This value, however, is not low enough to say with any real conclusiveness that VEGFR2 is basolaterally polarised.

The result from VEGFR2 was a promising start, as it demonstrated that HUVEC

surface proteins may show polarity. Taken further, other HUVEC surface proteins were stained for using the same immunofluorescence protocol. A further six surface proteins were tested for in the immunofluorescence assay: clathrin heavy chain (CHC), PECAM-1, P-glycoprotien, podocalyxin, robo 4 and flotillin 2. Due to efficacy variability of the primary antibodies, some of the immunofluorescence images failed to show a signal, or this signal was too weak to quantify. As a result, the polarity of these proteins could not be deduced. Figure 5.12 is a table showing the function of all the proteins investigated, as well as the outcome of the immunofluorescence experiment.

Of those tested, CHC and PECAM-1 antibodies generated a signal that could be detected and imaged (Figure 5.11). The remaining four antibodies failed to be effective at staining the HUVEC surface proteins. PECAM-1 is a major constituent of endothelial intercellular junctions and is involved in the extravasation of immune cells during inflammation. Its function implies that PECAM-1 will be laterally distributed and hence more or less non-polarised across the apical-basolateral axis. Figure 5.11, however, shows PECAM-1 to have a more apical polarity as the confocal image has a greater amount of staining visible above the nucleus than below. The apical/basolateral ratio, too, suggests an apical polarity. This ratio, 1.43, alludes to there being almost 50% more PECAM-1 present at the apical HUVEC surface membrane than at the basolateral. Again, this value is not great enough to conclusively say that PECAM-1 is apically localised, as there is still a substantial amount present at the basolateral surface.

CHC is the protein component composing the coat of vesicles and pits involved in vesicle trafficking. The amount of material endocytosed equals that which is exocytosed for a cell to achieve a steady trafficking state and homeostasis. Additionally, there are similar amounts of proteins at the apical and basolateral surfaces of cells. This would imply that there will be similar amounts of CHC coated pits at the apical surface of the cell as the basolateral surface. However, a greater amount of trafficking is likely to occur at the apical surface in HUVEC as this is in contact with the blood stream and hence with a more active trafficking environment. This is reflected in the apical: basolateral ratio, 1.31 (Figure 5.11). There is a greater average amount of CHC at the apical surface membrane than the basal, but again this value is too close to 1 for any real polarity to be deduced.

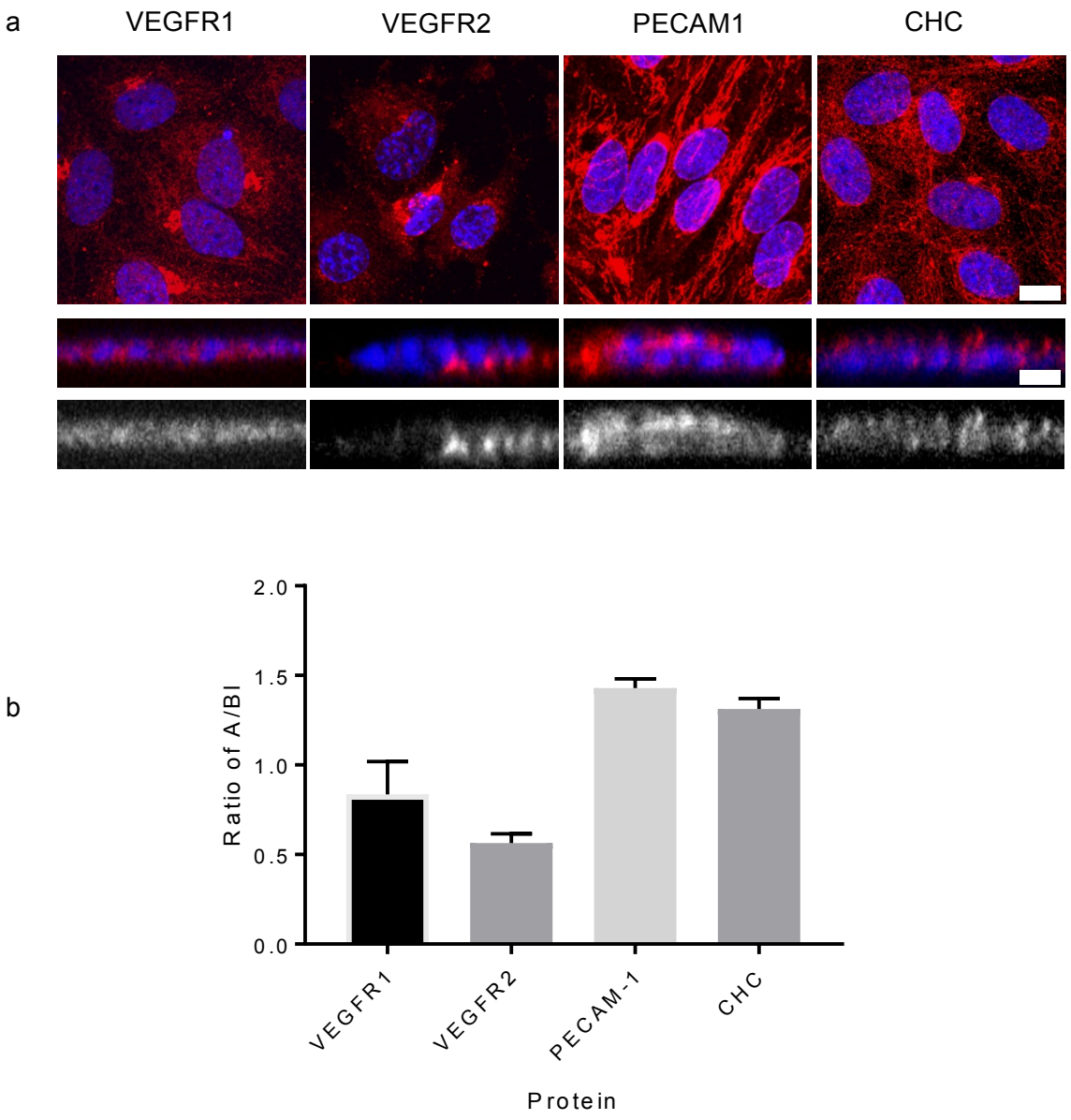

Figure 5.11 – HUVEC surface proteins show a propensity for either the apical or basolateral surface of HUVEC grown on coverslips. Coverslips were cultured with $6x10^4$ cells/ml and then fixed and stained with DAPI (blue) and for VEGFR-1, VEGFR-2, PECAM-1 and CHC (red). a) XY and XYZ images were captured using confocal microscopy. The polarity of both these proteins can clearly be seen from above and below the nucleus (DAPI stained to see thickest part of cell). b) The ratios of apical: basaolateral average pixel intensities were deduced from the XYZ images using imaging software. The bar graph shows the mean ± SEM of three experimental replicates for VEGFR-1, VEGFR-2, PECAM1 and CHC; n=3. Scale bar = 10μm.

Protein	Physiological function	Outcome
Integrin α5	One of two subunits that compose integrin α5. Together with the β1 subunit, α5 forms a receptor for fibronectin and so its main function is in cell surface adhesion to the ECM and in cellular signalling.	Success
ICAM-1	Cell surface glycoprotein that is present in low concentrations under normal conditions in EC and immune cell surface membranes but is upregulated during inflammation. It binds to complementary surface glycoproteins to allow for diapedesis.	Success
VEGFR-1	Cell surface receptor for VEGFA, VEGFB and PGF. Involved in vasculogenesis, angiogenesis and lymphatics development.	Success
VEGFR-2	The main mediator of VEGF-induced angiogenesis and vasculogenesis. Binds to VEGFA, VEGFC and VEGFD.	Success
Clathrin Heavy Chain	Three clathrin heavy chains and three clathrin light chains compose a subunit of clathrin. These form networks that coat vesicles and pits involved in endocytosis and exocytosis. Clathrin is heavily responsible for membrane deformation and vesicle formation.	Success
PECAM-1	Cell adhesion molecule found on the surface of platelets and cells of the immune system, and is also a major constituent of endothelial intercellular junctions. PECAM-1 on immune cells binds to other PECAM-1 glycoproteins exposed during increased endothelium permeability. This allows the guidance of immune cells into the interstitium during inflammation.	Success
P-glycoprotein	ATP-dependent efflux pump found in ECs with broad substrate specificity. Pumps foreign substances out of cells and back into the blood stream.	Only background signal detected
Podocalyxin	Type I transmembrane glycoprotein expressed, among others, on hemangioblasts and mature ECs. It is involved in hematopoietic cell differentiation and in binding to L-selectin, hereby participating in inflammation.	Very weak signal antibody
Robo 4	Involved in vasculogenesis, and in stability of vasculature in adults.	No signal detected
Flotillin 2	Caveolae-associated integral membrane protein. Caveolae are small vesicles on the inner membrane of the surface membrane involved in vesicular trafficking and signal transduction.	Only background signal detected

Figure 5.12 – Function and outcome of proteins investigated.

5.3 Discussion

The results from this chapter have showed that it is not yet possible to separately label HUVEC surface proteins without some label being lost to the other surface. Biointylation reagent added to the apical surface of the HUVEC resulted in label being observed at the basolateral surface, and vice versa. Furthermore, the ability of the reagent to bind to the basal surface was not as good as the apical surface. Both of these results combined invalidates any results obtained using proteins that have been labelled in this way.

The results from figures 5.5 and 5.6 show that sulfo-NHS-LC-biotin labels a greater amount of total protein when added apically, however this is distributed relatively evenly at the apical and basolateral surfaces. Less total protein is labelled when label added to the basolateral surface of the HUVEC, even when 4x as much biotin reagent added, reflecting the fact that it is less able to label proteins when added to this surface. Labelling from this surface, however, labels twice as much protein at the basolateral surface relative to apical. It can be deduced, then, that labelling from the apical surface is much more efficient at labelling surface proteins, however a relatively large amount of these labelled proteins are at the basal surface when the cells are fixed. When added basally, the biotinylation reagent struggles to reach the basal surface proteins to label them compared to when the reagent is added apically. These proteins are mostly situated at the basolateral surface when the cells are fixed and are likely to largely be constituents of the ECM. Taken further, for proteomic analysis of the two separate HUVEC surfaces, these two surfaces must be labelled independently.

In another attempt to label the apical surface of HUVEC in isolation, the incubatory times of HUVEC with the biotintinylation reagent at 37° and 0°C were reduced (Figure 5.7 and 5.8). An increase in apical surface protein labelling relative to basolateral surface protein labelling was seen for 5 and 10 min incubations at both temperatures. However, this difference in labelling across the two surfaces was relatively non-distinct. Reducing the temperature to 0°C did not improve relative apical to basolateral labelling.

As shown, this method of surface protein labelling cannot be used when researching proteomics as it is not possible to label one cell surface in isolation from the other. Biotinylated proteins are isolated from lysed cells using streptavidin, which cannot differentiate the apical from the basolateral cell surface. Hence, surface proteins from both the apical and basolateral surfaces will be analysed using SDS PAGE and western blotting. The polarity of surface proteins cannot be determined as there is no separation of proteins from each surface.

The results from analysis of HUVEC surface protein polarity using

immunofluorescence show great promise. This protocol uses fixed HUVECs, which have been surface membrane permeabilised, and so the polarity of proteins at the point of fixation can be accurately determined. Highly specific, tight binding of antibody-antigen ensures little cross-specificity and is highly accurate. Validation of this method using strong apical and basolateral markers, ICAM-1 and integrin α5 respectively, on Transwells was successful (Figure 5.19). However, these apical: basolateral ratios are still close to 1, meaning they are only marginally polarised at the apical and basolateral surfaces respectively. Their polarity pattern was reproduced on coverslips, which meant that it was possible to scale up the experiment to screen for other proteins.

Results obtained regarding the polarity of VEGFR-1 in HUVEC (Figure 5.11) contradicted that of Hudson et al [38]. This paper suggested that VEGFR1 was apically polarised in mouse MVECs isolated from cortical grey matter. This was the result from *in vitro* cryoimmunogold electron microscopy and both *in vitro* and *in vivo* immunofluorescence. However, my *in vitro* immunofluorescence assay of VEGFR-1 in HUVEC showed it to be basolaterally polarised. This discrepancy may be due to the different micro-environment of the ECs (brain vs umbilical cord matter), or the different animal model used.

Further immunofluorescence experiments were carried out on different surface proteins to determine their polarity within HUVECs (Figure 5.12). Neither PECAM-1 nor CHC produced a polarity index indicating any absolute polarity. VEGFR-2, which had previously suggested was basolaterally polarised [38], too, produced a relatively weak polarity index when assayed for immunofluorescence.

In summary, it was not possible to establish a protocol for labelling HUVEC apical and basolateral surface proteins separately. Initial protocols used EDTA as a reagent to increase the passage of labelling reagent to the basolateral surface when added apically. However, this is likely to interfere with the surface proteins; this research suggested that EDTA cleaved VEGFR-1. It is possible to label surface proteins without EDTA, the labelling reagent being incubated with the HUVEC at the apical or basolateral surfaces. At both surfaces however, the labelling reagent failed to remain at its intended surface. It was possible to demonstrate a more valid method of surface protein labelling using immunofluorescence. Some of these followed a polar distribution that was expected from their physiological function. Integrin α5 and ICAM-1 patterning agreed with initial predictions, however stronger relative staining patterns are needed to provide any conclusive evidence of surface protein polarity. This method is suitable for continuation of HUVEC surface protein studies.

Conclusion

The study of the endothelium in recent research has shown that it is at a hub of homeostasis, controlling normal physiological processes and being implicated in many pathologies. Work in this research project was aimed at studying ECs in cell culture to understand the fundamental cell biology of the endothelium. In doing this, I set out to learn the basics of EC culture and apply this to more complex cellular assays to study the interaction of ECs with other cell types *in vitro* and determine the polarity of a number of important EC surface proteins.

First, I learnt how to culture ECs *in vitro* and that their requirements are more complex than first thought. This cell type has a specialist requirement for culture media composition. The growth and proliferation of HUVEC was optimal when Lonza EGM-2 media was used, compared to different culture media compositions and other suppliers. EGM-2 media containing refined growth factors and signalling molecules at specific concentrations to promote optimal HUVEC proliferation. Having a statistically greater effect on HUVEC proliferation, I then used Lonza EGM-2 media as the culture media for future culture assays.

Secondly, having optimised HUVEC culture conditions I aimed to determine whether different biomaterials were suitable to support HUVECs grown on their surface. From this it was evident that not only do HUVECs not form a complete monolayer with stable cell-cell junctions when cultured on TiO_2, they are also prone to developing markers of genetic instability. Fluorescence microscopy of DAPI and phalloidin stained HUVEC showed the low confluency and high micro-nuclei and chromatin bridges in these cells grown on TiO_2.

The elevated levels of micro-nuclei and chromatin bridges seen in HUVECs grown on TiO_2 raised serious concern for the potential future clinical application of this biomaterial. These genetic instability markers are a likely prerequisite to transformation of the cell into a tumour cell. The obvious effects of this could be catastrophic to the health of the individual. I decided that further research on this would be unjustified using the limited resources present in my current research post. To be able to take this material further would require specialist equipment able to modify the surface topology and chemistry of the TiO_2, which is beyond the capability of my lab.

Although there is a deficit of novel bactericidal biomaterials for clinical applications, the use of this surface at this stage of development would be detrimental to the health of a patient, if said device is implanted. Further research needs to be conducted on the biochemical effect this surface has on physiological cells before clinical application can

be considered. This data, along with that of the immunofluorescence conducted within this research, would give researchers focussing on the development of these novel biomaterials an indication to the types of surface chemiphysical properties that should be avoided, or provide them with a basis for future surface developments.

Having optimised a cell culture protocol for HUVEC, I wanted to use this as a basis for generating a novel protocol for the culture of zebrafish ECs. Initially using Lonza EGM-2 media, I discovered that it is not a suitable culture medium for zebrafish larvae ECs to grow and replicate. Cell proliferation using this media was stunted and cell number declined after 24 h. Suggestions for further optimisation of this protocol would involve using FBS as a source of crude, undefined growth factors and other components necessary for cellular replication. Due to the variability and broad spectrum of its constituents, this media is a more versatile culture media relative to EGM-2, whose composition reflects the specific requirements of HUVEC. Further additions of growth supplements able to be recognised by zebrafish ECs may need to be added to the basal serum if the bovine versions do not allow for adequate cellular proliferation. Furthermore, during FACS, cells other than ECs may have been sorted, demonstrated as their cellular morphologies were dissimilar to that of ECs, and more characteristic of cells of the HPC lineage. This would have altered the outcome of the EC proliferation assay as cells other than ECs would have been counted. An additional variable affecting the reliability of the assay is the inclusion of dead and dying cells in the count. To evade these inappropriately high cellular counts, further rounds of EC validation are needed. Cellular markers specific for ECs need to be identified, such as VEGFR2, using immunofluorescence. In this way those cells that are successfully labelled with the antibodies will be counted. The application of a live/dead cell assay, using fluorophores that effectively stain live cells one colour and dead another, to the culture would allow for the exclusion of dead cells from the count.

Once the culture media has been optimised and a protocol to count only live ECs, the primary cells can be immortalised. hTERT is an enzyme that extends DNA telomeres thereby allowing a cell to replicate beyond the point of its Hayflick limit and potentially become immortal. Using hTERT that is compatible with zebrafish ECs, the primary cells have the capacity to become an immortal, non-transformed cell line. This will have application in future cell culture experiments that require a stable source of zebrafish ECs. These experiments are likely to gain in interest enormously to complement *in vivo* studies on zebrafish larvae. The data from which can be extrapolated back to human models due to their genetic similarities.

Culturing HUVEC with NHDF to generate blood vessels allowed me to understand the importance of cell-cell and cell-ECM interaction in the formation of vasculature. The addition of SW480 P and V tumour spheroids suggested a link between localised VEGF secretion and the upregulation of angiogenesis. This experiment also demonstrated how the incubatory period of the co-culture with each cell type depicts the resulting vasculature density. Work within this chapter has developed a protocol for this tumour angiogenesis assay, producing a blood vasculature density that would give quantifiable results regarding the angiogenic effect of VEGF. This provides the foundation for future opportunities in studying the effect of VEGF and other pro-angiogenic growth factors, as well as the effect of anti-angiogenic factors and drugs designed to inhibit the progression of vasculature expansion. Thus, this assay provides a screening assay for bioactive molecules and existing drugs which may have a second medical use.

Finally, work within this thesis attempted to develop a protocol for surface labelling HUVECs prior to proteomic analysis. Failure to separately label the apical and basolateral surfaces at 0°C with a biotinylating reagent demonstrated how difficult this is, even when the incubatory time of the HUVEC with the reagent was lowered to 5 min. From carrying out this experiment it is clear that basal surface labelling of HUVEC is more difficult than apical surface labelling, the majority of the label being trapped by the protein dense ECM and therefore not reaching the proteins on the basal surface of the cells. Additionally, there was a large amount of proteins being able to reach the basal surface of the HUVEC when the biotinylating reagent is added apically. Therefore, proteomic analysis wasn't possible. Direct labelling of surface proteins with antibodies specific for proteins proven in HUVEC gave encouraging results. There is polarity of surface proteins seen in HUVEC, that of α5 integrin and ICAM-1 following the distribution pattern expected based on their physiological function. This validates this method of surface protein labelling and presents opportunities for future surface protein analysis.

Put together, the results from this project show promise for future research on ECs. Each chapter has set up opportunities for further cell culture assays with various applications. However, the work that I think shows the most potential going forward for further study is the development of a cell surface protein labelling technique. It is clear that labelling all the proteins on the apical and basal surfaces separately is very difficult, however directly labelling specific proteins of interest and imaging them using immunofluorescence presents a reliable method to gain data on their relative surface polarities. The integrity of blood vasculature is critical to their function. For the majority of the endothelium, having a continuous, fence-like sheet of ECs is essential for the

protection and homeostasis of the sub-endothelial tissue. These cells rely on specialised receptor molecules on their surfaces for transcytosis of molecules for cellular growth and proliferation. Little is known of the amount and identities of EC surface proteins at each cellular surface, and so little can be deduced of their function in this important physiological process. Unveiling the polarity of important surface proteins in HUVEC will provide crucial information on their functioning within ECs and hence will have an application in the study of health and disease.

References

1 Bouïs, D., Hospers, G. A. P., Meijer, C., Molema, G. and Mulder, N. H. (2001) Endothelium in vitro: A review of human vascular endothelial cell lines for blood vessel-related research. Angiogenesis **4**, 91–102.

2 Soediono, B. (1989) Alberts - Molecular Biology Of The Cell 4th Ed. J. Chem. Inf. Model.

3 Cines, D. B., Pollak, E. S., Buck, C. A., Loscalzo, J., Zimmerman, G. A., McEver, R. P., Pober, J. S., Wick, T. M., Konkle, B. A., Schwartz, B. S., et al. (1998) Endothelial cells in physiology and in the pathophysiology of vascular disorders. Blood **91**, 3527–3561.

4 Galley, H. F. and Webster, N. R. (2004) Physiology of the endothelium. Br. J. Anaesth. **93**, 105–113.

5 Favero, G., Paganelli, C., Buffoli, B., Rodella, L. F. and Rezzani, R. (2014) Endothelium and its alterations in cardiovascular diseases: Life style intervention. Biomed Res. Int.

6 Peyvandi, F., Garagiola, I. and Baronciani, L. (2011) Role of von Willebrand factor in the haemostasis. Blood Transfus. **9**, s3-8.

7 Gale, A. (2011) Current understanding of hemostasis. Toxicol Pathol . **39**, 273–280.

8 Jain, R. K. (2003) Molecular regulation of vessel maturation. Nat. Med. **9**, 685–693.

9 Kubis, N. and Levy, B. I. (2003) Vasculogenesis and angiogenesis: molecular and cellular controls. Part 1: growth factors. Interv. Neuroradiol. **9**, 227–237.

10 Tammela, T. and Alitalo, K. (2010) Lymphangiogenesis: Molecular Mechanisms and Future Promise. Cell **140**, 460–476.

11 Pocock, G., Richards, C. D. and Richards, D. A. (Biochemist). (2013) Human physiology. Hum. Physiol.

12 Augustin, H. G. and Koh, G. Y. (2017) Organotypic vasculature: From descriptive heterogeneity to functional pathophysiology. Science (80-.). **357**, 1–12.

13 Attwell, D., Mishra, A., Hall, C. N., O'Farrell, F. M. and Dalkara, T. (2016) What is a pericyte? J. Cereb. Blood Flow Metab. **36**, 451–455.

14 Fakhrejahani, E. and Toi, M. (2012) Tumor angiogenesis: Pericytes and maturation are not to be ignored. J. Oncol.

15 Adair, T. H. and Montani, J.-P. (2010) Overview of Angiogenesis. Angiogenesis, Morgan & Claypool Life Sciences.

16 Korthuis, R. J. (2011) Skeletal Muscle Circulation. Integr. Syst. Physiol. From Mol. to Funct. to Dis.

17 Michiels, C. (2003) Endothelial cell functions. J. Cell. Physiol. **196**, 430–

443.

18 Margaris, K. N. and Black, R. A. (2012) Modelling the lymphatic system: Challenges and opportunities. J. R. Soc. Interface **9**, 601–612.

19 Zawieja, D. C. (2009) Contractile Physiology of Lymphatics. Lymphat. Res. Biol. **7**, 87–96.

20 Shi, C. Z., Collins, H. W., Garside, W. T., Buettger, C. W., Matschinsky, F. M. and Heyner, S. (1994) Protein databases for compacted eight□cell and blastocyst□stage mouse embryos. Mol. Reprod. Dev. **37**, 34–47.

21 Cao, N. and Yao, Z. X. (2011) The Hemangioblast: From Concept to Authentication. Anat. Rec. **294**, 580–588.

22 Kume, T. (2010) Specification of arterial, venous, and lymphatic endothelial cells during embryonic development. Histol. Histopathol. **25**, 637–646.

23 Christiansen, A. and Detmar, M. (2011) Lymphangiogenesis and Cancer. Genes and Cancer **2**, 1146–1158.

24 Drake, C. J. (2003) Embryonic and adult vasculogenesis. Birth Defects Res. Part C - Embryo Today Rev. **69**, 73–82.

25 Bauer, S. M., Bauer, R. J. and Velazquez, O. C. (2005) Angiogenesis, vasculogenesis, and induction of healing in chronic wounds. Vasc. Endovascular Surg. **39**, 293–303.

26 Schoenwolf, G. C., Bleyl, S. B., Brauer, P. R. and Francis-West, P. H. (2014) Larsen's human embryology. In Larsen's human embryology.

27 Gerecht-Nir, S., Osenberg, S., Nevo, O., Ziskind, A., Coleman, R. and Itskovitz-Eldor, J. (2004) Vascular Development in Early Human Embryos and in Teratoma-Derived from Human Embryonic Stem Cells. Biol Reprod **71**, 2029–2036.

28 Gilbert, S. F. (2013) Developmental Biology. Dev. Biol. 10th Editi.

29 Otrock, Z. K., Mahfouz, R. A. R., Makarem, J. A. and Shamseddine, A. I. (2007) Understanding the biology of angiogenesis: Review of the most important molecular mechanisms. Blood Cells, Mol. Dis. **39**, 212–220.

30 Adair TH, M. J. (2010) Angiogenesis. Angiogenesis.

31 Hoeben, A., Landuyt, B., Highley, M. S., Wildiers, H., Van Oosterom, A. T. and De Bruijn, E. a. (2004) Vascular endothelial growth factor and angiogenesis. Pharmacol. Rev. **56**, 549–580.

32 Chung, A. S. and Ferrara, N. (2011) Developmental and Pathological Angiogenesis. Annu. Rev. Cell Dev. Biol. **27**, 563–584.

33 Tahergorabi, Z. and Khazaei, M. (2012) A review on angiogenesis and its assays. Iran. J. Basic Med. Sci. **15**, 1110–1126.

34 Mendelsohn, J., Howley, P. M., Israel, M. A., Gray, J. W. and Thompson, C. B. (2008) The Molecular Basis of Cancer. Mol. Basis Cancer Third Edit.

35 Kitchens, C. S., Konkle, B. A. and Kessler, C. M. (2013) Consultative Hemostasis and Thrombosis: Third Edition. Consult. Hemost. Thromb. Third Ed.

36 Ortega, N., Hutchings, H. and Plouët, J. (1999) Signal relays in the VEGF system. Front. Biosci. **4**, 141–152.

37 Nishida, N., Yano, H., Nishida, T., Kamura, T. and Kojiro, M. (2006) Angiogenesis in cancer. Vasc. Health Risk Manag. **2**, 213–219.

38 Hudson, N., Powner, M. B., Sarker, M. H., Burgoyne, T., Campbell, M., Ockrim, Z. K., Martinelli, R., Futter, C. E., Grant, M. B., Fraser, P. A., et al. (2014) Differential apicobasal VEGF signaling at vascular blood-neural barriers. Dev. Cell **30**, 541–552.

39 Blanco, R. and Gerhardt, H. (2013) VEGF and Notch in tip and stalk cell selection. Cold Spring Harb. Perspect. Med. **3**, 1–15.

40 Lizama, C. O. and Zovein, A. C. (2013) Polarizing pathways: Balancing endothelial polarity, permeability, and lumen formation. Exp. Cell Res. **319**, 1247–1254.

41 Yang, Y. and Oliver, G. (2014) Development of the mammalian lymphatic vasculature. J. Clin. Invest. **124**, 888–897.

42 Srinivasan, R. S., Dillard, M. E., Lagutin, O. V., Lin, F. J., Tsai, S., Tsai, M. J., Samokhvalov, I. M. and Oliver, G. (2007) Lineage tracing demonstrates the venous origin of the mammalian lymphatic vasculature. Genes Dev. **21**, 2422–2432.

43 Oliver, G. and Alitalo, K. (2005) THE LYMPHATIC VASCULATURE: Recent Progress and Paradigms. Annu. Rev. Cell Dev. Biol. **21**, 457–483.

44 Yang, Y., García-Verdugo, J. M., Soriano-Navarro, M., Srinivasan, R. S., Scallan, J. P., Singh, M. K., Epstein, J. A. and Oliver, G. (2012) Lymphatic endothelial progenitors bud from the cardinal vein and intersomitic vessels in mammalian embryos. Blood **120**, 2340–2348.

45 Daneman, R. and Prat, A. (2015) The blood–brain barrier. Cold Spring Harb. Perspect. Biol. **7**.

46 Magistretti, P. J. and Allaman, I. (2015) A Cellular Perspective on Brain Energy Metabolism and Functional Imaging. Neuron **86**, 883–901.

47 Dickens, D., Chiduza, G. N., Wright, G. S. A., Pirmohamed, M., Antonyuk, S. V. and Hasnain, S. S. (2017) Modulation of LAT1 (SLC7A5) transporter activity and stability by membrane cholesterol. Sci. Rep. **7**, 1–13.

48 Rasche, H. (2001) Haemostasis and thrombosis: An overview. Eur. Hear. Journal, Suppl. **3**, Q3–Q7.

49 Pober, J. S. and Sessa, W. C. (2007) Evolving functions of endothelial cells in inflammation. Nat. Rev. Immunol. **7**, 803–815.

50 Janeway, C. J., Travers, P. and Walport, M. (2001) Immunobiology: The Immune System in Health and Disease. 5th edition. Garl. Sci.

51 Urb, M. and Sheppard, D. C. (2012) The role of mast cells in the defence against pathogens. PLoS Pathog. **8**, 1–3.

52 Ley, K., Laudanna, C., Cybulsky, M. I. and Nourshargh, S. (2007) Getting to the site of inflammation: The leukocyte adhesion cascade updated. Nat. Rev. Immunol. **7**, 678–689.

53 Rock, K. L. (2009) Pathobiology of Inflammation to Cell Death. Biol. Blood Marrow Transplant. **15**, 137–138.

54 Medzhitov, R. (2008) Origin and physiological roles of inflammation. Nature **454**, 428–435.

55 Sandoo, A., Veldhuijzen van Zanten, J. J. C. S., Metsios, G. S., Carroll, D. and Kitas, G. D. (2010) The Endothelium and Its Role in Regulating Vascular Tone. Open Cardiovasc. Med. J. **4**, 302–312.

56 Vinay Kumar, Abul K. Abbas, J. C. A. (1994) Robins Basic Pathology. J. Clin. Pathol. 9th Editio.

57 Underwood, J. (2009) General and systemic pathology 5th ed.

58 Kalogeris, T., Baines, C. P., Krenz, M. and Korthuis, R. J. (2012) Cell Biology of Ischemia/Reperfusion Injury. Int. Rev. Cell Mol. Biol. **298**, 229–317.

59 Tabas, I., García-Cardeña, G. and Owens, G. K. (2015) Recent insights into the cellular biology of atherosclerosis. J. Cell Biol. **209**, 13–22.

60 Lusis, A. J. (2000) Atherosclerosis. Nature **407**, 233–241.

61 Weber, C. and Noels, H. (2011) Atherosclerosis: Current pathogenesis and therapeutic options. Nat. Med. **17**, 1410–1422.

62 Dundar, Y. et al. (2004) Angioplasty and stents in coronary artery disease: a systematic review and meta□analysis. Scand. Cardiovasc. J. **38**, 200–210.

63 Wiseman, A. C. (2016) Immunosuppressive medications. Clin. J. Am. Soc. Nephrol. **11**, 332–343.

64 Jenkins, J. et al. (2018) Characterisation of bactericidal titanium surfaces using electron microscopy.

65 Jaggessar, A., Shahali, H., Mathew, A. and Yarlagadda, P. K. D. V. (2017) Bio-mimicking nano and micro-structured surface fabrication for antibacterial properties in medical implants. J. Nanobiotechnology **15**, 1–16.

66 Bjarnsholt, T. (2013) The role of bacterial biofilms in chronic infections. APMIS **121**, 1–58.

67 Jenkins, J., Nobbs, A. H., Verkade, P. and Su, B. (2018) Characterisation of bactericidal titanium surfaces using electron microscopy. Microsc. Anal. **34**, 17–22.

68 Park, J., Bauer, S., Von Der Mark, K. and Schmuki, P. (2007) Nanosize and vitality: TiO2 nanotube diameter directs cell fate. Nano Lett. **7**, 1686–1691.

69 Veldman, M. B. and Lin, S. (2008) Zebrafish as a developmental model organism for pediatric research. Pediatr. Res. **64**, 470–476.

70 Delov, V., Muth-Köhne, E., Schäfers, C. and Fenske, M. (2014) Transgenic fluorescent zebrafish Tg(fli1: EGFP)y1for the identification of vasotoxicity within the zFET. Aquat. Toxicol.

71 Mellor, H. MELLORLAB.

72 Bishop, E. T., Bell, G. T., Bloor, S., Broom, I. J., Hendry, N. F. K. and Wheatley, D. N. (1999) An in vitro model of angiogenesis: Basic features. Angiogenesis **3**, 335–344.

73 Hetheridge, C., Mavria, G. and Mellor, H. (2011) Uses of the in vitro endothelial–fibroblast organotypic co-culture assay in angiogenesis research : Figure 1. Biochem. Soc. Trans. **39**, 1597–1600.

74 Folkman, J. and Haudenschild, C. (1980) Angiogenesis in vitro. Nature **288**, 551–556.

75 Knight, E. and Przyborski, S. (2015) Advances in 3D cell culture technologies enabling tissue-like structures to be created in vitro. J. Anat. **227**, 746–756.

76 Kut, C., Mac Gabhann, F. and Popel, A. S. (2007) Where is VEGF in the body? A meta-analysis of VEGF distribution in cancer. Br. J. Cancer 978–985.

77 Park, J. E., Keller, G. A. and Ferrara, N. (1993) The vascular endothelial growth factor (VEGF) isoforms: differential deposition into the subepithelial extracellular matrix and bioactivity of extracellular matrix-bound VEGF. Mol. Biol. Cell 1317–1326.

78 Jonckheere, A. I., Smeitink, J. A. M. and Rodenburg, R. J. T. (2012) Mitochondrial ATP synthase: architecture, function and pathology. J. Inherit. Metab. Dis. **35**, 211–225.

79 Lodish, H., Berk, A., Zipursky, S. L., Matsudaira, P., Baltimore, D. and Darnell, J. (2000) Molecular Cell Biology. 4th edition. New York W. H. Free.

80 Huang, S. and Czech, M. P. (2007) The GLUT4 Glucose Transporter. Cell Metab. **5**, 237–252.

81 Gottardi, C. J., Dunbar, L. a and Caplan, M. J. (1995) Biotinylation and assessment of membrane polarity: caveats and methodological concerns. Am. J. Physiol. **268**, 285–295.

82 June, S. L., Semela, D., Iredale, J. and Shah, V. H. (2007) Sinusoidal remodeling and angiogenesis: A new function for the liver-specific pericyte? Hepatology **45**, 817–825.

83 DeSesso, J. M. (2017) Vascular ontogeny within selected thoracoabdominal organs and the limbs. Reprod. Toxicol. **70**, 3–20.

84 Kunkel, E. J. and Butcher, E. C. (2003) Plasma-cell homing. Nat. Rev. Immunol. **3**, 822–829.

85 Ooi, B., Goh, B. and Yap, W. (2017) Oxidative Stress in Cardiovascular Diseases: Involvement of Nrf2 Antioxidant Redox Signaling in Macrophage Foam Cells Formation. Int. J. Mol. Sci. **18**, 2336.